Università degli Studi di Padova

Industrial Engineering Department (DII)

Master's Degree in:
Environmental Engineering

Master's Thesis

A comparison of models for nitrogen and pathogen removal in horizontal subsurface flow constructed wetlands

Supervisor:
Prof. Luca Palmeri

Co-supervisor:
Dr. Alberto Barausse

Candidate:
Andrea Sacha Cannizzo

Academic Year 2014 / 2015

1. INTRODUCTION

1.1 Introduction

Today the interest in the use of constructed wetland (CWs) plants as tertiary wastewater treatments and more is increasing, principally for small communities or in the context of wastewater treatment plants designed for few equivalent inhabitants. It is a very interesting technology for developing countries too (Kivaisi, 2001), not only as post-treatment, and in addition it could be very interesting for the industrial wastewater treatment (Vyzamal, 2014).

This kind of plants, miming what occurs in natural wetland, contributes to remove nutrients and organics dissolved and suspended in the wastewater as well as the pathogens and promote the removal of some toxic substances (for example some aromatic compounds such phenols, benzene, BTEX) and heavy metals (Vyzamal, 2014).

The use of this kind of plants and research studies regarding them are increasing principally because CW plants can be defined as low cost technologies; constructed wetland plants or wetland-like treatment plants (facultative ponds or lagoons for example) are characterized by low realization and maintenance costs compared to the traditional intensive technologies (activated sludge plants for example). Wu et al. (2015) remind us of the fact that CWs plants are characterized by very low maintenance, construction and operation costs. However, they also remind that these technologies could produce an important soil occupation and consumption. A complete and valid evaluation of a constructed wetland plants require to take all potential environmental impacts into account.

An important part of research studies are focused on constructing, investigating, and evaluating the performance of models that simulate and describe the pollutants and nutrients fate and their dynamics in wetlands; there are important informations for plant design and critical evaluation. For example, several authors (Mayo et al, 2005; Senzia et al, 2002; Wang et al, 2009) have investigated and evaluated models useful to describe the nitrogen compounds removal that occurs into horizontal sub-surface constructed wetland or wetland-like systems (facultative primary ponds); all these authors have modelled the nitrogen dynamic in wetlands taking into account its cycle and using a continuous stirred tank reactor (CSTR) model.

Very interesting and articulate is the CW2D model developed by Langergraber et al. that is

described and implemented in several studies (Langergraber et al. 2005, 2006, 2007); this model describes the dynamics of organic matter, nitrogen compounds, phosphorus compounds, and others (sulphites for example) applying a modified activated sludge model (ASM), that, afterwards, they called CWM1 (Langergraber et al., 2009), using such as hydraulic model a modified HYDRUS-2D and 1D application. The CW2D now is a package that is possible to use with the HYDRUS-2D software.

Another very interesting experience is the one developed by Giraldi et al. (2010) that have implemented a model to describe the pollutants behaviour in a subsurface vertical flow constructed wetland called FITOVERT, which stands for "FITOdepurazione VERTicale". This kind of model is capable of describing the dynamics that occur in unsaturated porous media in 1 dimension and is capable to model: the transport of dissolved and particulate compounds, the oxygen exchange and the dynamic of clogging that develops over time.

The dynamic of organics and nitrogen compounds into constructed wetland plants can be described also using simpler models such as the k-C* first order kinetics model, as showed by Rousseau et al. (2004) and as is remarked by Kadlec et al. (2008). However, Kadlec (2000), in a study, shows that the choice of a k-C* first order kinetics model and a plug flow reactor model alone is inadequate for the design of a constructed wetland plant. He has demonstrated that the rate constant (k) and the apparent background concentration (C*) are strongly influenced by some characteristic of the CWs tank such as hydraulic loading, inlet concentration, short circuiting and spatial distribution of vegetation.

Research studies about the pathogens removal in constructed wetland plant are very common too; as I have said above, the interest in using CWs as tertiary disinfection treatment is increasing. Usually, a first order kinetics model is used to describe the removal of pathogens (principally Coliform, Streptococci and Escherichia coli) into wetlands or ponds (Mayo, 2004; Mayo et al, 2007; Von Spelling, 1998; Xu et al, 2002; Craggs et al, 2004; Cirelli et al, 2009; Hamaamin et al, 2014) using a plug and flow model, a CSTR model or a dispersed flow model.

1.2 Aim of thesis

The aim of this thesis is to build several models with different levels of complexity that describe the nitrogen and pathogens removal into constructed wetland basins and to compare them using different indicators, to understand which kind of wetland model performs better.

To evaluate model performance, I used both classical indicators of goodness-of-fit (such as the Nash-Sutcliffe efficiency) and indicators taking both goodness-of-fit and model simplicity into account (such as the Akaike's information criterion AIC). The models were applied to a real-world application, represented by two constructed wetland tanks sited in the Vigonza (Padova province, North-eastern Italy) wastewater treatment plant, where the Department of Industrial Engineering (DII, former DPCI) of the University of Padova carried out monitoring activities between July 2011 and June 2012.

In the following chapters, after a brief description of the area and the constructed wetland plants where the research study was conducted (Chapyter 2), all the information used to build models and the methodology applied to realize, implement, fit and evaluate them are described (Chapter 3). Chapter 4 and 5 are dedicated to reporting results, discussing them and drawing some conclusions.

2. SITE DESCRIPTION

2.1 The Vigonza Wastewater treatment plant

The wastewater treatment plant (WWTP), where the constructed wetland basins were built, is sited in the Vigonza municipality, about 10 km far from the centre of Padova city (fig 2.1). It was built during the 1999 and, at present, is managed by ETRA s.p.a. This plant was designed in order to treat the urban wastewater produced by 7 municipalities for a total of 70000

Figure 2.1: The position of Vigonza wastewater treatment plant (orange) with respect the Padova municipality. Imagine by Google Earth.

equivalent inhabitants. The wastewater that enters into the plant is, firstly, pretreated: the screening, the grit removal and oils removal are the most important pre-treatments; three primary sedimentation tanks were built during the 1999, but now are not used in order to increase the treatment efficiency; all pre-treatments occur indoor, into a shed (fig 2.2). After the oils removal, the wastewater is sent to anoxic tanks where denitrification phenomena occur (fig 2.2); then, the sewage is directed to aerobic tanks where the removal of biodegradable organics and ammonia occur (fig 2.2). The outflow wastewater from the aerobic tanks undergoes a sedimentation process in order to remove the particulate biodegradable and not biodegradable organics; the Vigonza WWTP is characterized by three secondary settler in parallel (fig 2.2). At the end, the wastewater is disinfected and post-treated using per-acetic acid, a filtration process and, at the end, ultraviolet method. It is then

Figure 2.2: The Vigonza WWTP: the pre-treatments indoor area (red); the anoxic tanks (yellow); the aerobic tanks (green); the secondary settlers (blu); the four constructed wetland basins (violet).

discharged into the rio Fiumicello or rio dell'Arzere, little channels that arrive to the lagoon of Venice.

During 1999 four constructed wetland basins (fig 2.2, 2.4) were built, principally for the implementation of experiments and research studies in order to verify and calculate the removal efficiency of nutrients or pathogens. The constructed wetland plant is characterized by three tanks with an horizontal subsurface flow (HSSF) (fig 2.4) and one equalization tank (fig 2.4) that collects the wastewater out of the HSSF basins and sends it to the head of WWTP, again. These basins have worked since 1999 and 2001; after, two of four tanks were reactivated by the Padova University for research studies: from the September 2009 until the end of 2012. Now, the constructed wetland tanks do not work. In a HSSF constructed wetland

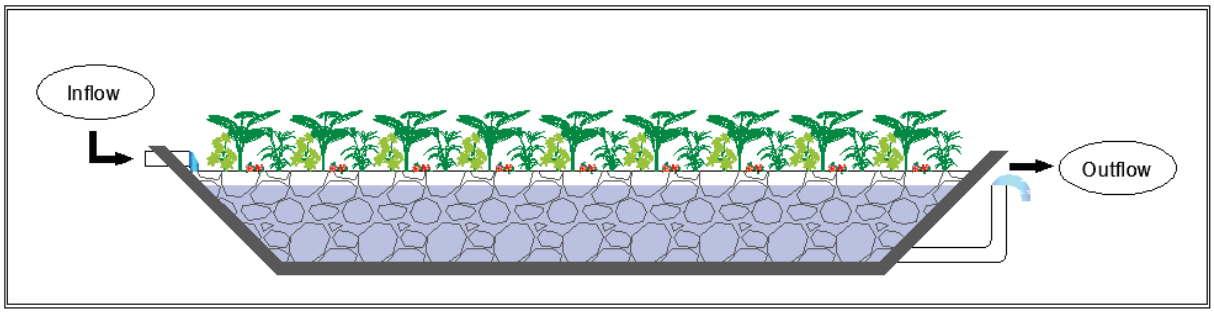

Figure 2.3: The horizontal subsurface flow (HSSF) constructed wetland configuration

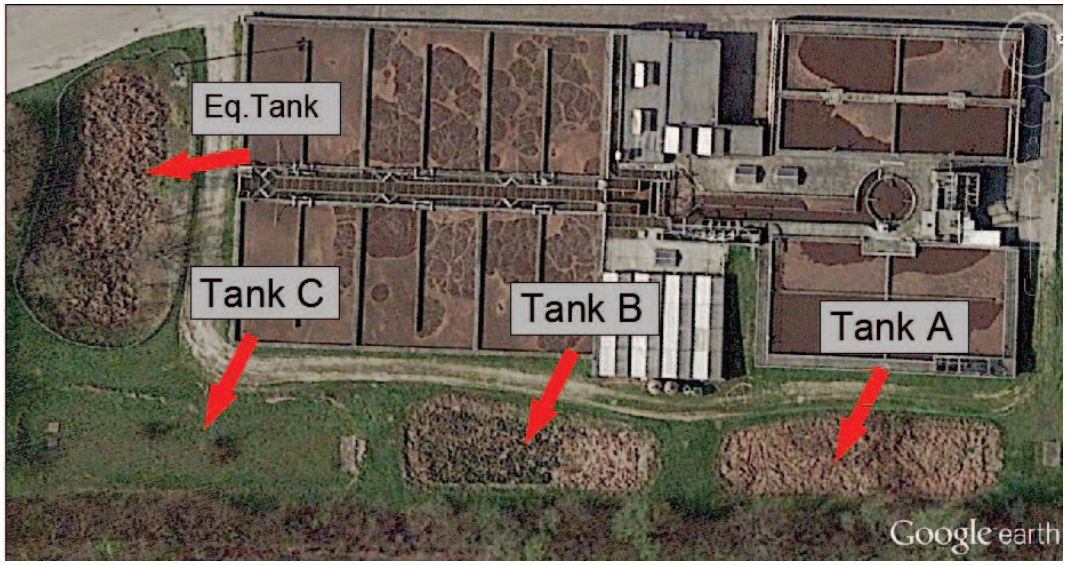

Figure 2.4: The tanks A,B and C and the equalization one that compose the constructed wetland plant in Vigonza WWTP

(fig. 2.3) the water flows longitudinally with respect to the tank length. Usually, the wastewater is injected, through pipes, in the upper part of the basin and comes out in the bottom, from the opposite side (fig 2.3). The tank is filled with a permeable porous medium where the plants roots and bacteria can grow and water can flow. In this kind of constructed wetland basin, the porous medium is saturated; the water free surface is slightly below the surface of materials which fill the tank (fig 2.3). The saturation conditions are guaranteed thanks a regulating trap: the point where the wastewater come out (in the pipes) have the same distance, from the tank bottom, as the water free surface into the tank (fig 2.3).

2.2 The constructed wetland plant

From the September 2009 the Padova University has used two of the four constructed wetland tanks for research; henceforth these will be called in A tank and B tank (fig 2.4). Aims of such studies were to: verify and calculate the abatement efficiency of nutrients and pathogens; improve the knowledge of the hydraulic of tanks, thanks to the conduction of several tests useful for the calculation of average wastewater retention time and the presences of dead zone.

The tank A is characterized (tab 2.1) by an average surface of 362 m^2 with an average length of 36 m, while the tank B (tab 2.1) is about 336 m^2 and 33 m long. Both tanks are characterized by an depth of 1 meter. The bottom liner of all basins is impermeable consisting of a HDPE geomembrane which is protected by a geotextile; this solution avoids the wastewater infiltration into the underlying natural soils. The porous media that fill all basins

are (from bottom to up) (fig 2.7): a fine gravel layer (4-6 mm diameter) 10 cm thick; a gravel layer (100-150 mm diameter) with a thickness of 60 cm; a large gravel layer (20-30 mm diameter) 10 cm thick; a fine gravel layer (4-6 mm diameter) with 10 cm thickness; a layer of 20 cm composed by compost (fig 2.7).

Table 2.1: The constructed wetland plant basins: Tank A and B characteristics

	Tank A	Tank B
Average Tanks Lenght (m)	35.7	32.8
Average Tanks Depth (m)	1	1
Average Tanks Width (m)	10.3	10.3
Average Tanks Surface (m^2)	362.53	336.53

Until May 2011 the tank A was the only one planted with a mix of Phragmites australis and Scirpus sylvaticus; from June 2011 the tank B was covered by Iris pseudacorus and Canna indica. During the 2011 piezometers were installed into both tanks in order to understand the wastewater hydraulics behaviour into the constructed wetland basins and so to understand if there are preferential wastewater flow zones; they were used also in order to understand if there are dead zones where the wastewater tends to stop with an increase of wastewater retention time. In the tank A and B 12 piezometers were installed, divided in 4 transects (fig. 2.5) and 3 series (fig. 2.5) at 40 cm from the surface of basin, and two piezometers (P1, P2) at 70 cm from the surface (fig. 2.5).

The inflow wastewaters, into the constructed wetland basins, were taken through a pump from a tank placed downstream the secondary settler and upstream the filtration process. After this,

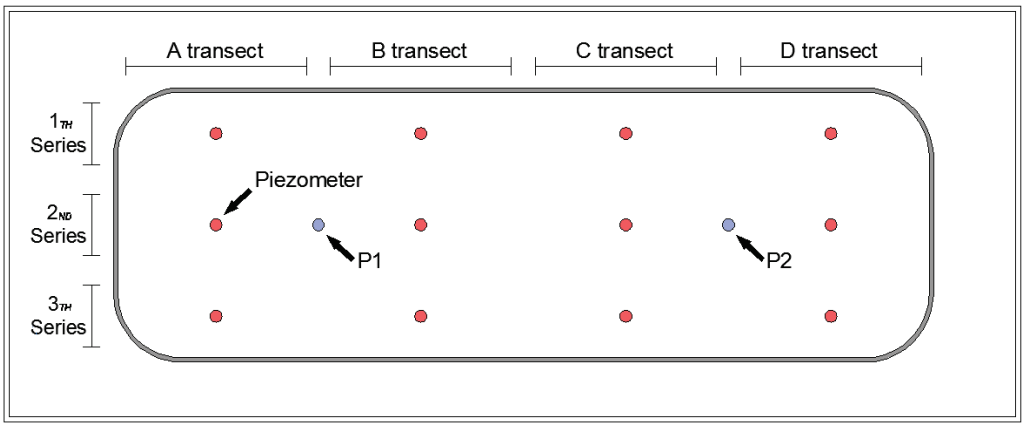

Figure 2.5: Piezometers installed configuration in the Tank A and B

the wastewater flow was divided in two fluxes through an T divergence device, where the water flow was regulated using three valves and where water volume counters were installed. The designed wastewater inflow for each basin was 0.5 m^3/h.

Figure 2.6: The wastewater divergence device installed upstream the constructed wetland tanks

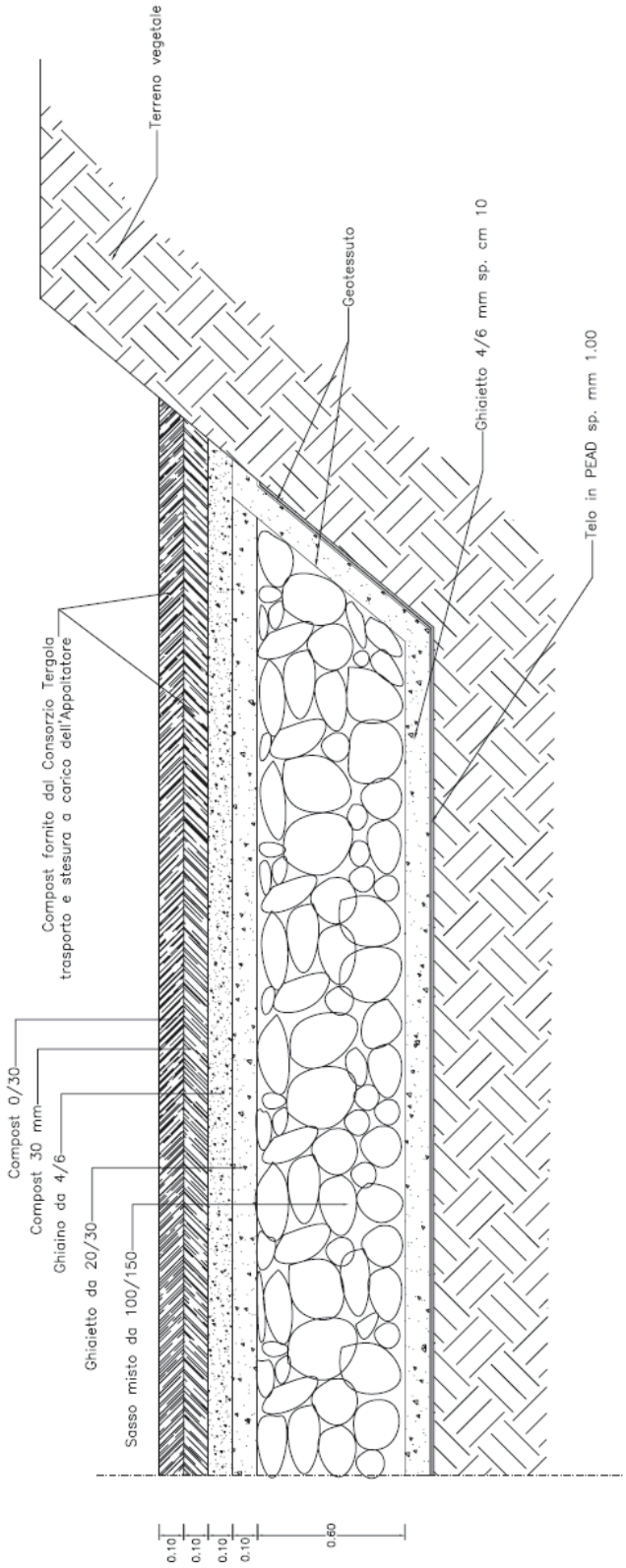

Figure 2.7: The constructed wetland tanks filling

3. MATERIALS AND METHODS

3.1 The wastewater chemical-physical characteristics

The calculation of nutrient and microbiological abatement efficiency was made comparing the nutrient and microbiological concentration of inflow wastewater and outflow one.

The nutrients taken into account in a previous study are: Ammonia nitrogen [NH_4], Nitrates [NOx], Dissolved organic nitrogen [DON] and so the total inorganic dissolved nitrogen [TDIN] (calculated adding up the NH_4 and NOx concentrations) and the total dissolved nitrogen [TDN] (calculated adding up the concentrations of NH_4, NOx and DON).

The microbiological parameters considered are: Faecal coliform (UFC/100ml); Escherichia coli (UFC/100ml); Faecal streptoccocci (UFC/100ml); Total streptoccocci (UFC/100ml); Clostridium (UFC/100ml).

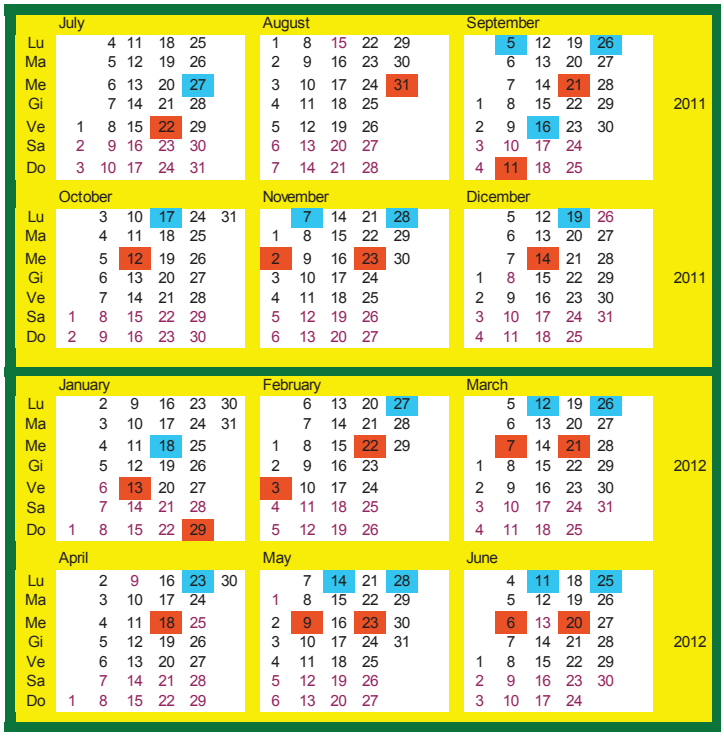

Figure 3.1: Sampling calendar: days when the inflow wastewater sampling (red) and the outflow wastewater sampling (blue) occurred.

The sampling of inflow and outflow wastewater was made between the 22 July 2011 and 20 June 2012; in this period a total of 18 sampling campaigns was carried out, on average, every 14 days (fig.3.1).

The sampling of outflow wastewater typically occurred the fifth day after the corresponding inflow sampling to approximately account for water residence time in the plant; therefore the precise hydraulics retention time in the system was not taken into account strictly during the campaigns; the wastewater flow, into the constructed wetland basins, was designed in order to have a retention time value equal or higher than 4 days, a value recommended for tertiary treatment (Kadlec et al, 2009). The analysis (par.3.2) for understanding the wastewater hydraulics behaviour, and so, the calculation of average retention time was made in the same period when the nutrient sampling occurred.

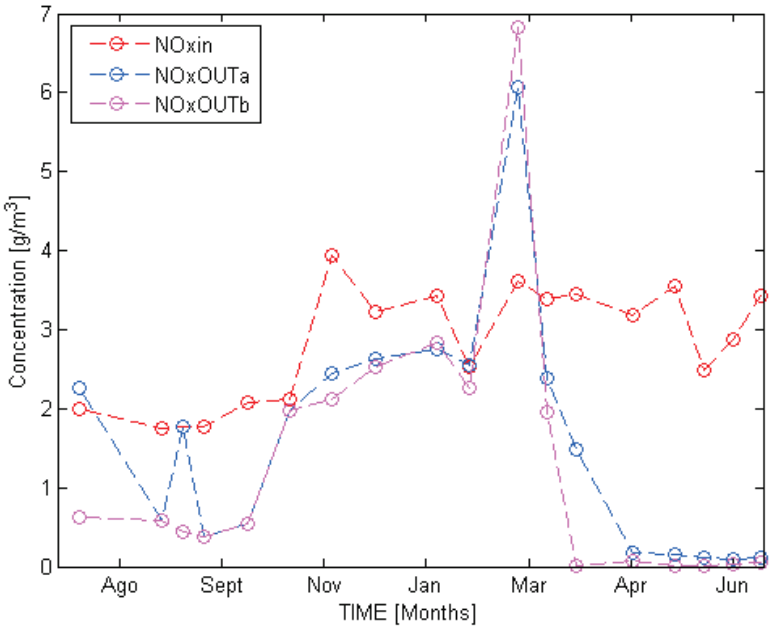

Figure 3.2: Inflow Nitrates (NOx) (red) compared to the outflow NOx of A basin (blue) and B basin (pink) measured between July 2011 and June 2012

3.1.1 The nitrogen compounds dynamics in the constructed wetlands basins

Globally all campaigns show that both constructed wetland plants are generally capable to reduce the concentration of the TDN (fig. 3.5), DON (fig. 3.4) and Nitrates (fig. 3.2). The nitrates averages removal efficiencies[1] of A basin and B basin were 44% and 56% respectively while the global removal efficiencies of DON were 47% and 42% respectively. The ammonia nitrogen dynamics into the wetlands tend to be more irregular than DON and nitrate ones (fig.

1 The tank removal efficiency of nitrogen compounds and pathogens was calculated with the following equation:

$$R_{EFF} = \frac{\sum_{(v=1)}^{N} (1 - (C_{Ov} / C_{Iv}))}{N} \cdot 100$$

where: C_{Ov} is the outflow concentration observed during the sampling v; C_{Iv} is the inflow concentration observed during the sampling v; N is the number of sampling; R_{EFF} is the removal efficiency in percentage.

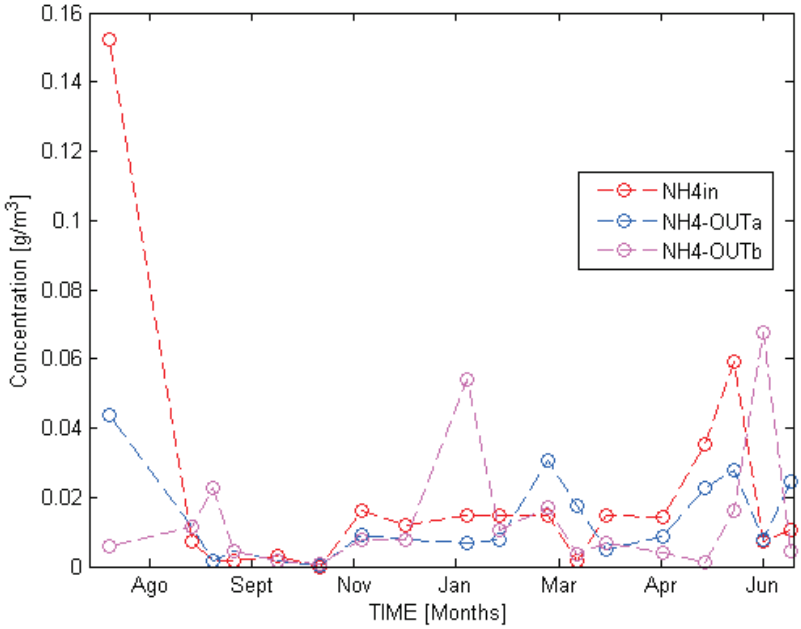

Figure 3.3: Inflow Ammonia Nitrogen (NH4) (red) compared to the outflow NH4 of A basin (blue) and B basin (pink) measured between July 2011 and June 2012

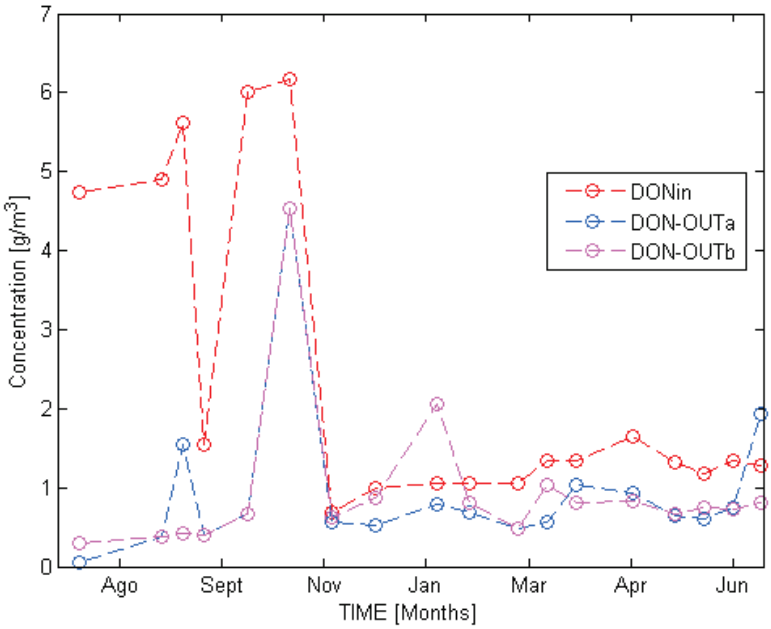

Figure 3.4: Inflow Dissolved organic nitrogen (DON) (red) compared to the outflow DON of A basin (blue) and B basin (pink) measured between July 2011 and June 2012

3.3); the averages removal efficiencies of ammonia nitrogen is negative referred to A basin and B basin respectively. The explanation is related to the low values of ammonium measured in wastewater. Loro (2011) shows in his thesis work that it did not make sense to apply

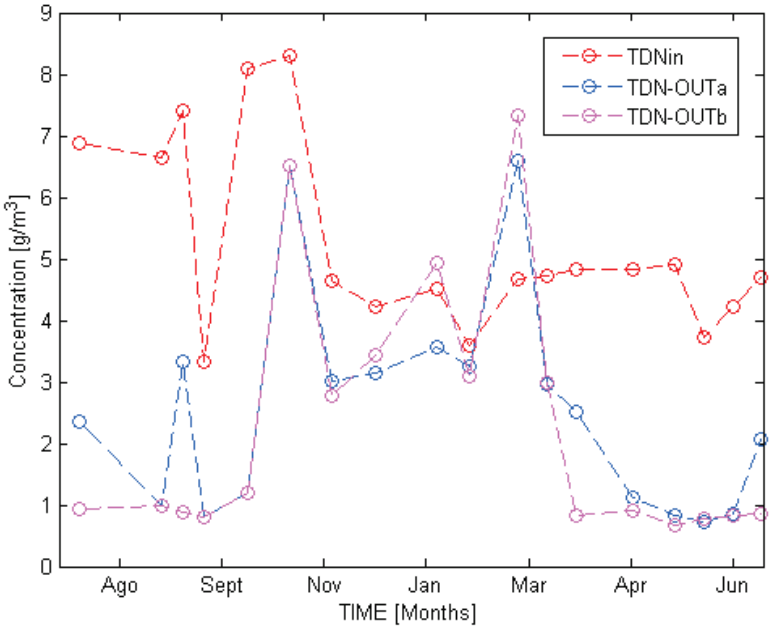

Figure 3.5: Inflow Total dissolved nitrogen (TDN) (red) compared to the outflow TDN of A basin (blue) and B basin (pink) measured between July 2011 and June 2012

statistical tests to assess the ammonia nitrogen removal into the basins because the inflow and outflow wastewater ammonia concentration was below the sensitivity instrument threshold used to measure the concentration. Globally the A basin and B basin are characterized by a total nitrogen (TDN) removal efficiency of 50% and 54% respectively.

Tab. 3.1: Microbiological averages removal efficiencies and DEC for constructed wetland basins

	A-Basin		B-Basin	
	% Abatement	DEC[2]	%Abatement	DEC[2]
Clostridium	36	1.04	3	0.58
Total Streptococci	-100.9	-0.13	-121	-0.14
Faecal Streptococci	86.1	1.75	71.4	1.65
Faecal Coliform	84.8	1	63.9	0.69
Escherichia Coli	97.7	3.23	87.6	1.42

2 DEC means ***D**ecimal **E**limination **C**apacity*. This can be used to evaluate the pathogens removal and was calculated with the following equation:

$$DEC = \log_{10}\left(\frac{C_I}{C_{OUT}}\right)$$

where: C_I is the inflow average pathogens concentration ; C_{OUT} the outflow average pathogens concentration. If this value tends to 1 means that the abatement is about 90%; a DEC value of 2 means that the abatement is about 99% while with a value of 3 about 99.9%; on contrary a DEC of -1 means a pathogens production of 90%.

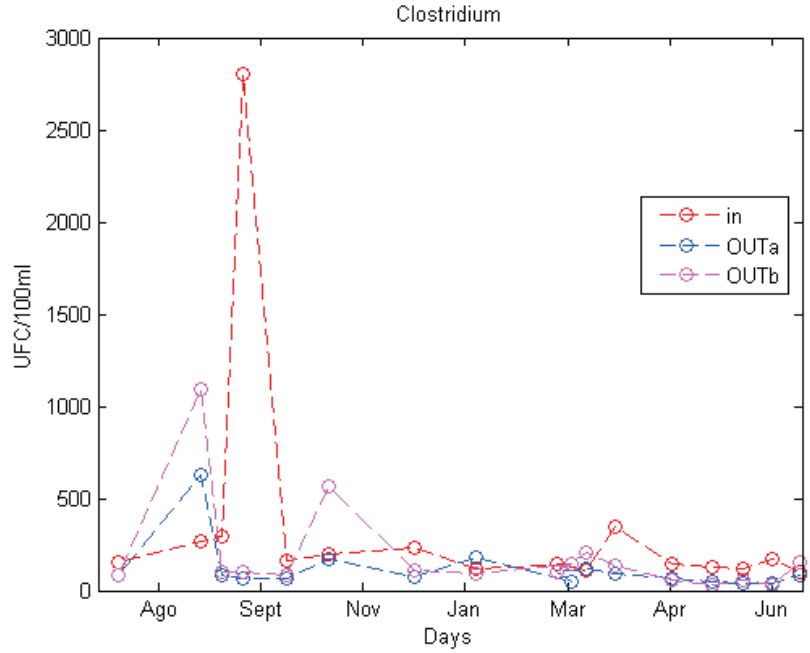

Figure 3.6: Inflow Clostridium (red) compared with the outflow concentration of A basin (blue) and B basin (pink) measured between July 2011 and June 2012

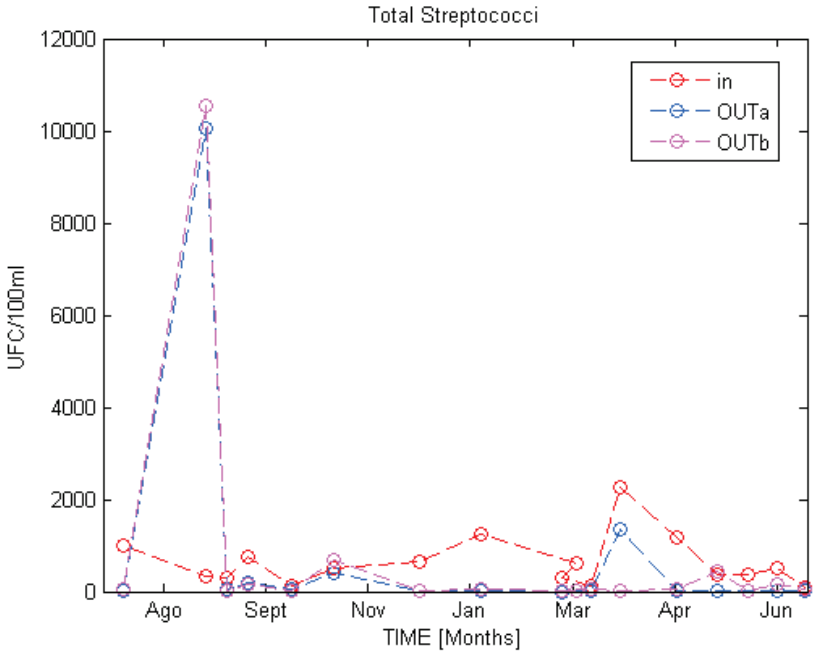

Figure 3.7: Inflow Total Streptococci (red) compared with the outflow concentration of A basin (blue) and B basin (pink) measured between July 2011 and June 2012

3.1.2 The microbiological abatement

From the microbiological analysis it emerges that the constructed wetland plants are capable of removing pathogens with some exceptions (tab. 3.1); in particular, the A tank is capable to

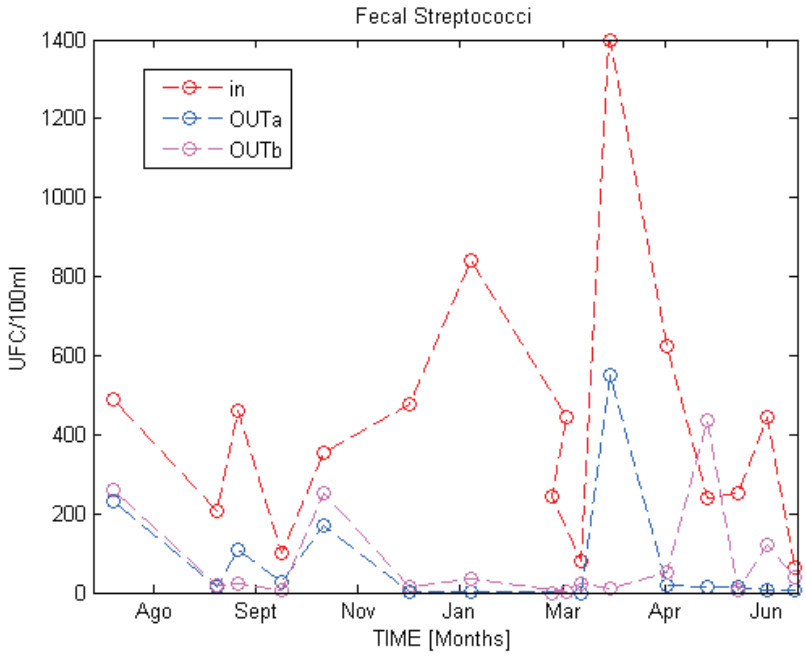

Figure 3.8: Inflow Faecal Streptococci (red) compared with the outflow concentration of A basin (blue) and B basin (pink) measured between July 2011 and June 2012

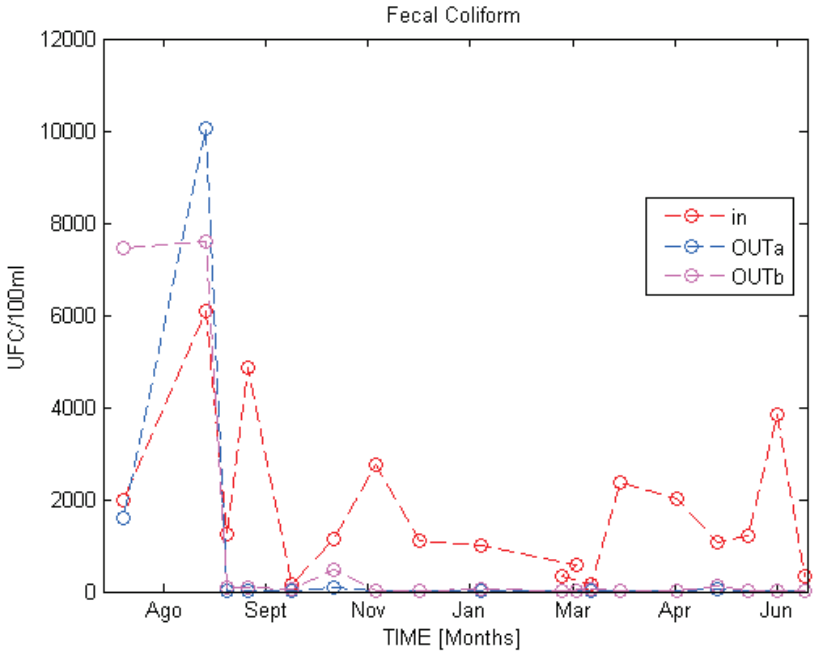

Figure 3.9: Inflow Faecal Coliform (red) compared with the outflow concentration of A basin (blue) and B basin (pink) measured between July 2011 and June 2012

remove better the pathogens than the B one (tab. 3.1): the averages removal efficiencies of Clostridium are 36% for A basin and 3% for B basin; the efficiencies of Total and Faecal

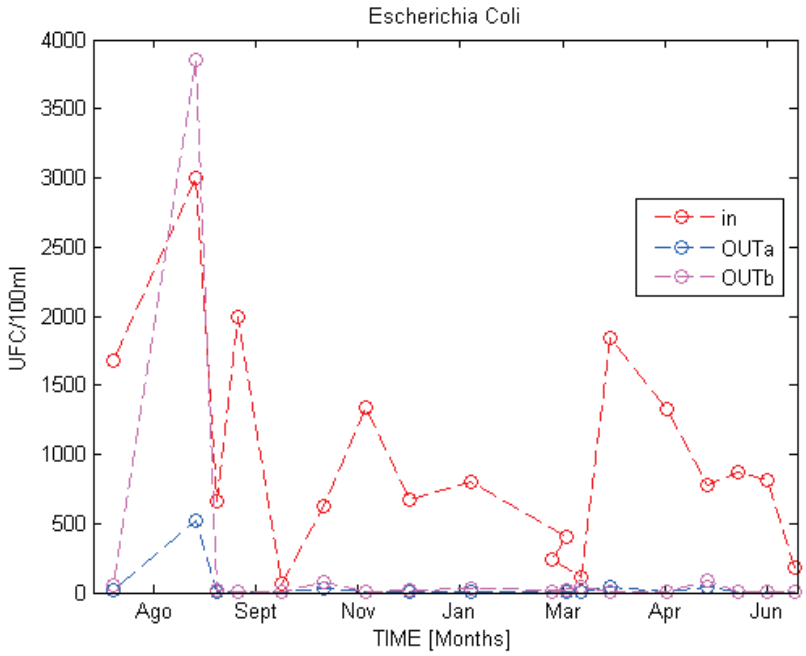

Figure 3.10: Inflow Escherichia Coli (red) compared with the outflow concentration of A basin (blue) and B basin (pink) measured between July 2011 and June 2012

Streptococci removal are the -100%[3] and 86.1% and for the A basin respectively, and the -121%[3] and 71.4% for the B basin respectively; the averages removal efficiencies of Faecal Coliform and Escherichia Coli are the 84% and 97.7% and for the A basin, and the 64% and 88% for B basin. The figures 3.6, 3.7, 3.8, 3.9, 3.10 listed below show the inflow and outflow (UFC/100 ml) of Clostridium, Total and Faecal Streptococci, Faecal Coliform and Escherichia Coli respectively. From the figures 3.6, 3.7, 3.9 and 3.10 is possible to observe that the calculation of percentage abatement and DEC are strongly influenced by a particular pathogens peak concentration, measured during the august 2011.

3.1.3 Temperature data

In order to have indications about the temperature dynamics in the wetland, I have used informations published by Tamburini (2010) in his thesis. He started his research work supported by DII during 2010. In this study, Tamburini, measured the temperature of the inflow and outflow wastewater in tank A and B (the latter was not planted during the 2010) putting them in relation with the average external air temperature (fig. 3.11). These informations could be very interesting in order to find a correlation between the inflow and outflow temperature of A and B tanks with the average external temperature.

3 A negative removal efficiency value means that pathogens production occurs into HSSF wetland tanks.

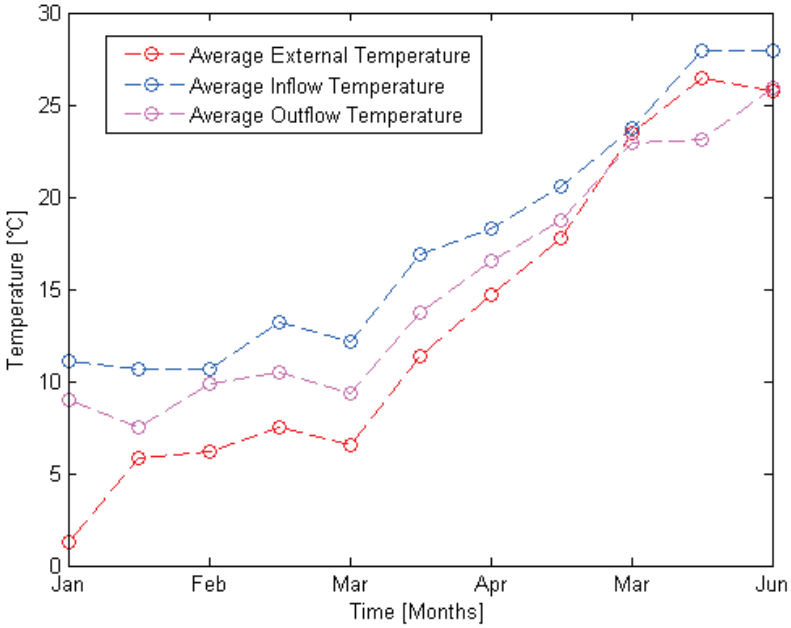

Figure 3.11: Tank A inflow wastewater Temperature (blue) and outflow one (pink) measured by Tamburini (2010) and related to the average external temperature (red)

3.2 The constructed wetland tanks hydraulics

The constructed wetland basins were fed using a pump which took the outflow sewage from the secondary treatment plants and loaded a cockpit from where the wastewater infiltrate into the basins. The pump was automatically activated for 15 minutes every hour and so for a total of 6 hours per day. The wastewater discharge occurred through a telescopic pipe into a pit; this system allows to control the water depth into the basins.

Aims of the hydraulics studies were: the calculation of hydraulics retention time; the knowledge of wastewater hydro-dynamics into the constructed wetland plants.

3.2.1 The calculation of hydraulics retention time

The hydraulic retention time was calculated with a tracer test using Rhodamine WT, a fluorescent tracer. The Rhodamine was injected instantaneously (in a very few seconds) near the wastewater injection point; the outflow fluorescent tracer concentration was measured with a special instruments used for this kind of experiments and properly calibrated. The temporal outflow concentration distribution was used to calculate the average hydraulics retention time of the constructed wetland basins.

The Rhodamine tracer test study was conducted three times: the first during July 2011 (from 18 July 2011 to 28 July 2011), the second between November and December 2011 (from 25

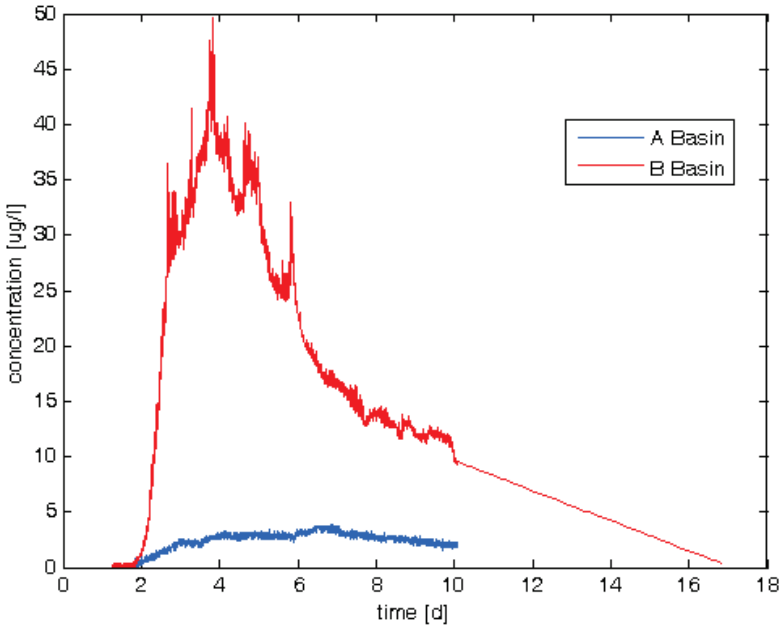

Figure 3. 12: Rhodamine residence time distribution in the A basin (blue) and B basin (red) measured during the July 2011

November 2011 to 12 December 2012) and the third between March and April 2012 (from 26 March 2012 to 6 April 2012); during the tests, the tracer was measured into several intermediate points, also, using piezometers in addition to wastewater outflow point. In the same period (when occurred the tracer test), a wastewater flow test was conducted in order to measure exactly the inflow wastewater flows and the outflow ones.

The first test was conducted injecting into both basins about 4.3 g of Rhodamine WT. The wastewater inflow and outflow trial occurred during five days (from 18 to 22 July 2011); these trials were conducted measuring the time need for inflow and outflow sewage to fill a container of 2.15 litres, the wastewater inflow test was repeated four times per day, twice when the pump was on (one in the morning and one in the evening) and twice when the pump was off (one in the morning and one in the evening), while the wastewater outflow test occurred only two times per day, one in the morning and one in the evening when the pump was off. From the first Rhodamine experiment two residence time distribution was produced, one for A basin and one for the B basin (fig. 3.12), and a hydraulics retention time of 6.2 days emerged for the A basin and a time of 4.5 days for the B basin; from the sewage flow trials it emerged an average wastewater inflow of 0.48 m^3/h for A basin and 0.43 m^3/h for B basin and an average wastewater outflow of 0.3 m^3/h for A basin and 0.27 m^3/h for B basin. It should be noted, however, that during the test, a failure in the pumping system, which interrupted the

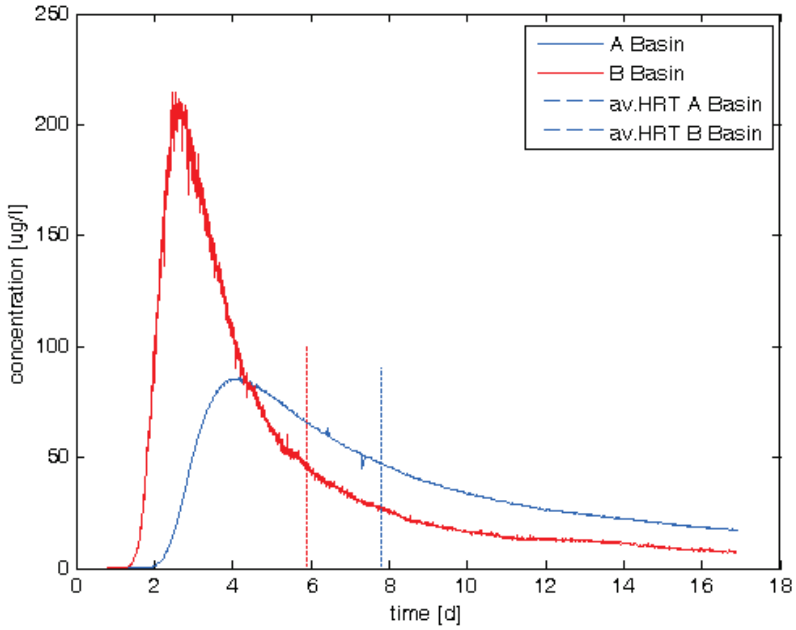

Figure 3.13: Rhodamine residence time distribution in the A basin (blue) and B basin (red) evaluated between November and December 2011

power supply for 12 hours, and a modest precipitation, have evidently changed residence times making the results less significant.

The second test was conducted injecting into both basins about 10.5 g of Rhodamine WT. The wastewater inflow trial occurred during five days (25, 28 November and 1, 6, 12 December) while the test to calculate the outflow wastewater occurred only on the 12 December; these trials were conducted measuring the time need for inflow and outflow sewage to fill a container of 2.15 litres and were repeated twice a day, one time when the pump was on (in the morning) and one time when the pump was off (in the evening); the test of wastewater outflow was conducted only one time when the pump was off.

From the experiments conducted between November and December 2011 it emerges a hydraulics retention time of 7.8 days for the A basin (fig. 3.13) and 5.3 days for the B basin (fig. 3.13); from the sewage flow trials it emerges an average wastewater inflow of 0.45 m^3/h for A basin and 0.54 m^3/h for B basin and an average wastewater outflow of 0.45 m^3/h for the A basin and 0.39 m^3/h for the B basin.

In the same used to conduct the second test, the third was characterized by the injection into both basins of about 10.5 g of Rhodamine WT. The wastewater inflow and outflow trial occurred during six days (from 26 March to 2 April 2012); differently by the precedent trials,

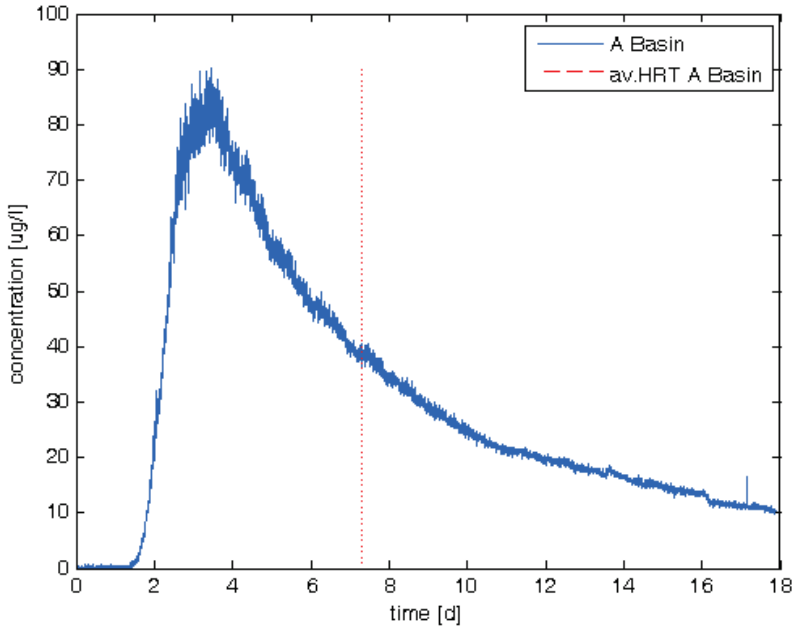

Figure 3.14: Rhodamine residence time distribution in the A basin (blue) evaluated between March and April 2012

these were conducted measuring the volume occupied by the wastewater after 15 seconds when the pump was on and after 30 second when the pump was off (the outflow wastewater were measured considering a time of 15 seconds only). The wastewater inflow and outflow test was repeated four times per day, twice when the pump was on (one in the morning and one in the evening) and twice when the pump was off (one in the morning and one in the evening). From the third experiment it emerged a hydraulics retention time of 7.3 days for the A basin (fig. 3.14) and 5.9 days for the B basin; from the wastewater flow trials it emerges an average wastewater inflow of 0.49 m^3/h for A basin and 0.51 m^3/h for B basin and an average wastewater outflow of 0.51 m^3/h for A basin and 0.32 m^3/h for B basin. However, it should be noted (fig. 3.14) that I do not have information useful to display the RTD curve for B tank.

3.2.2 The wastewater hydro-dynamics into the constructed wetland tanks

Another important test using the Rhodamine WT was conducted in order to understand the hydrodynamics within the constructed wetland tanks. The aim of this test was to verify the presence and location of zones with preferential flow or dead zones in the CW basins; the Rhodamine was injected near the inflow wastewater point and, after, its concentration was measured in several intermediate points using piezometers; the wastewater was sampled from piezometers using a pump characterized by a flow of about 90 litres per hour. Implementing

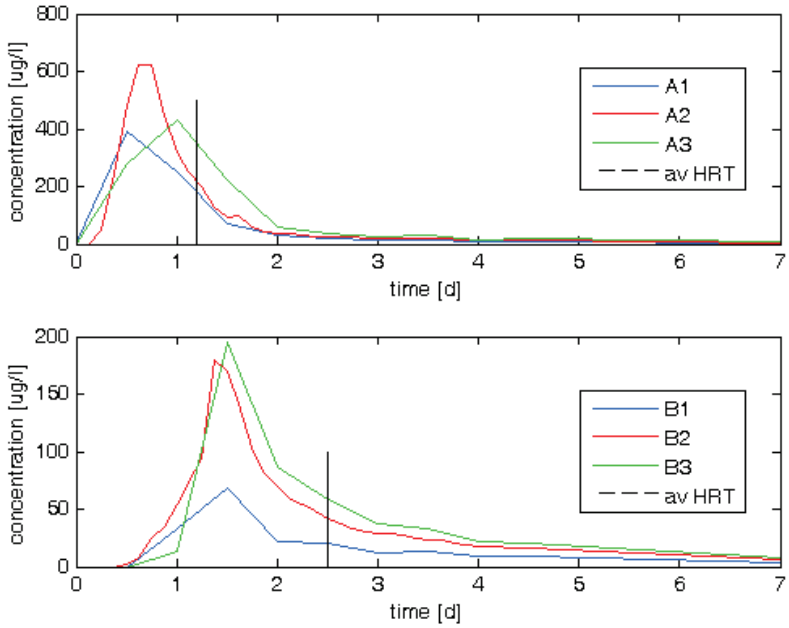

Figure 3.15: Rhodamine residence time distribution measured in the A and B transects of the B basin evaluated during July 2011

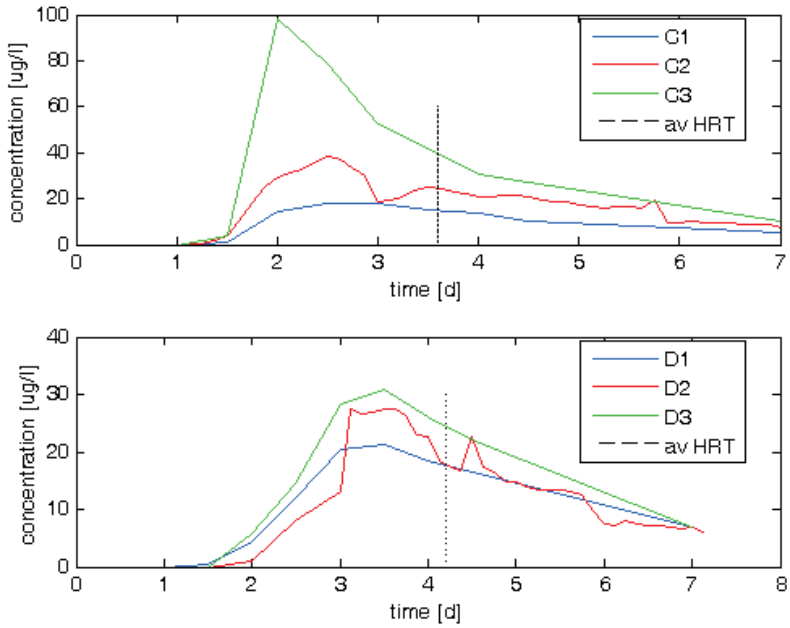

Figure 3.16: Rhodamine residence time distribution measured in the C and D transects of the B basin evaluated during July 2011

this trial, it was possible to build one residence time distribution for each measured point and so calculate the residence time for each point. The intermediate Rhodamine tracer test was conducted two times: one between 18 July 2011 and 25 July 2011 and the last between 26

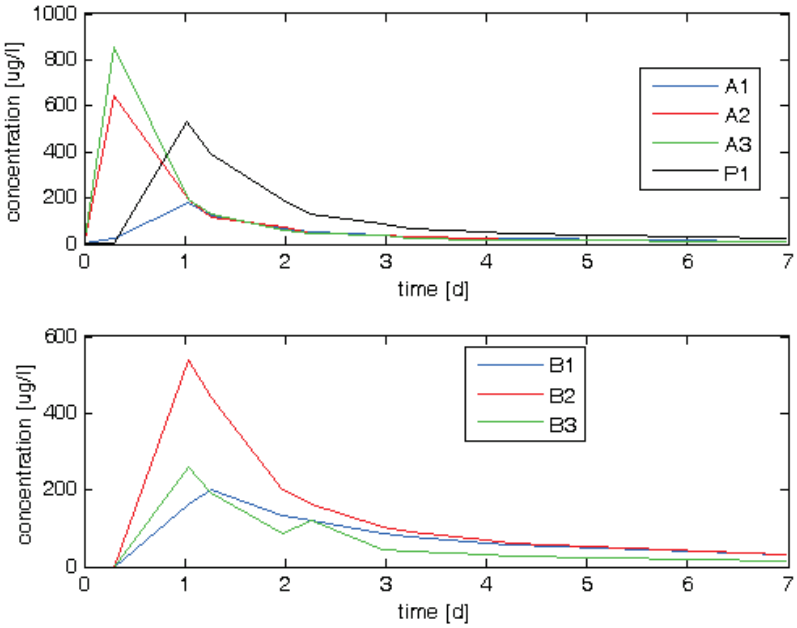

Figure 3.17: Rhodamine residence time distribution measured in the A, B and P1 transects of the A basin evaluated between March and April 2012

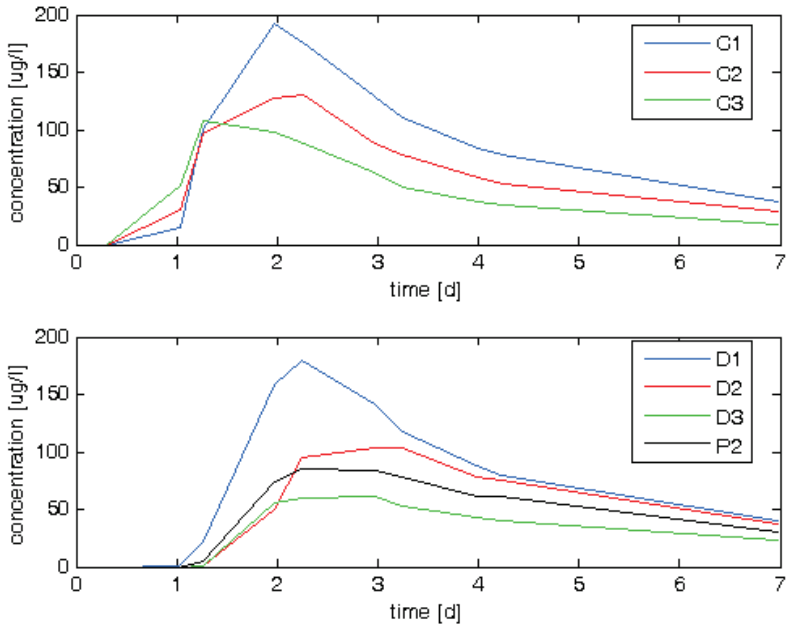

Figure 3.18: Rhodamine residence time distribution measured in the C, D and P2 transects of the A basin evaluated between March and April 2012

March 2012 and 2 April 2012. The intermediate Rhodamine trial, conducted during July 2011, was implemented only for the B basin. From the figures 3.15, 3.16 is possible to observe that, at the beginning, the wastewater tends to flow in the central part of the tank, in fact the

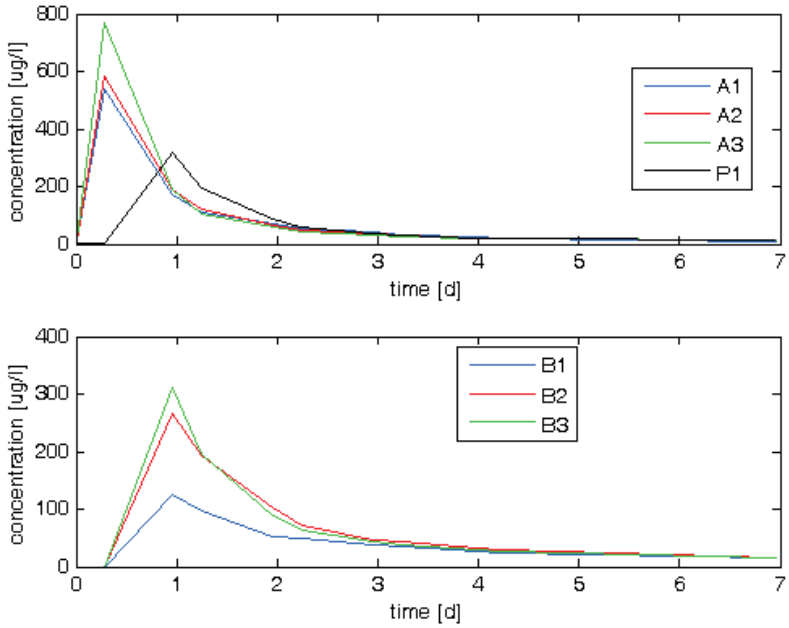

Figure 3.19: Rhodamine residence time distribution calculated in the A, B and P1 transects of the B basin evaluated between March and April 2012

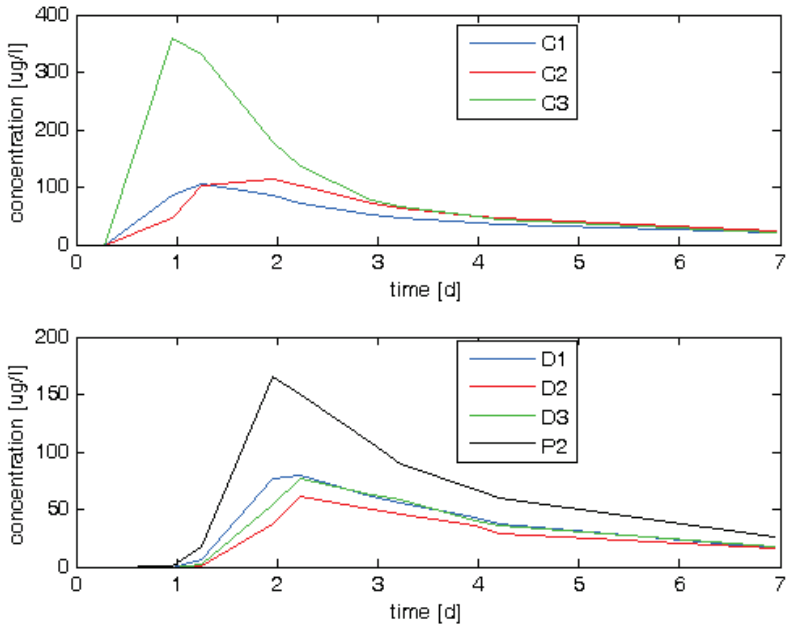

Figure 3.20: Rhodamine residence time distribution calculated in the C, D and P2 transects of the B basin evaluated between March and April 2012

piezometer A2 (fig. 2.5) has the highest concentration peak; after, it tends to flow the lateral areas of the wetland, the piezometer B3, C3 and D3 tend to have the highest peak (fig. 2.5). The average retention time to reach the A, B, C, D transects was 1.2, 2.5, 3.6 and 4.2 days

respectively (fig. 3.15, 3.16).

The test conducted between 26 March 2012 and 2 April 2012 was implemented for both basins. From the figures 3.17, 3.18 is possible to observe that in the tank A, at the beginning, the wastewater tends to flow laterally of the basin and the concentration is greater at 0.4 m from the surface than at 0.7 m, indeed the piezometer A3 (fig. 2.5) has the highest peak and the P1 (fig. 2.5) peak is lower than A2 and A3 piezometers (fig. 2.5); travelling towards the exit point, the wastewater tends to flow in the central part of the tank (the piezometer B2 has the highest peak) and afterwards it moves laterally again, but on the opposite side than the initial one (the piezometer C1 has the highest peak); at the end the sewage tends to continue to flow laterally and, also in this case, the concentration tends to flow greater at 0.4 m from the surface than at 0.7 m, in fact the piezometer D1 has the highest peak and the P2 peak is lower than D1 and D2 piezometers (fig. 3.17, 3.18).

The figures 3.19 and 3.20 show the Rhodamine dynamics into the B basin. Into the B basin, near the injection point, the wastewater tends to flow laterally of the basin and the rhodamine concentration tends to flow greater at 0.4 m from the surface than at 0.7 m, the piezometer A3 has the highest peak and the P1 peak is lower than A1, A2 and A3 piezometers; travelling towards the exit point, the wastewater tends to remain on the same side (the piezometer B3 and C3 have the highest peak); at the end it tends to flow uniformly in the whole wetland and the concentration tends to flow greater at 0.7 m from the surface than at 0.4 m (the piezometer D1, D3 and C3 have similar peak and the P2 piezometer has the highest peak).

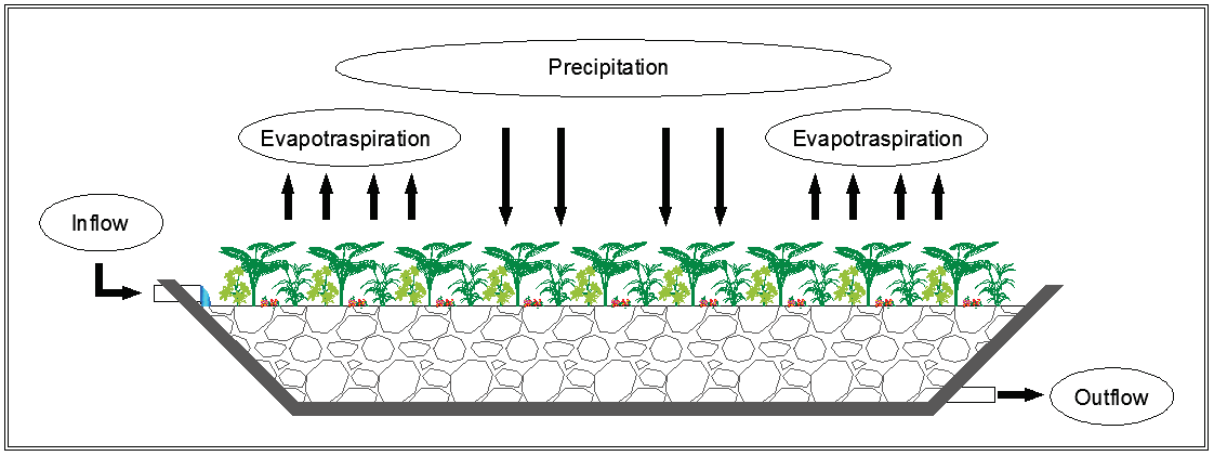

Figure 3.21: The hydro-geological model used in the models

3.3 The Hydraulic Mass Balance

The hydro-geological model (fig. 3.21) used to simulate the hydraulic mass balance into the

constructed wetland basins can be written as (1) (simplified respect the equation showed by kadlec et al. (1996)) :

$$\frac{dV}{dt} = Q_I - Q_{OUT} + P - ET \quad (1)$$

where: Q_I is the inflow wastewater [m^3/d]; Q_{OUT} is the outflow wastewater [m^3/d]; P is the water infiltrated due to the precipitation process [m^3/d]; ET is the water lost due to evapotranspiration [m^3/d].

The Precipitation and the inflow wastewater contribute to increase the water volume and water flow into the natural tanks (fig. 3.21) while the evapotranspiration phenomena and the outflow wastewater contribute to reduce the volume and water flow from the constructed wetlands basin (fig. 3.21). Wastewater losses from the bottom of CW tanks were not considered; the bottom liner was considered not permeable.

I have considered steady state conditions (2) in order to simplify the models; the variation of water volume into the constructed wetland tanks due to evapotranspiration, precipitation and water flow is negligible.

$$0 = Q_I - Q_{OUT} + P - ET \quad (2)$$

3.3.1 The inflow wastewater in tank A and B

The wastewater inflow data that I have considered in the models were chosen based on the hydraulic studies mentioned above. I have taken into account the second and the third Rhodamine tracer test in order to choose the wastewater inflow into the tank A and B and the average hydraulic retention time.

Table 3.2: Hydraulics information on the constructed wetland basins used in the models

	Tank A	Tank B
Wastewater Inflow (m^3/d)	11.28	12.6
Water Average Retention Time (d)	7.55	5.6
Water volume stored in tank (m^3)	85.164	70.56
Average Water flow velocity (m/d)	4.73	5.86
Average section wet area (m^2)	2.38	2.15

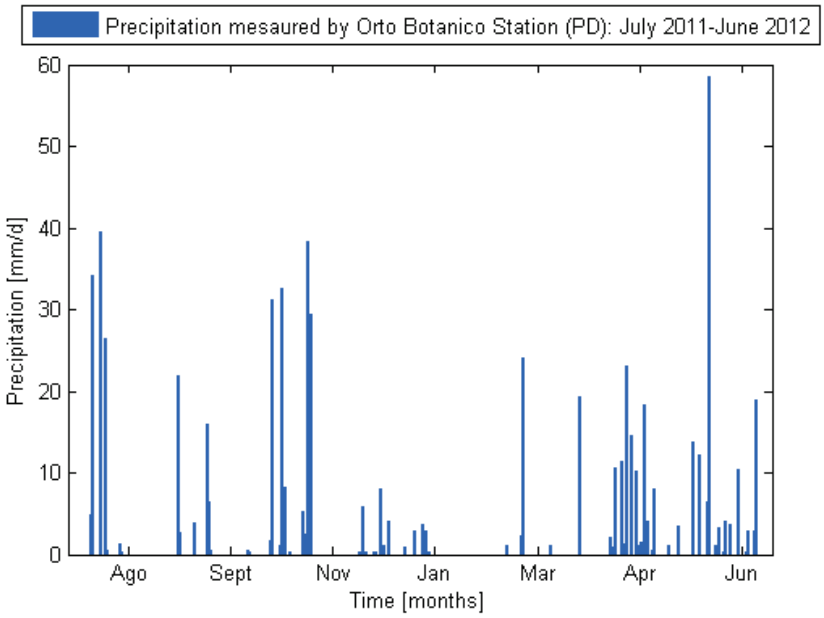

Figure 3.22: Daily precipitation intensity (mm/d) measured by Padova Orto Botanico weather station between July 2011 and June 2012

Based on the second and the third Rhodamine tracer tests I have chosen an inflow wastewater of 0.47 m^3/h for the tank A and 0.525 m^3/h for B basin and an average hydraulics retention time of 7.55 days for the tank A and 5.6 days for the tank B. Based on these assumptions emerges that the water volume stored into the basins is 85.164 m^3 into the tank A and 70.56 m^3 into the tank B while the average water velocity in basins, considering the basins length showed above and the respective average water retention time values, are 4.73 m/d in the A tank and 5.86 m/d in the B basin.

3.3.2 The water infiltration and precipitations

The water volume which enters into the system (P) due to precipitation phenomena during the sampling period, was calculated, and so simulated, taking into account the values of daily precipitation intensity, measured at Padova Orto Botanico weather station (data kindly provided by ARPAV-Servizio Meterologico), and considering the surface occupied by the constructed wetlands tanks (3):

$$P = \frac{I \cdot A}{1000} \tag{3}$$

where: I is the daily precipitation intensity [mm/d]; A is the area occupied by the constructed wetland basins [m^2].

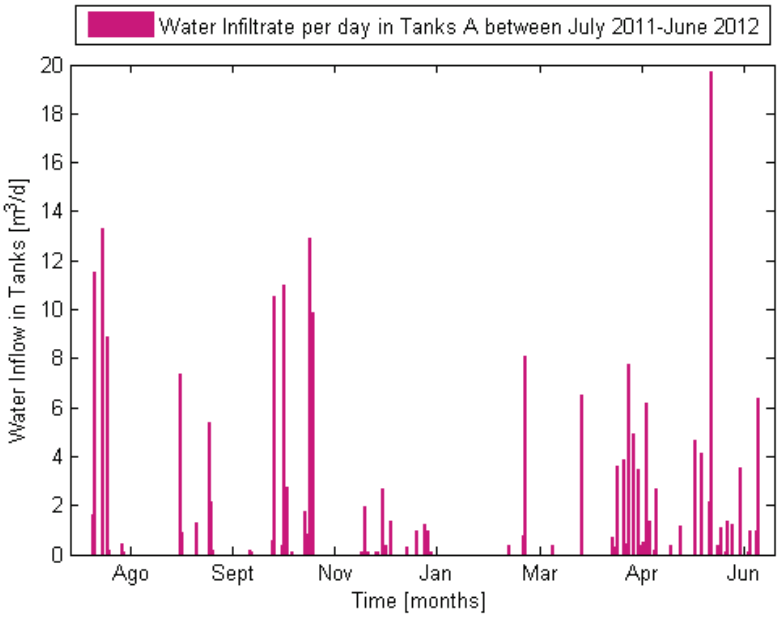

Figure 3.23: Daily water infiltrated (m^3/d) in tank A between July 2011 and June 2012 through rainfall

I have chosen the data collected by the Padova Orto Botanico weather station because it should represent in a good way the weather that occurred in the Vigonza area; the Padova Orto Botanico area is far from the Vigonza one only about 10 km, and furthermore no closer weather stations are present. Considering the surface of constructed wetland basins showed above and the daily precipitation intensity values (mm/d) (fig. 3.22), the wastewater flow

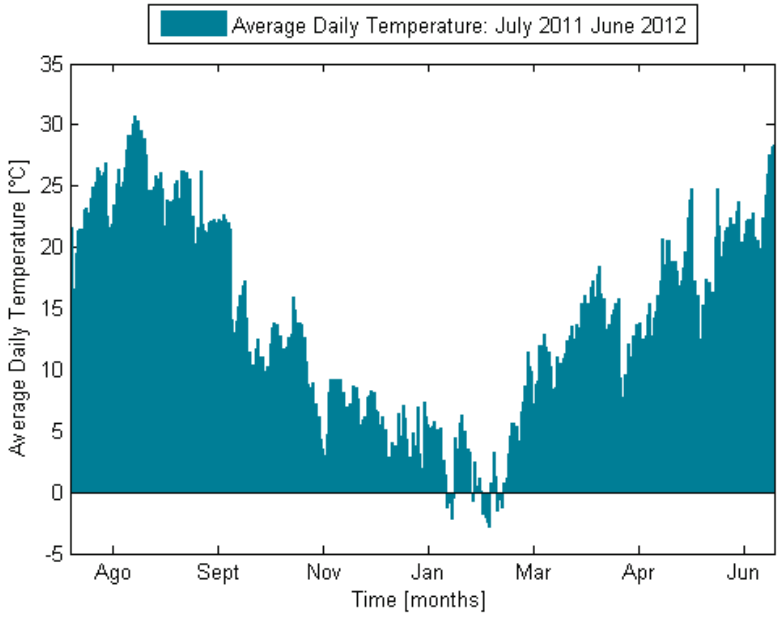

Figure 3.24: Average daily temperature measured by Padova Orto botanico weather station between July 2011 and June 2012

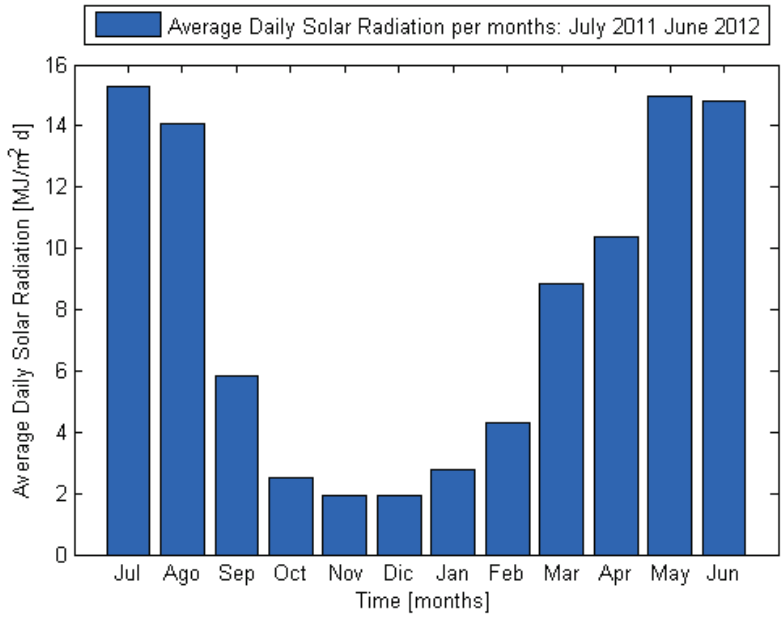

Figure 3.25: Daily average global radiation per months between July 2011 and June 2012 used for the calculation of evapotranspiration

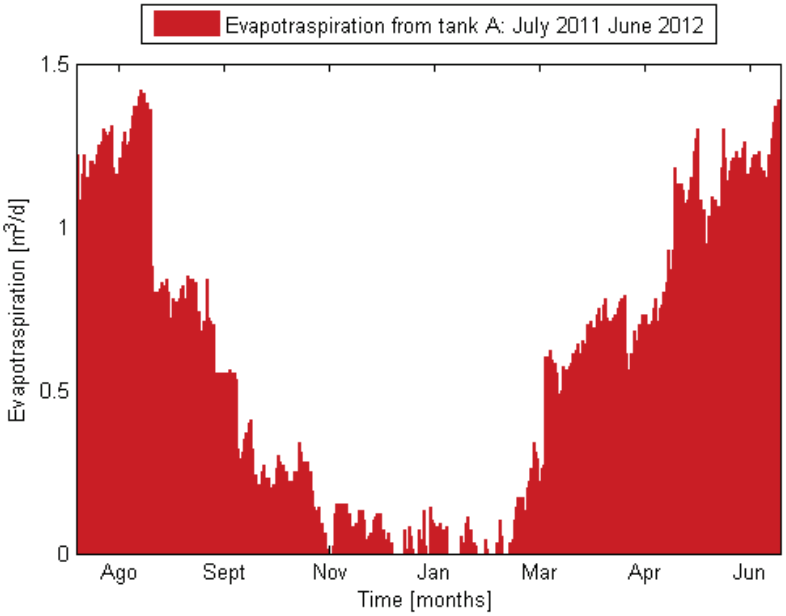

Figure 3.26: Water lost (m^3/d) from tank A between July 2011 and June 2012

(m^3/d) that entered in the constructed wetland basins through rainfall during the sampling period (July 2011-June 2012) is reported in the figure 3.23 (the figure 3.23 shows the water volume entered in the tanks A only; the inflow wastewater due to precipitation in the tank B is very similar to one that occurs in the tank A).

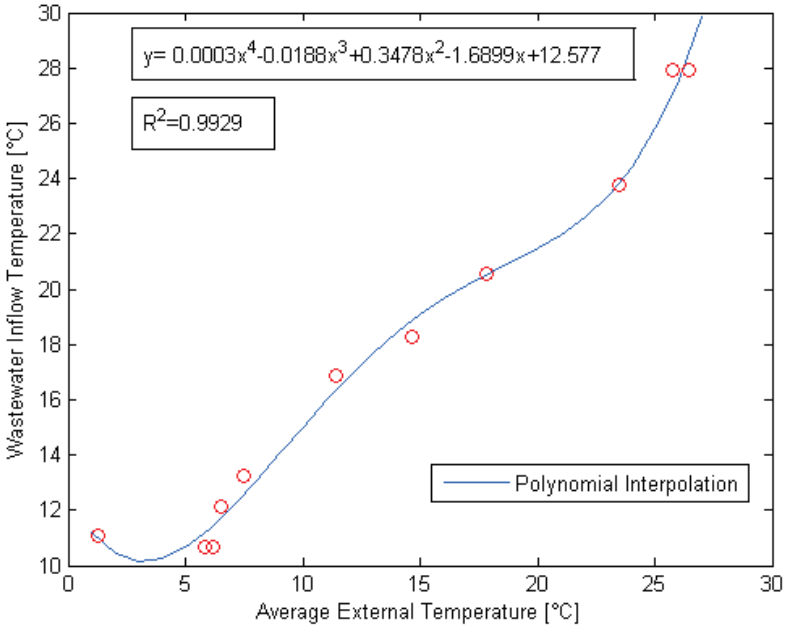

Figure 3.27: Polynomial relation between the average external temperature and the inflow wastewater temperature in tank A during 2010.

3.3.3 The Evapotranspiration

The evapotranspiration that occurred in the Vigonza area during the sampling period was calculated with the equation (4) (Alkaeed et al., 2006) and with it was calculated the total water which comes out of the tanks (5):

$$ET_o = -0.611 + 0.149R_s + 0.079T_{mean} \quad (4)$$

$$ET_T = \frac{ET_o \cdot A}{1000} \quad (5)$$

where: ET_o is the evapotraspiration [mm/d]; R_S is the short-wave solar radiation [MJ m^{-2} d^{-1}]; T_{mean} is the average daily temperature [°C], ET_T is evapotraspiration flux from constructed wetland tanks [m^3/d]; A is the tank surface area of constructed wetland basins [m^2].

The global evapotranspiration (fig. 3.26) was calculated considering the daily average temperature (fig. 3.24), calculated taking into account the instantaneous temperature measured by the Padova Orto Botanico weather station, the daily average global radiation (fig. 3.25), calculated knowing the total monthly global radiation measured by Padova Orto Botanico weather station too (Data kindly provided by ARPAV – Servizio Meteorologico).

3.4 The wastewater temperature used in the Models

I have built a relation between the average external air temperature and the inflow wastewater temperatture in tank A and a relation between the inflow wastewater temperature in tank A with the outflow one started from informations showed above (fig. 3.11). I have calculated these relation using a polynomial interpolation (fig. 3.27, 3.28). In this way by the knowledge of the average external temperature that occurred during the sampling period (2011/2012) I have been able to calculate and simulate the inflow and outflow wastewater temperature in tank A and B. The polynomial relation between the average external temperature of 2010 with the inflow wastewater in tank A is described by the (6), while the relation between the inflow and outflow wastewater temperature is described by the (7).

$$T_I = 0.003T_{av}^4 - 0.0188T_{av}^3 + 0.3478T_{av}^2 - 1.6899T_{av} + 12.577 \quad (6)$$

$$T_{OUT} = -0.0058T_I^3 + 0.3281T_I^2 - 4.789T_I + 29.619 \quad (7)$$

where: T_I is the inflow wastewater temperature [°C]; T_{OUT} is the outflow wastewater temperature [°C]; T_{av} is the average external temperature [°C].

3.5 The Reactor Models

The dynamics of the nitrogen compounds and microbiology into the constructed wetland basins was modelled taking into account three kind of reactor models: a continuous flow stirred tank reactor (CSTR) model, a continuous flow stirred tank reactor (CSTR) in series model and a plug and flow reactor (P&F) model with and without dead zones.

3.5.1 The CSRT Model and CSTR in series model

In a CSTR reactor (fig. 3.29) it is assumed that complete mixing occur instantaneously and that there are no concentration gradients transversely and longitudinally to water flow. In this kind of reactor the diffusion phenomena and the advection one are not considered. In this kind of reactor, the influent (QI) and effluent stream (Q) (fig. 3.29) bring with them solutes or particulates that enter and come out from the system, whose concentrations can change due to reactions that occur inside the tanks. The dynamics of concentration and the mass balance into a CSTR can be described by (8) (Tchobanoglous et al. 2014, Grady et al. 2011):

$$\frac{dC}{dt}V = Q_I C_o - Q_{OUT} C \pm kCV \quad (8)$$

where: Q_I is the inflow wastewater [L^3/T]; Q_{OUT} is the outflow wastewater [L^3/T]; V is the water volume stored into the basin [L^3]; C_o is the inflow concentration [ML^{-3}]; C is the outflow concentration equal to the concentration inside the reactor [ML^{-3}]; *k* is reaction constant [T^{-1}].

The models dependent on temperature that use a CSTR reactor were implemented considering the average of inflow and outflow wastewater temperature calculated as the average of (6) and (7).

In a CSTR in series model (fig. 3.30) the reactor is represented, ideally, as chain of a N CSTR tanks characterized each by a volume V and each by a particular residence time. This kind of reactor series model is used to describe some non-ideal flow that occur in the reality; a tank or a basin is not completely well mixed (Tchobanoglous et al. 2014) and is possible to observe a solute residence time distribution (RTD) with a bell shape. As Kadlec et al. (2008) show, the tanks in series flow model bridges the gap between the idealized extremes represented by the plug and flow and CSTR reactor models. A system that can be modelled with few CSTR in series has a behaviour similar to a CSTR, on contrary if a system could be described with a number of tanks that tend to infinity it behaves as a P&F reactor.

In a CSTR in series model, the upstream tank feeds the downstream one: the first tank, that at

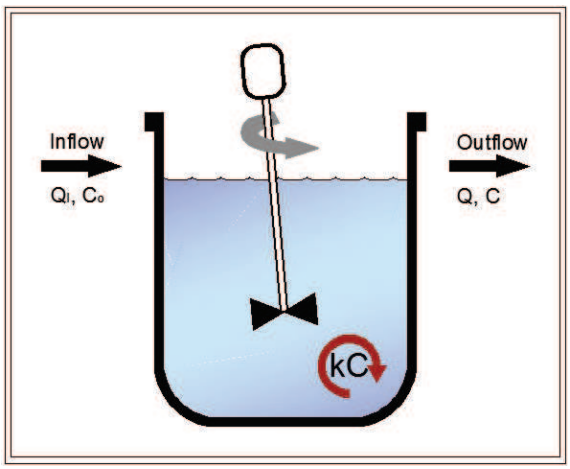

Figure 3.28: A CSRT Reactor representation

time 0 is characterized by a inflow Q_I and a solute concentration Co, produces as response the feed of a second tank that will be characterized by a inflow Q_I and a solute concentration C_1;

the response of second tank will be the feed of third tank (fig. 3.30) etc.

In order to understand the number N of tanks that could be representative of our system (the constructed wetland basins) and so the plug-flow grade I have used the relationship (9) (Dal Cin et al, 2002):

$$N = \frac{t_{mean}}{t_{mean} - t_p} \tag{9}$$

where: t_{mean} the average retention time of wastewater in the system [T]; t_P is the peak time [T] or the time passed from the injection of a tracer when is possible measured the peak concentration in the residence time distribution (RTD) curve of such tracer.

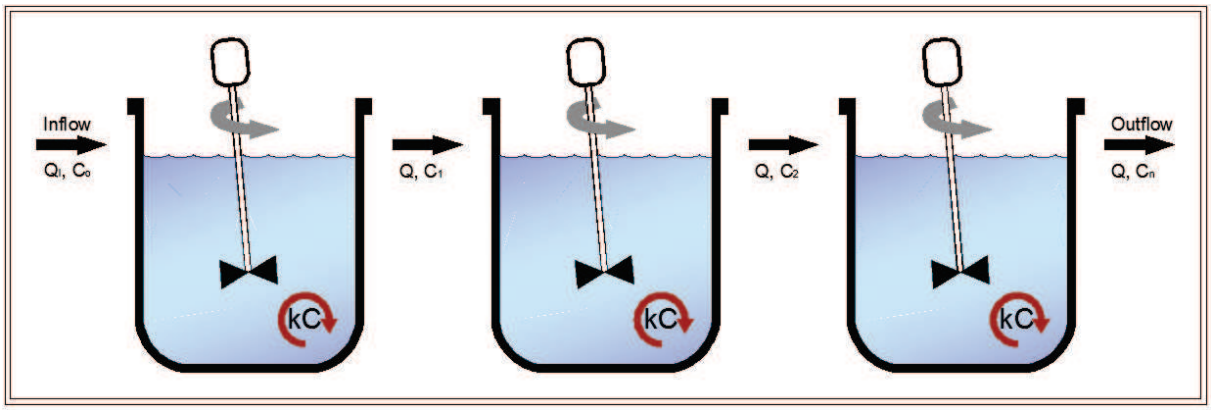

Figure 3. 29: A CSTR in series model

In order to calculate the number of tanks that could be representative for tank A, I have considered the RTD curve produced with the Rhodamine tracer tests conducted during the autumn 2011 and spring 2012; while to calculate the number of tanks that could be representative for tank B, I have considered the RTD curve formulated with the Rhodamine tracer conducted during the autumn 2011 only.

Table 3.3: Representative Number of CSTR tanks for A basin and B basin

	Tank A (2011)	Tank A (2012)	Tank B (2011)
Average residence time (d) t_{mean}	7.8	7.3	5.6
Peak time (d) t_P	4.17	3.45	2.54
Number of CSTR tank	2.14	1.9	1.93

By the knowledge of average wastewater residence time and the peak time, and applying (9) it

emerges (tab. 3.3) that both tanks could be represented with two tanks in series. I have described the solutes dynamics and mass balance in a CSTR in series model, characterized by two tanks, with a system of two equations (10) (11):

$$\frac{dC_1}{dt} V_1 = Q_I C_o - Q_1 C_1 \pm kCV_1 \quad (10)$$

$$\frac{dC}{dt} V_2 = Q_1 C_1 - Q_{OUT} C \pm kCV_2 \quad (11)$$

where: Q_I is the inflow wastewater in the system [L^3/T]; Q_1 is the outflow wastewater in the ideal tank 1 and the inflow one in tank 2 [L^3/T]; Q_{OUT} is the outflow wastewater from the system [L^3/T]; V_1 is the water volume stored into the first ideal basin [L^3]; V_2 is the water volume stored into the second ideal basins [L^3]; C_o is the inflow concentration [ML^{-3}]; C is the outflow concentration [ML^{-3}]; C_1 is the inflow concentration in the ideal second tank [ML^{-3}]; *k* is a reaction constant [T^{-1}].

In order to better simulate what occurs in nature, the models dependent on temperature using a CSTR in series reactor were implemented considering that in the hypothetical tank 1 the wastewater temperature is equal to the inflow one, as it is expressed by (6), while in the second hypothetical tank it was considered a wastewater temperature equal to the outflow one as is expressed by (7).

3.5.2 The Plug and Flow model with and without the dead zone

In a Plug and Flow reactor model it is assumed that the solute is optimally mixed transversely to the water flow and is not well mixed longitudinally; the solute is longitudinally dispersed a along the reactor during the water flow. The solute dispersion is a phenomenon that occurs due to the combination of molecular diffusion, turbulent diffusion and due to the traversal gradient velocity of a water flow in tanks. In a plug and flow reactor the solute is also subject to the advection phenomenon. The dynamics of concentration and mass balance could be described by (12) (Tchobanoglous et al. 2014, Grady et al. 2011):

$$\frac{dC}{dt} + \frac{Q_I}{A}\frac{dC}{dx} = D_c \frac{d^2C}{dx^2} \pm kC \quad (12)$$

where: Q_I is the inflow wastewater [L^3/T]; A is the cross-sectional area of water flow [L^2]; C is

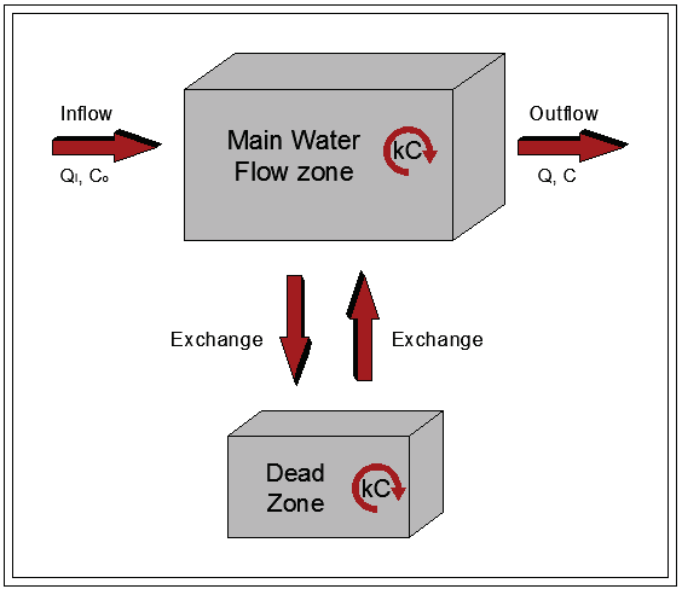

Figure 3.30: Conceptual model that describe the relations between the dead zone and the main water flow zone.

the concentration [ML^{-3}]; *k* is the reaction constant [T^{-1}]. D_C is the longitudinal dispersion coefficient [L^2T^{-1}].

The dispersion of a solute along a river or, in our case, in a porous media is influenced by the presence of dead zones or hyporheic zones. The dead zones are the part of a river or porous medium system where the solute tends to remain for a longer time before its output with respect to the solute in the main flow (fig. 3.31); every dead zone is characterized by a particular residence time distribution. The dead zone presence could influence strongly the global residence time distribution of a system.

The system of equations that is used to describes all processes that occur between a dead zone and the principal water flow area, in the case of a reactive solute, is (Runkel, 1998) (13)(14):

$$\frac{\partial C}{\partial t} + U\frac{\partial C}{\partial x} = D_L\frac{\partial^2 C}{\partial^2 x} + \alpha(C_s - C) \pm kC \qquad (13)$$

$$\frac{dC_s}{dt} = -\alpha\frac{A}{A_s}(C_s - C) \pm kC_S \qquad (14)$$

where C is the solute concentration of the stream [ML^{-3}], U is the mean flow velocity [LT^{-1}]; α is a transfer coefficient [T^{-1}], $A\backslash A_S$ is the ratio of stream to storage cross-sectional areas; C_S is the concentration of solute in the storage zone [ML^{-3}], D_L is the longitudinal dispersion coefficient for the flow in the main channel [L^2T^{-1}], and t is time [T].

3.6 Pathogens removal in constructed wetland plants

The pathogens removal in a wetland and a wetland-like systems (such as lagoons and stabilization ponds) is strictly influenced by several environmental factors.

Generally, the pathogens removal in a wetland depend on biotic and abiotic factors. The temperature for example is an important factor that influences the pathogens life; usually the greater is the temperature the higher is pathogens die-off (Stevik et al, 2004; Maynard et al, 1998). Other important abiotic factors that influence the pathogens removal are: light, dissolved oxygen on water/wastewater and pH. For example, Davis-Colley et al. (1998) that had studied the inactivation of faecal indicator microorganisms in waste stabilization ponds show that: the Escherichia coli and Enterococci inactivation is strongly influenced by the dissolved oxygen concentration (the greater is the dissolved oxygen in the system the higher is the inactivation of Escherichia coli and Enterococci), and by the pH of solution. Davis-Colley et al. (1998) show that E.coli inactivation occurs principally at low and high pH, and the inactivation of Enterococci is not strongly influenced by pH; finally, Colley et al. (1998) show that all faecal microorganisms inactivate when they are subjected principally to light-wave near the ultraviolet frequency.

The removal of pathogens is also influenced by biotic factors. Maynard et al. (1998), that have spoken about the removal processes of nutrients and pathogens in tertiary treatment lagoons, remind us that coliphages play an important role in E. coli removal from lagoons, that coliforms are unable to compete with other bacteria for nutrients and that predation and competition are extremely important in the removal of faecal coliforms.

An interesting review that gives us informations on pathogens retention and removal in porous media, and so, important to understand some processes in a HSSF wetland, is the one published by Stevik et al. (2004). In this work, Stevik et al. remind us that the porous media tend to be a retention and removal mechanism to pathogens; for example, the dominant mechanism for retention of bacteria is the adsorption, that can occur in porous media and biofilms, dependent on: physical factors such as the characteristics of porous media, presence of organic matter and biofilm, temperature and water flow velocity; chemical factors such pH; and microbiological factors such as hydro-phobicity or electrostatic charges on the cell surface. Another important process that influences the pathogens retention is straining: a mechanism that involves the physical blocking of movement through pores smaller than the

bacteria, dependent in the grain size of the porous media, bacterial cell size and shape, degree ofwater saturation and clogging of filter media.

3.6.1 Pathogens removal model: The First Order Kinetic Model

Usually, a first order kinetics model is used to describe the removal of pathogens (principally coliform, streptococci and escherichia coli) into a wetland or ponds (Mayo, 2004; Mayo et al, 2007; Von Spelling, 1998; Xu et al, 2002; Craggs et al, 2004; Cirelli et al, 2009; Hamaamin et al, 2014) coupling it a plug and flow model or a CSTR model or a dispersed flow model.

From the literature it emerges that several factors that influence the pathogens removal are, usually, taken into account in order to calculate the kinetic reaction or mortality rate (d^{-1}); Hamaamin et al. (2014) show that the first order kinetic can depend on the temperature, solar radiation and adsorption, filtration and sedimentation phenomena that occur in a constructed wetland basin (15) (16) (17) (18):

$$k = k_I + k_T + k_F \tag{15}$$

$$k_T = k_{T,20}\,\theta^{(t-20)} \tag{16}$$

$$k_I = \phi \cdot I_{avg} \tag{17}$$

$$k_F = \frac{4}{\pi} \cdot \eta \cdot \alpha \, \frac{u(1-\varphi)}{d} \tag{18}$$

where: k is the global first order kinetics value or mortality rate (d^{-1}); k_I is the mortality rate due to solar radiation (d^{-1}); k_T (d^{-1}) is the mortality rate due to temperature; k_F (d^{-1}) is the mortality rate due to the adsorption, filtration and sedimentation phenomena; k_{T_20} (d^{-1}) is the mortality rate at 20 °C; θ is a temperature-related coefficient; I_{avg} ($cal/m^2/d$) is the average solar radiation; η is the single collector removal efficiency; α is the sticking efficiency; u is the flow velocity (m/d); d is the collector diameter (m); φ porosity of wetland bed.

Mayo et al. (2007) use a first order kinetics depending on: environmental parameters such as temperature, pH, dissolved oxygen (DO) and solar radiation; a mortality rate due to the sedimentation processes that occur into the wetland; a mortality rate due to the adsorption on plant biofilm or due to the attachment of bacteria on the plants.

3.6.2 The models implemented to describe the Pathogens removal

Based on what published by literature, and based on data and informations that I have, in order to describe and predict the microbiological removal and retention in the HSSF wetland, I will use a first order kinetic model: a first order kinetic model with a global mortality rate that will depend on temperature (19) and a first order kinetic model with a global mortality rate that will not be depend on temperature (20). The first order kinetic model for pathogens removal will be implemented in a CSTR model, CSTR in series model and in a P&F model.

$$r_{pathogens} = k_{pathogens,20}\,\theta^{(t-20)}\,P \tag{19}$$

$$r_{pathogens} = k_{pathogens}\,P \tag{20}$$

where: $r_{pathogens}$ = is the pathogens removal rate (g/m^3 d); $k_{pathogens,20}$ is the pathogens mortality rate at 20 °C (d^{-1}); θ temperature coefficient (Arrhenius); $k_{pathogens}$ is the pathogens mortality rate not dependent on temperature (d^{-1}); P pathogen concentration in the constructed wetland tanks (g/m^3).

3.7 The Nitrogen dynamics in wetlands

The most important inorganic forms of nitrogen in wetlands are: ammonium (NH_4^+), nitrite (NO^{2-}) and nitrate (NO^{3-}). Gaseous nitrogen may exist as dinitrogen (N_2), nitrous oxide(N_2O), nitric oxide (NO_2 and N_2O_4) and ammonia (NH_3).

Into a wetland, the nitrates, the ammonia and the nitrogen compounds are assimilated by microorganisms and plants, which transform them into particulate nitrogen (PN) which is then subjected to the decomposition and sedimentation processes. The sedimentation and burial participate in the retention and removal of nitrogen compounds from the water column and could be a way to remove the nitrogen in the long-term. During the decomposition process, that is characterized principally by the hydrolysis, there is the production of dissolved organic nitrogen (DON). After, the DON is principally subjected to the mineralization processes with the production of ammonium (NH_4^+).

The ammonia nitrogen can be affected by volatilization process, assimilation by plants and microorganisms, by nitrification processes, by adsorption on porous media and by anaerobic oxidation (ANAMMOX). During the volatilization, the ammonium (NH_4^+) is transformed in ammonia that diffuses in the atmosphere; the reaction that produces ammonia depends

principally by the pH of solution and by the temperature. Another important process that participates to the transformation of nitrogen compounds from wetlands is the anaerobic ammonia oxidation; under reducing condition, ammonium reacts with nitrite and/or nitrate to form gaseous nitrogen (N_2) that diffuses in the atmosphere. The nitrification process is a mechanism that leads to the production of nitrite and, after, nitrate operated by several microorganisms which use the ammonia such electron acceptor in the absence of oxygen under reducing conditions. An important process that participates to the retention of ammonia in the wetland system is the adsorption process: in fact this cation could be exchanged with the detritus, inorganic media and soil present in the wetland or chemisorbed by humic substance; the ammonia adsorption such as the phosphorus one is strongly influenced by temperature, pH and variation of concentration on the water phase.

The nitrite and nitrate are interested by denitrification processes and assimilation by plants and microorganisms and, as explained above, can participate to ANAMMOX process. The denitrification process as well as the ammonium volatilization contribute to the removal of nitrogen to the wetland system. The denitrification process is operated by microorganisms and leads to production of elemental nitrogen gas using the nitrite and nitrate such electron acceptor under reducing conditions.

The ammonium and nitrate compounds are the only plants available nitrogen forms, are used by plants such nutrient for their growth; in this way, inorganic nitrogen compounds are transformed in organic forms, the particulate one. The nitrogen plant uptake process and the absorbing rate varies with the season, the cycle of the plant (germination, growth period, senescence) and the species. part of nitrogen assimilated will be removed definitely only with the harvesting; the nitrogen uptaken by plants if harvesting does not occur, will tend to sediment or decompose in a cyclic way.

The nitrogen can enter in the wetland system, in solution with the rain (nitrates) or thanks to some processes such as the fixation that consists on the conversion of nitrogen gas to ammonia by some microorganism that live in the soils or in symbiosis with the plants root. In wetland soils, biological N_2 fixation may occur in the floodwater, on the soil surface, in aerobic and anaerobic flooded soils, in the root zone of plants, and on the leaf and stem surfaces of plants.

3.7.1 The Nitrogen cycle in a HSSF wetland

The nitrogen cycle in a HSSF constructed wetland, is strongly influenced by its hydraulics and design. In a HSSF basin, the volatilization process does not influence the nitrogen removal from the system (Vymazal et al, 2007).

In an artificial constructed wetland, and in particular, in a HSSF basin, the sedimentation and burial processes are strongly limited: the sedimentation and re-suspension (and so the burial taking into account a long time period) phenomena are strictly influenced by the media that composes the constructed wetlands basin.

Vyzmal (2007) remind us that in a HSSF constructed wetland that is characterized principally by reducing conditions, an important nitrogen removal process is the denitrification processes that is characterized by an important magnitude.

In a SSF constructed wetlands, the necromass (plant detritus) does not return in the water column but is deposited on the top of wetland bed that could be unsaturated, partially saturated or intermittent saturated (Kadlec et al, 2008); for these reasons, the degradation and decay of detritus tends to be slower than the ones that could occur in natural or FWS wetlands.

3.7.2 The models implemented to describe the Nitrogen removal

In order to describe the Nitrogen removal in the constructed wetland tanks I have compared, totally, three kind of models:

- (model n°1) a first order kinetic model that describes the dynamic of total dissolved nitrogen;
- (model n°2) a model that describe the nitrogen removal taking into account of the dynamics of DON, NH_4 and NO_3 separately using a first order kinetic model;
- (model n°3) a model that describe the nitrogen removal taking into account the dynamics of DON, NH_4 and NO_3 using saturation kinetic constants (Monod Kinetics), to describe the nitrification and the uptake process, and a first order model (to describe the mineralization, the denitrification an other processes).

The model n°1 was implemented using a CSTR model, CSTR in series model, in a P&F model and in a P&F model with dead zone; the first order kinetics used depended by temperature (21):

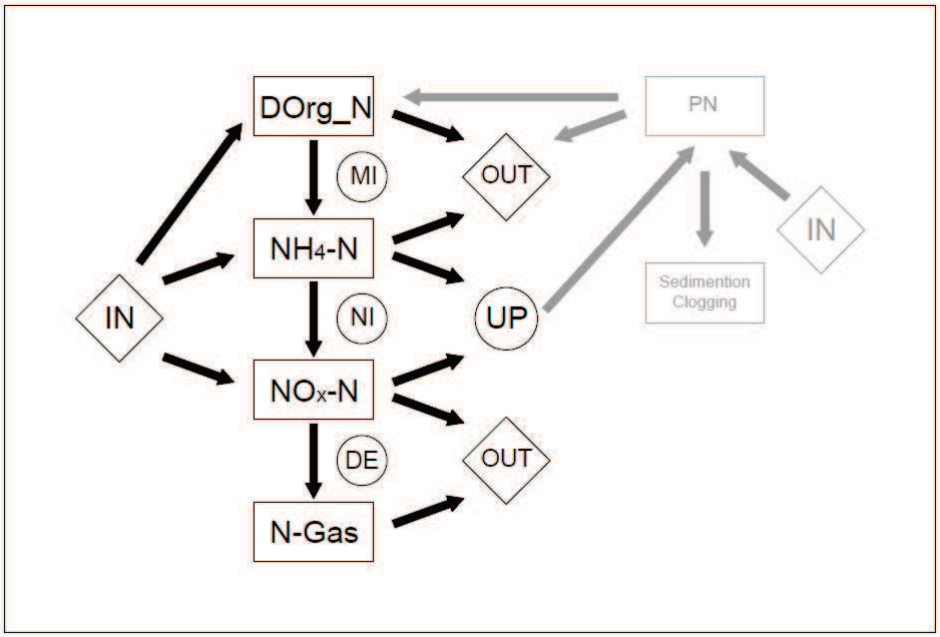

Figure 3.31: The conceptual model built for describe the dissolved N dynamics into a HSSF constructed wetland: conceptual model n°3

$$r_{TN} = k_{N,20}\theta^{(T-20)}TN \quad (21)$$

where: r_{TN} = is the total nitrogen removal rate (g/m^3 d^{-1}); $k_{N,20}$ is the total nitrogen removal rate at 20 °C (d^{-1}); θ temperature coefficient (Arrhenius); T is the wastewater temperature; TN is the total nitrogen concentration (g/m^3).

3.7.2.1 The Nitrogen removal models number 2 and 3

The dynamics of DON, NH_4 and NO_3 used in the models n° 2 and 3 are showed in the figure 3.32. I have built this conceptual model taking into account the nitrogen cycle in wetlands. The dissolved organic nitrogen entered and produced in the system, starting from the degradation of particulate organic nitrogen, is subjected to the mineralization processes forming ammonium. The ammonium will be transformed to nitrate by the denitrification process and absorbed by microorganisms and plants, no volatilization will occur. The nitrates entered and produced in the system will be subjected to denitrification processes and will be used by plants and microorganisms to growth.

In the model n° 2 all processes (mineralization, nitrification, denitrification and the absorption by plant and microorganism) were modelled using a first order kinetics depending by temperature at the same way described above (21); while in the model n°3 the nitrification (22) (Hence et al, 2008), and the uptake by plant and microorganism (25) (26) was described

using Monod kinetics; the denitrification process was modelled with a first order kinetic (Hence et al, 2008; Tchobanoglous et al. 2014).

$$r_n = k_{oxidation}\theta^{(T-20)}\frac{NH4}{K_N + NH4} \tag{22}$$

$$K_N = 10^{(0.51T-1.158)} \tag{23}$$

$$r_D = k_{D,20}\theta^{(T-20)}NO_3 \tag{24}$$

$$r_U = k_{AMM}\theta^{(T-20)}\frac{NH_4}{K_{NH_4} + NH_4} \tag{25}$$

$$r_{NO3} = k_{Nitr}\theta^{(T-20)}\frac{NO_3}{K_{NO_3} + NO_3} \tag{26}$$

where: r_n is the nitrification rate (g/m^3 d^{-1}); r_D is the denitrification rate (g/m^3 d^{-1}); r_U is the ammonia uptake rate (g/m^3 d^{-1}) by plants and bacteria; r_{NO3} is the nitrates uptake rate (g/m^3 d^{-1}) by plants and bacteria; $k_{oxidation}$ is the nitrification rate at 20 °C (d^{-1}); K_N is ammonia oxidation half saturation constant for nitrosomonaas (g/m^3) which is temperature dependnt (Senzia et al. 2002); K_{NO3} is ammonia oxidation half saturation constant (g/m^3); K_{NH4} is ammonia oxidation half saturation constant (g/m^3); $k_{D,20}$ is the denitrification kinetic at 20 °C (d^{-1}); k_{AMM} is the ammonium uptake rate at 20 °C (d^{-1}); k_{NO3} is the nitrate uptake rate at 20 °C (d^{-1}); θ temperature coefficient (Arrhenius); T is the wastewater temperature. The model that I implemented will describe only the dynamics of dissolved organic nitrogen, ammonium and nitrates because I have not informations about the dynamic of particulate organic nitrogen in the constructed wetland basins system.

3.8 Models Implementation

The model implementation started from the choice of periods useful to build and to validate it. This choice was made by: searching for intercept periods of the year characterized by more than one season and searching to have a number of observations that would have guaranteed a good model calibration. It is very important to say that a total of 18 observations are relatively few to support the construction of complex models.

After the mathematical formulation of models, that was described above, they were written

and implemented using Matlab software, and after the models construction and after a first evaluation, using the different coefficients described in the following (Chap. 3.9), the calibration and a sensitivity analysis of parameters calibrated in the models were made.

The models validation was the last step; during the validation, the models implemented were run using the coefficients (Chap. 3.9) found during calibration.

3.8.1 Periods and number of observations used to build and validate the models

An average (over both tanks) of 10 observations measured between the 23 November 2011 and the 20 June 2012 were used to implement the models used to simulate nitrogen dynamics (tab. 3.4) into the tank A and B, while 6 observations collected between 22 July 2011 and November 2011 were chosen for its validation in both tanks (tab. 3.4).

For the implementation of the first order kinetic model, describing the dynamics of Clostridium in both tanks, an average of 8 observations measured between the February 2011 and June 2012 were used and about an average 6 observations between July and December 2012 were used its validation (tab. 3.4).

An average of 10 observations measured between the 23 January 2011 and the 20 June 2012 were used to implement the first order kinetic model used to simulate dynamics of Total and Faecal Streptococci, Coliform and Escherichia Coli (tab. 3.4) in the tank A and B, while 6/7 observations collected between 22 July 2011 and December 2011 were chosen for them validation (tab. 3.4).

Table 3.4: Periods of the year and observations used to implement and validate the models in tank A and B

	Implementation				Validation			
	Tank		Observations		Tank		Observations	
	A	B	A	B	A	B	A	B
Nitrogen Compounds	23/11/11-20/06/12	23/11/11-20/06/12	11	10	22/07/11-02/11/11	22/07/11-02/11/11	6	6
Clostridium	29/01/12-20/06/12	13/01/12-06/06/12	9	7	22/07/11-14/12/11	22/07/11-14/12/11	5	5
Total Streptococci	13/01/12-20/06/12	13/01/12-20/06/12	10	9	22/07/11-14/12/11	22/07/11-14/12/11	6	5
Coliform	13/01/12-20/06/12	13/01/12-20/06/12	10	10	22/07/11-14/12/11	11/09/11-14/12/11	7	6
Escherichia Coli	13/01/12-20/06/12	13/01/12-20/06/12	10	10	22/07/11-14/12/11	22/07/11-14/12/11	7	7

3.8.2 The Calibration and the Sensitivity Analysis

Globally, the first-order kinetic models using a CSTR and a CSTR in series reactor has been used for the calibration of 2 parameters (tab. 3.5): the kinetics at 20 °C and the Arrhenius constants; four parameters and six parameters were calibrated in the first-order kinetic models implemented with a P&F reactor with and without dead zones respectively (tab. 3.5): the kinetics at 20 °C, the Arrhenius constants, the dispersion coefficients, the flux sectional area, the exchange rate (P&F with dead zone model) and the area ratio (P&F with dead zone model); four kinetics at 20 °C and four Arrhenius constants were calibrated in the nitrogen removal model n°2 while a maximum of 10 parameters were calibrated in the nitrogen removal model n°3 (tab. 3.5).

The calibration was made considering the Residual sum of square value (RSS) (27):

$$RSS = \sum_{(t=1)}^{T} \left(Q_o - Q_M\right)^2 \tag{27}$$

where: Q_o is the value of observed data; Q_M is the value of modelled data.

Table 3.5: Kind and number of parameters calibrated per models

	Parameter Calibrated	***Kind of Parameters***
First-order kinetic model		
CSTR-CSTRs	2	Kinetics at 20°C, Arrhenius Constants
Plug and Flow	4	Kinetics at 20°C, Arrhenius Constants, Dispersion Coefficient, Section Area
P&F with dead zone	6	Kinetics at 20°C, Arrhenius Constants, Dispersion Coefficient, Section Area, Ex. Rate and Area ratio
Nitrogen removal models		
Model n°2	9	Kinetics at 20°C, Arrhenius Constants
Model n°3	Max 10	Kinetics at 20°C, Arrhenius Constants

The Sensitivity Analysis was conducted by observing the behaviour of the models that occurs changing some of the parameters values. In particular it was observed the response considering, on average, a variation of 10% of Arrhenius constants and a variation of 30% of kinetics rates. It was estimated the Condition Number (28) for each parameter, which is an indicator of sensitivity:

$$CN = \frac{\left|S - S_c\right| / S}{\left|P - P_c\right| / P} \tag{28}$$

where: S is the value of the modelled state variable; S_c is the value of the modelled state

variable with the changed parameter; P is the value of parameter; P_c is the value of changed parameter.

3.9 Models evaluation

Three kind of indicators were used to evaluate the performance of the models implemented and validated: the Nash-Sutcliffe Efficiency Coefficient; the Roots Mean Square Error (RMSE) and the Akaike's information criterion (AIC).

The Nash Sutcliffe efficiency (NASH) (29) is a measure that gives information of how well the model fits the observed data and so, describes how well the observed data are simulated by the model. It can range from negative values to 1.

$$NASH = 1 - \frac{\sum_{(t=1)}^{T} (Q_o - Q_M)^2}{\sum_{(t=1)}^{T} (Q_o - Q_A)^2} \tag{29}$$

where: Q_o is the value of observed data; Q_M is the value of modelled data; Q_A is the value of average of modelled data.

If Nash parameter tends to 1, the modelled data fits perfectly the observed ones and if it is below 0 the model does not describe in a good way the observations.

The roots mean square error is another parameter used to evaluate the models performance; the RMSE ranges from 0 to $+\infty$. If RMSE is 0 the model fits perfectly the observed data. It is calculated as the square root of the mean of the squared differences between measured data and modelled ones (30):

$$RMSE = \sqrt{\frac{\sum_{(t=1)}^{T} (Q_o - Q_M)^2}{n}} \tag{30}$$

where: Q_o is the value of observed data; Q_M is the value of modelled data; n is the number of observation in the model.

The Akaike's Information Criterion permits to evaluate models based on its capacity to describe the observed data and based on its complexity. The complexity of a model depend on the parameters that are used in it: the greater is the number of parameters used in the model to describe a phenomena the greater is the model complexity. Comparing several models, used to describe the same phenomenon, the best is one that is characterized by the lowest AIC

coefficient, i.e. by a good compromise between simplicity and goodness of fit. The AIC coefficient was calculated by the (31):

$$AIC = n\log\frac{RSS}{n} + 2k \tag{31}$$

where: RSS is the residual sum of square; n is the number of observations in the model; k is the number of parameter used in the model and (in my case) the calibrated parameters ones.

4. RESULTS

4.1 The first order kinetics models for total dissolved nitrogen dynamics

After the calibration (tab. 4.1) it emerges that all the first order kinetics models were capable in a good way to describe the total nitrogen dynamics in both constructed wetland tanks (fig. 4.1, 4.2, Annex 1); the calculated Nash-Sutcliffe coefficients range between 0.4 and 0.64 and the RMSE is comprised between 0.66 g/m^3 and 0.77 g/m^3 (fig. 4.1, 4.2).

Table 4.1: Total nitrogen reaction rate (k), Arrhenius Constants (theta), Wet Area (A), Dispersion Coefficients (D), Wet/Dead zone areas ratio (Ar) and Exchange rate (a) after calibration

Reactor Model	Paramenter Calibrated	Tank A	Tank B	Units
CSTR model	Nitrogen Removal rate (k)	0.3115 (26.7*)	0.7486 (57.29*)	d^{-1} (m/yr)
	Arrhenius Constant (theta)	1.1759	1.2	
CSTR model in series	Nitrogen Removal rate (kS)	0.2269 (19.45*)	0.4894 (37.45*)	d^{-1} (m/yr)
	Arrhenius Constant (theta_S)	1.1523	1.185	
Plug and Flow model	Nitrogen Removal rate (k)	0.1394 (11.95*)	0.4699 (35.96*)	d^{-1} (m/yr)
	Arrhenius Constant (theta)	1.1119	1.2	
	Wet Area (A)	2.3956	2.1343	m^2
	Dispersion Coefficient (D)	0.505	0.2384	m^2/s
Plug and Flow model with dead zone	Nitrogen Removal rate (k)	0.1514 (12.98*)	0.4913 (37.6*)	d^{-1} (m/yr)
	Arrhenius Constant (theta)	1.1269	1.2	
	Wet Area (A)	2.3782	2.1974	m^2
	Dispersion Coefficient (D)	0.6076	0.4397	m^2/s
	Wet/Dead Zone area ratio (Ar)	240	200	
	Exchange rate (a)	7.06E-07	9.99E-04	d^{-1}

The calibration (tab. 4.1) shows similar total nitrogen reaction rates for each tank, with the same magnitude: comprised between 0.13 d^{-1} (11.95* m/yr) and 0.31 d^{-1} (26.7* m/yr) in tank A and 0.47 d^{-1} (35.96* m/yr) and 0.75 d^{-1} (57.29* m/yr) in tank B. These values were similar than

* The relationship between the first-order total nitrogen kinetics removal rate k_{TN} (d^{-1}) and the area-based first-order total nitrogen reduction rate k_{ATN} (m/yr), used to convert both values, is (Kadlec et al. 1996):

$$\frac{k_{ATN}}{q} = k_{TN} * \tau \quad \text{with} \quad q = \frac{Q}{A}$$

where: q hydraulic loading rate (L/T); τ = wastewater detention time (T); Q = wastewater flow in HSSF tank (L^3/T); A is the wetland surface area (L^2).

the ones showed by literature: Kadlec et al. (1996), based mostly on North American SSF wetlands, show an area-based TN first order kinetics comprised between 3.73 (m/yr) and 36.79 (m/yr); Vymazal et al. (2008) show, in their book, an area-based TN first order kinetics of 12 (m/yr) for municipal wastewater, 149 (m/yr) for agricultural wastewater; Vymazal et al. (1998), in others studies, suggest for design an HSSF tank an area-based TN first order kinetics comprises between 12 (m/yr) and 20 (m/yr). Trang et al. (2010), in a study that investigate on role of the hydraulic load rate on pollutant removal in HSSF wetlands, show a TN area-based kinetic removal rate that ranges from 12 and 24 (m/yr).

The CSTR and CSTRs models have better described the nitrogen removal: these model were characterized by slightly higher Nash-Sutcliffe coefficients (an average of 0.58 for tank A and 0.64 for tank B) and by a lower RMSE (average 0.66 g/m^3 for tank A and 0.64 g/m^3 for tank B) than P&F and P&F with dead zone models that, on contrary, were characterized by an average Nash-Sutcliffe coefficient of 0.43 for tank A and 0.55 for tank B and by an average RMSE of 0.77 g/m^3 for tank A and 0.71 g/m^3 for tank B (fig. 4.1, 4.2).

In the validation, it emerges, globally, a decrease of the Nash-Sutcliffe coefficient (except for the P&F and P&F with dead zone models in tank A) and an increase of RMSE for all models implemented in both tanks (fig. 4.1, 4.2). In the tank A, the P&F and P&F with dead zone models were slightly stabler than CSTR and CSTRs ones (fig. 4.1): the P&F and P&F with

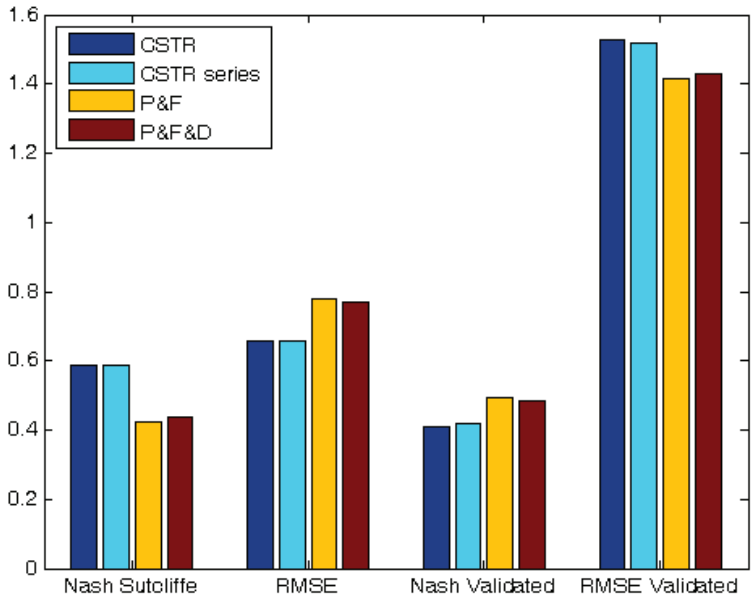

Figure 4.1: The Nash-Sutcliffe coefficient and the RMSE (g/m^3) value calculated for tank A after the models calibration and validation

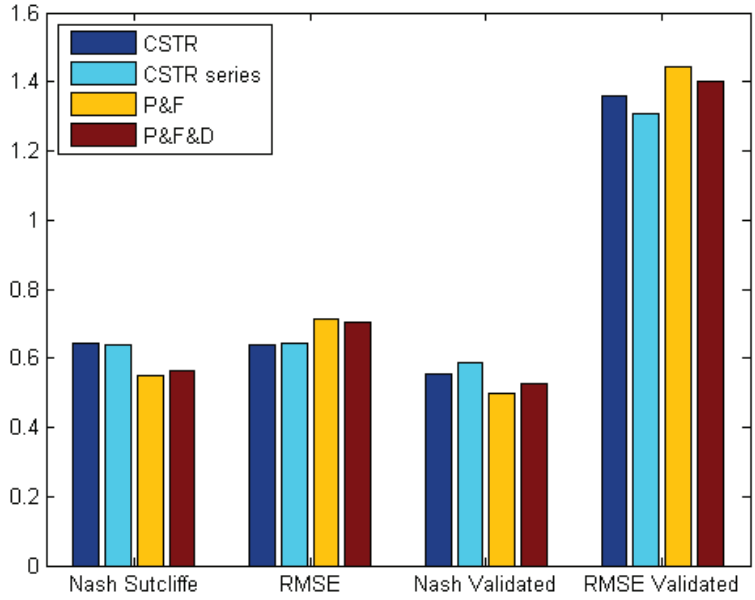

Figure 4.2: The Nash-Sutcliffe coefficient and the RMSE (g/m^3) value calculated for tank B after the models calibration and validation

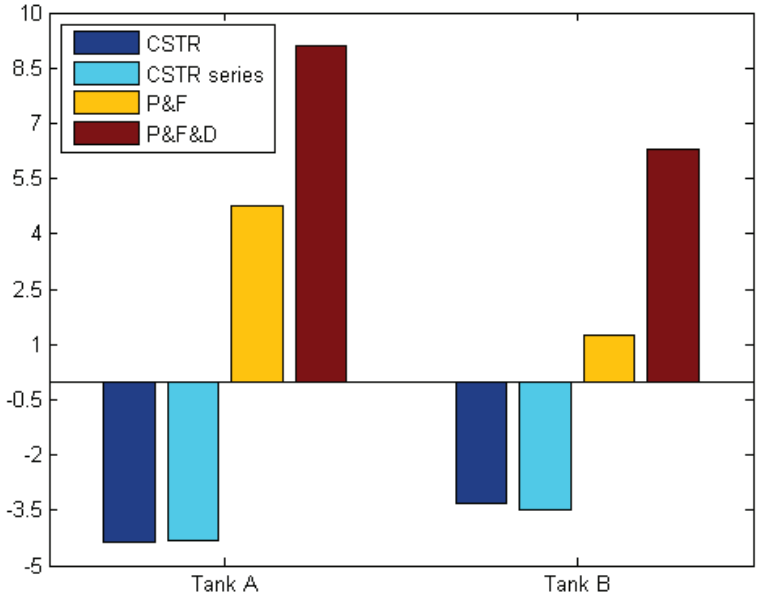

Figure 4.3: Models AIC parameters calculated in tank A and B after the calibration

dead zone models were characterized by an average increase of 13.5% of Nash-Sutcliffe coefficients after validation, and, their RMSE (with an average of 1.42 g/m^3) were lower than CSTR and CSTRs models (with an average of 1.52 g/m^3). On contrary, the CSTR and CSTRs models implemented for the tank B were able to describe the nitrogen removal slightly better than the P&F ones (fig. 4.2) because characterized by higher Nash coefficient and lower

RMSE; however, the validation had produced a decrease of the Nash parameter and an increase of the RMSE for all models respect the calibration phase (fig. 4.2).

After the calibration phase it emerges that the CSTR and CSTRs models were characterized by lower (fig. 4.3) AIC values (about an average of -4.35 for tank A and -3.4 for the tank B) than the P&F and P&F with dead zone ones, characterized by an average AIC parameter of 4.8 and 9.09 for tank A and 1.26 and 6.3 for the tank B, respectively (fig. 4.3).

Table 4.2: Curve Number of nitrogen reaction rate (k), Arrhenius Constants (theta), Wet/Dead Zone area ratio (Ar) and Exchange rate (a) calculated during the sensitivity analysis.

	Tank A				**Tank B**			
	CSTR	CSTRs	P&F	P&F&D	CSTR	CSTRs	P&F	P&F&D
K +30%	0.3923	0.6578	0.6405	0.5504	0.4757	0.7568	1.189	0.9474
K -30%	0.5601	0.9469	0.8356	0.7191	0.7059	1.5007	5.5559	2.0906
Theta +10%	2.0211	2.281	2.5069	2.1952	2.7030	3.5360	4.505	3.7559
Theta -10%	2.8232	3.1789	4.3003	3.6891	3.2691	3.1886	11.0602	6.2458
Ar +30%				1.03E-20				5.41E-14
Ar -30%				1.03E-20				5.41E-14
a +30%				5.16E-06				0.0018
a -30%				5.16E-06				0.0018

From the sensitivity analysis it emerges that the variation of the nitrogen reaction rate (k) and the Arrhenius constants (theta) have influenced strongly all models (tab. 4.2): the average condition number (of all models) of k, increased and decreased by a 30%, is about 0.66 and 1.61 respectively; the average theta condition number, increased and decreased by a 10%, is about 2.94 and 4.71 respectively. On contrary the wet/dead zone area ratio (Ar) and the exchange rate between the zones (a) do not influence a lot the P&F and P&F with dead zone models: the average condition number of the areas ratio (Ar), increased and decreased by a 30%, is about 2.7E-014; while the average condition number of the exchange rate increased and decreased by 30% is about 9.03E-04; this means that the use of these kind of models, considering the AIC comparison also, could be defined useless than the other models proposed. The wet/dead zone area ratio (Ar) and the exchange rate between the zones (a) were calibrated, despite their low influence in the model, because no informations about this conditions could be to measured.

4.2 The model n°2 and model n°3 for total dissolved nitrogen dynamics

After the calibration (tab. 4.3) it emerges that the model n°2 and model n°3 were able to

describe the total nitrogen dynamics in both constructed wetland tanks (fig. 4.4, 4.5, Annex 2); however, the validation have showed that they can be defined not stable (fig. 4.4, 4.5): the validate models present a Nash coefficient values lower of 90% and an RMSE values higher of 64% in average than the calibrated ones.

Table 4.3: Parameters of models n°2 and 3 calibrated

	Model n°2 CSTR		Model n°3 CSTR		
Parameters	**Tank A**	**Tank B**	**Tank A**	**Tank B**	**Units**
Mineralization kinetics 20°C (k)	0.0662	0.0789	0.0746	0.098	d^{-1}
Mineralization Arrhenius Constant (theta)	1.058	1.0726	1.0581	1.0697	
Nitrification kinetics Constant 20°C (u)	3.3943	3.625	1.6275	6.0415	d^{-1}
Nitrification Arrhenius Constant (theta N)	1.0017	1.0017	1.0312*	1.0312*	
NH4 Uptake kinetics 20°C (Kb_{NH4})	5.99E-04	5.56E-01	9.5625	8.8584	d^{-1}
NOx Uptake kinetics 20°C (Kb_{Nox})	0.0922	0.0063	4.23E-04	7.90E-03	d^{-1}
Uptake Arrhenius Constant (thetaBIO)	1.2	1.2	1.0023	1.0023	
Denitrification kinetics 20°C (DN)	0.4722	1.2249	0.4521	1.0237	d^{-1}
Denitr. Arrhenius Constant (thetaDN)	1.2	1.2	1.2	1.2	
Ammonium Half Sat. Constant (K_{NH4})			2.5078	1.6088	g/m^3
Nitrates Half Sat. Constant (K_{NOx})			21.6816	30	g/m^3
	Model n°2 CSTRs		Model n°3 CSTRs		
Parameters	**Tank A**	**Tank B**	**Tank A**	**Tank B**	**Units**
Mineralization kinetics 20°C (k)	0.0651	0.0888	0.0651	0.1107	d^{-1}
Mineralization Arrhenius Constant (theta)	1.059	1.1079	1.0405	1.0727	
Nitrification kinetics Constant 20°C (u)	3.2969	3.2814	8.5895	7.7091	d^{-1}
Nitrification Arrhenius Constant (theta N)	1.0004	1.0004	1.0312*	1.0312*	
NH4 Uptake kinetics 20°C (Kb_{NH4})	0.0451	1.147	8.961	10.0469	d^{-1}
NOx Uptake kinetics 20°C (Kb_{Nox})	4.03E-04	6.30E-03	5.55E-07	5.55E-07	d^{-1}
Uptake Arrhenius Constant (thetaBIO)	1.1715	1.1906	1.0003	1.0023	
Denitrification kinetics 20°C (DN)	0.4442	0.8801	0.3659	0.7956	d^{-1}
Denitr. Arrhenius Constant (thetaDN)	1.2	1.2	1.2	1.2	
Ammonium Half Sat. Constrat (K_{NH4})			2.4766	1.8828	g/m^3
Nitrates Half Sat. Constrat (K_{NOx})			30	40	g/m^3

*= Parameters not Calibrated but hypothesized from literature

In the Tank A, the model n°3 was characterized by an average Nash parameter of 0.58 and an average RMSE of 0.66 g/m^3 (fig. 4.4) against an average Nash parameter of 0.56 and an average RMSE of 0.68 g/m^3 of model n°2 (fig. 4.4). In the tank B, the model n°3 was characterized by an average Nash parameter of 0.55 and an average RMSE of 0.72 g/m^3 (fig. 4.5) against an average Nash parameter of 0.51 and an average RMSE of 0.75 g/m^3 of model

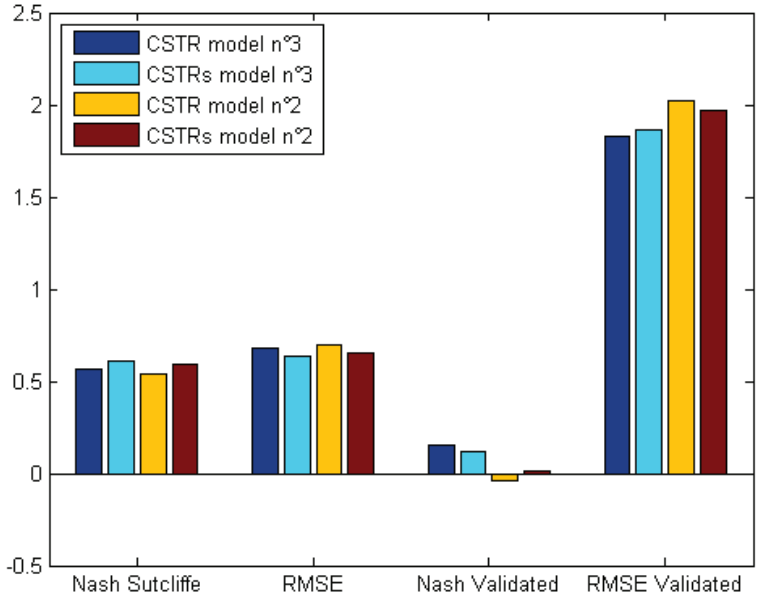

Figure 4.4: The Nash coefficient and the RMSE (g/m³) value calculated for tank A with the model n°2 and 3 after the calibration and validation

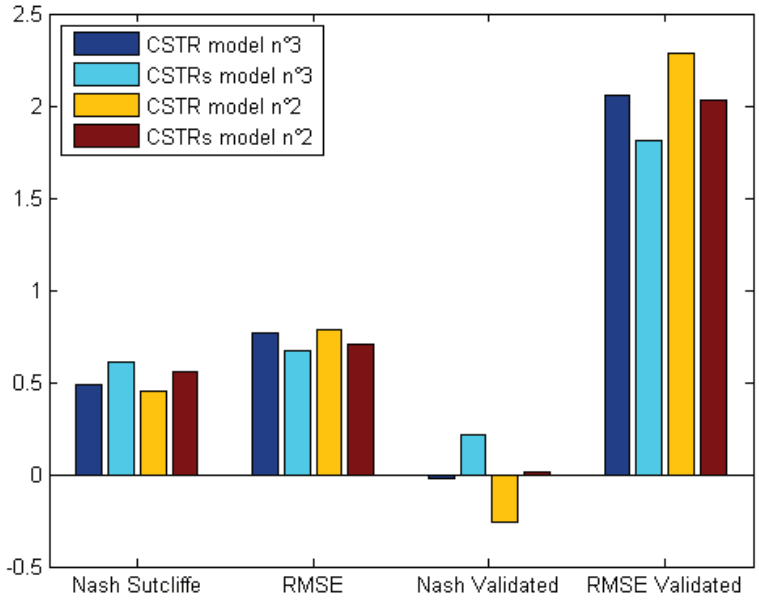

Figure 4.5: The Nash coefficient and the RMSE (g/m³) value calculated for tank B with the model n°2 and 3 after the calibration and validation

n°2 (fig. 4.5).

Globally, for all tanks, the model n°3 was able to describe the Nitrogen dynamics better than model n°2; in the tank A (fig. 4.4) the model n°3, with an average Nash parameter of 0.14 and an average RMSE of 1.85 g/m^3, was more stable than model n°2, that was characterized by an

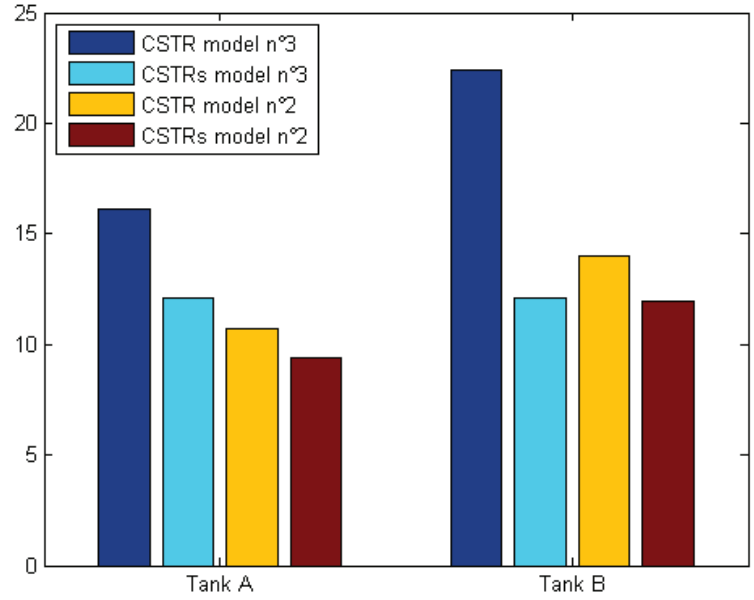

Figure 4.6: AIC parameters calculated with the model n°2 and 3 after the implementation in tank A and B

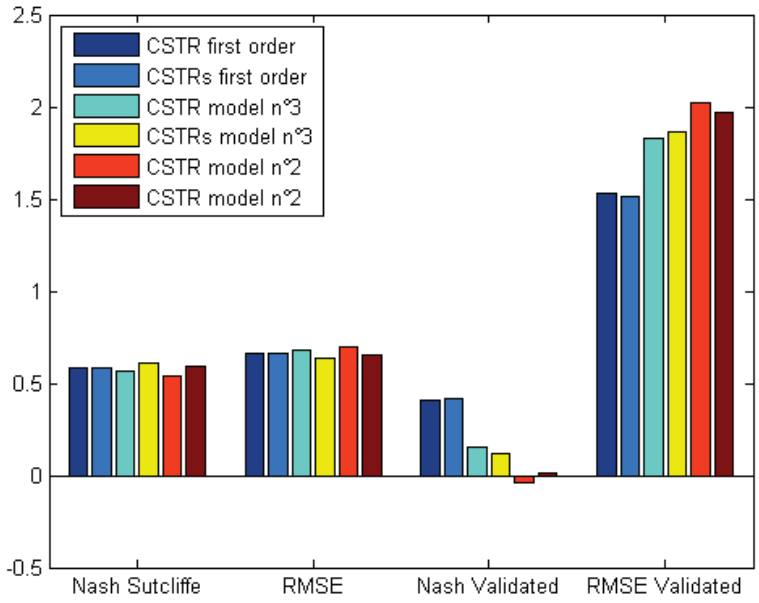

Figure 4.7: The Nash-Sutcliffe coefficient and the RMSE (g/m^3) values calculated for tank A applying all model used to describe the nitrogen removal

average Nash and RMSE parameters of 0.01 and 2 respectively (fig. 4.4). The same dynamic was observed in the tank B (fig. 4.5).

In the tank B, the CSTR in series models were capable to describe the Nitrogen dynamics better than the CSTR reactor models applied both in the model n°2 and 3 (fig. 4.5): the

average Nash parameter and RMSE of the CSRT in series models are 0.58 and 0.69 g/m^3 respectively against and the 0.47 and 0.78 g/m^3 of the CSTR models (fig. 4.5). It was possible say the same in the tank A with an exception: the CSTRs model was more stable than the CSTR one, only applying the model n°2 (fig. 4.5).

During the implementation it emerged that (fig. 4.6), in the tank A, the model n°2 was characterized by lower (fig. 4.6) AIC parameter than the model n°3: an average of 14.1 against 10.1; the same is showed for the tank B with an exception: the CSRTs model n°3 has the lowest AIC parameter (fig. 4.6).

Table 4.4: Condition Numbers of parameters used in model n°2 and 3.

	Model n°2 CSTR		Model n°3 CSTR		
Parameters	**Tank A**	**Tank B**	**Tank A**	**Tank B**	**Units**
Mineralization kinetics 20°C (k)	0.0725	0.0893	0.1144	0.1455	d^{-1}
Mineralization Arrhenius Constant (theta)	0.2537	0.3339	0.5087	0.6548	
Nitrification kinetics Constant 20°C (u)	0.0138	0.0104	0.0049	0.0048	d^{-1}
Nitrification Arrhenius Constant (theta N)	0.8151	0.5567	0.0355	0.0260	
NH4 Uptake kinetics 20°C (Kb_{NH4})	0.0047	0.0078	0.0139	0.0125	d^{-1}
NOx Uptake kinetics 20°C (Kb_{Nox})	0.0512	0.0038	0.0000	0.0000	d^{-1}
Uptake Arrhenius Constant (thetaBIO)	0.4548	0.0462	0.6602	0.4870	
Denitrification kinetics 20°C (DN)	0.2647	0.3237	0.2978	0.3290	d^{-1}
Denitr. Arrhenius Constant (thetaDN)	1.5972	1.9410	1.7087	1.9246	
Ammonium Half Sat. Constrat (K_{NH4})			0.0666	0.0875	g/m^3
Nitrates Half Sat. Constrat (K_{NOx})			2.96E-05	9.66E-08	g/m^3
	Model n°2 CSTRs		Model n°3 CSTRs		
Parameters	**Tank A**	**Tank B**	**Tank A**	**Tank B**	**Units**
Mineralization kinetics 20°C (k)	0.0790	0.1056	0.1375	0.1760	d^{-1}
Mineralization Arrhenius Constant (theta)	0.2338	0.3258	0.5812	0.7503	
Nitrification kinetics Constant 20°C (u)	0.0159	0.0076	0.0112	0.0073	d^{-1}
Nitrification Arrhenius Constant (thetaN)	3.1089	3.1600	0.0900	0.0461	
NH4 Uptake kinetics 20°C (Kb_{NH4})	0.0095	0.0119	0.0144	0.0130	d^{-1}
NOx Uptake kinetics 20°C (Kb_{Nox})	0.0004	0.0046	0.0000	0.0000	d^{-1}
Uptake Arrhenius Constant (thetaBIO)	0.0319	0.0757	5.1958	0.4051	
Denitrification kinetics 20°C (DN)	0.3689	0.3793	0.3424	0.3849	d^{-1}
Denitr. Arrhenius Constant (thetaDN)	2.0314	2.1512	1.9023	2.1661	
Ammonium Half Sat. Constrat (K_{NH4})			0.0714	0.0999	g/m^3
Nitrates Half Sat. Constrat (K_{NOx})			3.96E-08	1.76E-08	g/m^3

From sensitivity analysis (tab 4.4), it emerges that the model n°2 (in both tanks) is strongly

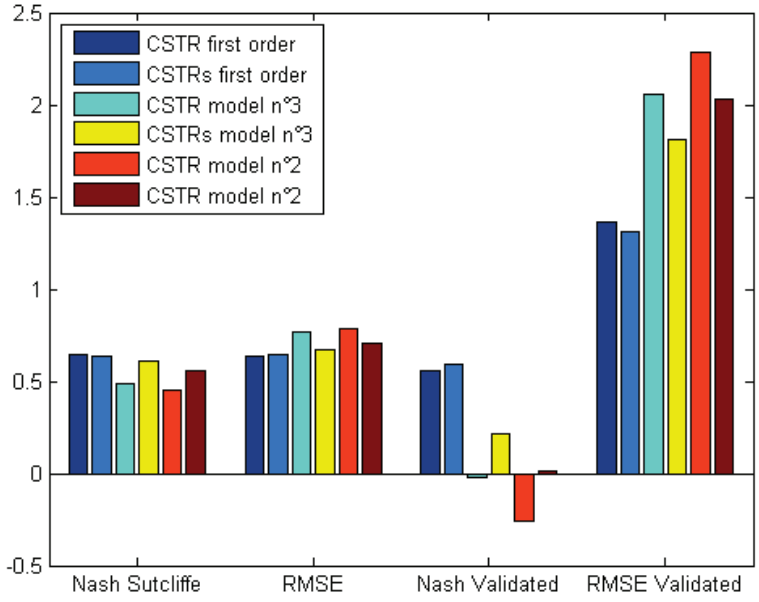

Figure 4.8: The Nash-Sutcliffe coefficient and the RMSE (g/m^3) values calculated for tank B applying all model used to describe the nitrogen removal

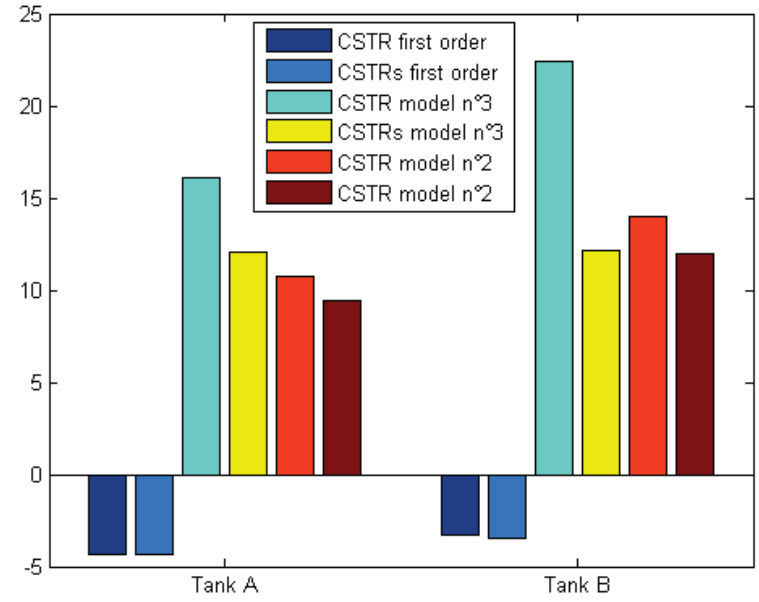

Figure 4.9: AIC parameters calculated applying all model used to describe the nitrogen removal after the implementation in tank A and B

influenced by the mineralization (k) and denitrification (DN) kineticss and by the Arrhenius constants associated with the mineralization (theta), nitrification (thetaN), and denitrification (thetaDN) (tab 4.4). The model n°3 behaviour depends principally on the mineralization (k)

and denitrification (DN) and by the Arrhenius constants associated with the mineralization (theta), denitrification (thetaDN) and biological uptake (thetaBIO) (tab 4.4). According to the sensitivity analysis, it emerges that the calibration of model n°2 and 3 had to be conducted considering the calibration of 5 or 6 parameters; however, 9 parameters and 10 parameter was calibrated for model n°2 and 3 respectively because no important publication was found in order to hypothesize a sensible value for some parameters. The condition numbers (CN) of kineticss showed in table 4.4 represent the average CN calculated increasing and decreasing the kineticss of 30%; while the Arrhenius parameter CN was calculated taking into account the average change between the increase of such parameter by 10% and the decrease of it to assign it equal to 1.

4.2.1 Comparison of all models used to describe the nitrogen removal

By a simply comparison (fig. 4.7, 4.8) of all models used to describe the dynamics of total nitrogen in both constructed wetland tanks, it emerges that all model implemented simulate in a good way the data observed; however, the first order kinetics models were the stabler in the long period and with respect to models n°2 and 3: the validated first order kinetics models have the highest Nash parameter and are characterized by the lowest RMSE value in both tanks (fig. 4.7, 4.8).

In addition, by the comparison of AIC parameters (fig. 4.9) emerges that the use of first order kinetics models permits a good description of nitrogen dynamics into the wetlands combined with the choice of a simple, parsimonious model structure: the AIC parameters of first order kinetics model applied with a CSTR and CSRTs reactor is below the 0 while the other models that are characterized by an average AIC parameter greater than 10 (fig. 4.9), which makes a large differences according to Anderson (2008).

4.3 The first order kinetics models for pathogens removal

The first order kinetics models implemented, do not describe in a perfect way the pathogens removal observed during the sampling periods; the modelled data were not able to fit in a perfect way the data observed since in the most cases the efficiency is resulted negative even if (principally in the tank A) they were characterized by a low RMSE value. The models described the pathogens removal better in tank A than in tank B (tab. 4.5): in the tank A, the models implemented for Clostridium, Coliform and Escherichia removal were characterized by an average RMSE of 18 UFC/100ml and 30 UFC/100ml after the calibration and

validation respectively and by an average RMSE of 307 UFC/100ml and 143 UFC/100ml respectively for Streptococci; while in the tank B, was possible to observe an average RMSE of 30 UFC/100ml and 150 UFC/100ml after the calibration and validation respectively and an average RMSE of 52 UFC/100ml and 58 UFC/100ml for Streptococci removal.

Table 4.5: The average AIC parameters, Nash coefficients and RMSE (UFC/100ml) calculated implementing all first order kinetics models proposed for each pathogens observed in this work

	Tank A			
	Clostridium	Coliform	Escherichia	Streptococci
AIC	66.136	55.59	53.706	119.299
Nash Sutcliffe Efficiency	-0.326	-0.389	0.344	0.411
RMSE (UFC/100ml)	30.189	12.953	11.166	306.510
Nash Validated Model	-0.419	0.978	-1.046	-0.092
RMSE validated (UFC/100ml)	44.174	31.225	15.418	142.880
	Tank B			
AIC	46.823	79.616	71.308	75.394
Nash Sutcliffe Efficiency	0.662	-0.334	-0.259	-0.586
RMSE (UFC/100ml)	19.902	41.304	28.171	52.379
Nash Validated Model	-0.481	-0.438	-0.402	-0.436
RMSE validated (UFC/100ml)	221.157	195.988	29.259	58.032

Globally, in tank A, the P&F model was better fitting and stabler than other models for describe the dynamics of Clostridium, Faecal coliform and Escherichia coli even if was characterized by the higher AIC parameter (higher than 3-4% respect the average).

In both tanks (and principally in the tank B), except the Clostridium dynamics, it emerges that the pathogens removal could be describe in a good way using models not dependent on temperature: the CSTR and CSTRs models used to describe the dynamics of Coliform, Escherichia and Streptococci without the temperature dependency were characterized by lower AIC parameters than the same models dependent by temperature and were capable to describe the pathogens dynamics in the same way or better.

4.3.1 The first order kinetics models for Clostridium removal

The modelled Clostridium dynamics (Annex 3) in Tank A was characterized by an average Nash Sutcliffe parameter of -0.33 and -0.42, and an average RMSE of 30 UFC/100ml and 44.2 UFC/100ml after the calibration (tab 4.7) and validation respectively; in Tank B, this dynamic, was characterized by an average Nash Sutcliffe parameter of 0.66 and -0.48, and an

average RMSE of 20 UFC/100ml and 221 UFC/100ml after the calibration (tab 4.7) and validation respectively.

Table 4.6: Clostridium mortality rate (k), Arrhenius Constants (theta), Wet Area (A), Dispersion Coefficients (D) after calibration

	Tank A			Tank B		
Parameters Calibrated	**CSTR**	**CSTRs**	**P&F**	**CSTR**	**CSTRs**	**P&F**
Mortality rate d^{-1}	0.2094	0.1638	0.0930	0.4481	0.3230	0.1214
M. rate No Temp. Model d^{-1}	0.1508	0.1208		0.2928	0.2049	
Arrhenius Constant (theta)	1.0930	1.0783	1.0461	1.1339	1.1139	1.1675
Dispersion Coefficient (m^2/d)			5.0903			0.6227
Wet Area Calibrated (m^2)			2.3995			2.1039

The most efficient model (in Tank A) was the P&F one, despite it was characterized by the highest AIC parameter (tab 4.7): the P&F model has described the Clostridium dynamics with a calculated Nash parameter of -0.101 and -0.249, and an RMSE of 27.6 UFC/100ml and 41.5 UFC/100ml after the implementation and validation respectively; its AIC parameter is higher by 3% with respect the average.

Table 4.7: The AIC parameter, the Nash-Sutcliffe coefficient and the RMSE (UFC/100ml) values calculated applying the first order kinetics models used to describe the Clostridium removal

	Temperature Model			No Temp. Model	
	CSTR	CSTRS	P&F	CSTR	CSTRS
			Tank A		
AIC	66.614	65.370	67.912	65.944	64.840
Nash Sutcliffe Efficiency	-0.347	-0.166	-0.101	-0.613	-0.401
RMSE (UFC/100ml)	30.506	28.376	27.579	33.376	31.107
Nash Validated Model	-0.332	-0.326	-0.249	-0.568	-0.623
RMSE validated (UFC/100ml)	42.841	42.752	41.491	46.489	47.297
			Tank B		
AIC	44.688	44.810	49.445	47.576	47.595
Nash Sutcliffe Efficiency	0.762	0.760	0.756	0.527	0.502
RMSE (UFC/100ml)	16.942	17.009	17.151	23.892	24.514
Nash Validated Model	-0.371	-0.383	//	-0.473	-0.451
RMSE validated (UFC/100ml)	213.025	213.897	//	220.782	219.126

Taking into account the dependency on temperature, emerges that the Clostridium dynamic is slightly influence by it: globally, the temperature models were characterized by average Nash parameters of -0.21 after the implementation and -0.3 after the validation against an average of -0.5 and -0.6 of models no temperature dependent (tab 4.7); similarly, the RMSE was lower

of 10% in the dependent temperature models than in the not dependent ones (tab 4.7).

It was possible observed the same dynamics in the tank B with an exception (tab 4.7): the most efficient model was the CSTR dependent on temperature that was characterized by the highest Nash parameter (tab 4.7), after the implementation and validation, and by the lowest RMSE (tab 4.7).

Table 4.8: Coliform mortality rate (k), Arrhenius Constants (theta), Wet Area (A), Dispersion Coefficients (D) after calibration

	Tank A			Tank B		
Parameters Calibrated	**CSTR**	**CSTRs**	**P&F**	**CSTR**	**CSTRs**	**P&F**
Mortality rate d^{-1}	24.01	3.1562	0.5451	15.42	2.836	0.5882
M. rate No Temp. Model d^{-1}	24.39	3.14		15.22	2.831	
Arrhenius Constant (theta)	1	1	1	1	1	1
Dispersion Coefficient (m^2/d)			9.98			15.78
Wet Area Calibrated (m^2)			2.3			2.196

4.3.2 The first order kinetics models for Faecal coliform removal

After the calibration (tab 4.8, Annex 4), the models of Faecal coliform removal in Tank A were characterized by an average Nash Sutcliffe parameter of -0.39 and an RMSE of 13 UFC/100ml (tab 4.9) while an average Nash Sutcliffe parameter of 0.98 and a RMSE of 31.22 UFC/100ml was calculated after the validation (tab 4.9). In Tank B, the models were characterized by an average Nash Sutcliffe parameter of -0.33 and -0.44 and an average RMSE of 41 UFC/100ml and 196 UFC/100ml after the calibration and validation respectively. As described above, the most efficient model (in Tank A) was the P&F, despite it was characterized by the higher AIC parameter (tab 4.9) (higher than 4% with respect to the average): the P&F model has described the Faecal coliform dynamics with a Nash parameter of -0.132 and 0.978 (tab 4.9), and an RMSE of 11.7 UFC/100ml and 30.9 UFC/100ml after the implementation and validation respectively (tab 4.9).

The most efficient model (in Tank B) was the CSTR in series not dependent on temperature; however, all models applied in tank B describe with the same accuracy the Faecal coliform dynamic: the Nash and RMSE parameters calculated after the models implementation and calibration are very similar (tab 4.9). The CSTR in series model not dependent on temperature describes the Coliform dynamics with a Nash parameter of -0.33 and -0.433, and an RMSE of 41.2 UFC/100ml and 195.6 UFC/100ml after the implementation and validation respectively (tab 4.9); it has the lowest AIC parameter: 77.3 against the 77.5 of CSTR model without

temperature and the average 81 of models dependent by temperature (tab 4.9).

Table 4.9: The AIC parameter, the Nash-Sutcliffe coefficient and the RMSE values (UFC/100ml) calculated applying the first order kinetics models to describe the Faecal coliform removal

	Temperature Model			No Temp. Models	
	CSTR	CSTRs	P&F	CSTR	CSTRs
			Tank A		
AIC	56.237	56.107	57.260	54.220	54.119
Nash Sutcliffe Efficiency	-0.470	-0.436	-0.132	-0.469	-0.436
RMSE (UFC/100ml)	13.344	13.188	11.707	13.340	13.188
Nash Validated Model	0.978	0.978	0.978	0.978	0.978
RMSE validated (UFC/100ml)	31.349	31.277	30.873	31.353	31.272
			Tank B		
AIC	79.501	79.324	84.440	77.492	77.321
Nash Sutcliffe Efficiency	-0.344	-0.330	-0.324	-0.344	-0.330
RMSE (UFC/100ml)	41.457	41.236	41.135	41.458	41.236
Nash Validated Model	-0.440	-0.434	-0.445	-0.439	-0.433
RMSE validated (UFC/100ml)	196.122	195.680	196.457	196.029	195.655

4.3.3 The first order kinetics models for Escherichia coli removal

The modelled Escherichia coli dynamic (Annex 5), in Tank A, was characterized by an average Nash Sutcliffe parameter of 0.34 and -1.05, and an RMSE of 11.17 UFC/100ml and 15.42 UFC/100ml after the calibration and validation respectively; while, in Tank B, it was characterized by an average Nash Sutcliffe parameter of -0.26 and -0.4 and an average RMSE of 28.2 UFC/100ml and 29.3 UFC/100ml.

Table 4.10: Escherichia coli mortality rate (k), Arrhenius Constants (theta), Wet Area (A), Dispersion Coefficients (D) after calibration

	Tank A			Tank B		
Parameters Calibrated	**CSTR**	**CSTRs**	**P&F**	**CSTR**	**CSTRs**	**P&F**
Mortality rate d^{-1}	8.5439	1.8692	0.6146	15.6279	2.8741	1.3746
M. rate No Temp. Model d^{-1}	8.5903	1.8662		14.9803	2.828	
Arrhenius Constant (theta)	1	1	1	1	1	1.1167
Dispersion Coefficient (m^2/d)			58.957			0.6953
Wet Area Calibrated (m^2)			2.3624			2.1899

In this case the P&F was able to describe the Escherichia dynamic better than others models: it was characterized by a Nash parameter of 0.272 and -0.775 (tab 4.11), and an RMSE of 11.76 UFC/100ml and 14.37 UFC/100ml after the implementation and validation respectively (tab 4.11). The other models were characterized by an higher Nash parameter after the

calibration (an average of 0.362) (tab 4.11) but were less stable than P&F with an average Nash and RMSE parameter of -1.11 and 15. 68 UFC/100ml respectively (tab 4.11).

Table 4.11: The AIC parameter, the Nash-Sutcliffe coefficient and the RMSE values (UFC/100ml) calculated applying the first order kinetics models to describe the Escherichia coli removal

	Temperature Model			No Temp. Models	
	CSTR	CSTRs	P&F	CSTR	CSTRs
			Tank A		
AIC	53.537	54.018	57.445	51.518	52.014
Nash Sutcliffe Efficiency	0.371	0.351	0.272	0.372	0.352
RMSE (UFC/100ml)	10.933	11.107	11.761	10.930	11.100
Nash Validated Model	-1.172	-1.059	-0.775	-1.160	-1.067
RMSE validated (UFC/100ml)	15.893	15.474	14.369	15.850	15.504
			Tank B		
AIC	71.020	70.917	76.700	69.001	68.902
Nash Sutcliffe Efficiency	-0.237	-0.230	-0.359	-0.237	-0.230
RMSE (UFC/100ml)	27.937	27.854	29.280	27.933	27.851
Nash Validated Model	-0.38	-0.36	-0.539	-0.373	-0.362
RMSE validated (UFC/100ml)	28.978	28.858	30.658	28.957	28.841

The most efficient and stable model (in Tank B) was the CSTR in series without the temperature that is characterized by the lower AIC parameter (68.9 against an average of 72.6 of temperature models), an average Nash parameter of -0.230 and -0.362, and an RMSE of 27.8 UFC/100ml and 28.84 UFC/100ml after the implementation and validation respectively (tab 4.11).

4.3.4 The first order kinetics models for Streptococci removal

The models used to describe the Streptococci removal (Annex 6) in Tank A was characterized by an average Nash Sutcliffe parameter of 0.41 and -0.09, and by an RMSE of 306 UFC/100ml and 142 UFC/100ml calculated after the calibration (tab 4.13) and validation respectively; while, in Tank B was characterized by an average Nash Sutcliffe parameter of -0.60 and -0.44 and an average RMSE of 52.4 UFC/100ml and 58 UFC/100ml.

The most efficient implemented model in Tank A was the CSTR one dependent and not dependent on temperature (tab 4.13): the CSTR models (with and without temperature) were characterized by an average AIC parameter of 117.66, against an average of 120.5 of other models, by an average Nash and RMSE parameter of 0.49 and 287 UFC/100ml respectively against an average of 0.36 and 318 UFC/100ml of the other models.

However, the most stable models in tank A were the CSTR in series with and without temperature (tab 4.13) characterized by an average Nash and RMSE parameter of -0.06 and 140 UFC/100ml respectively against an average of -0.11 and 144 UFC/100ml of the other models.

Table 4.12: Streptococci Mortality rate (k), Arrhenius Constants (theta), Wet Area (A), Dispersion Coefficient (D) after calibration

	Tank A			Tank B		
Parameters Calibrated	**CSTR**	**CSTRS**	**P&F**	**CSTR**	**CSTRS**	**P&F**
Mortality rate d-1	0.2187	0.2020	3.2E-07	7.1024	1.8249	0.4577
M. rate No Temp. Model d-1	0.1912	0.1891		7.11	1.8396	
Arrhenius Constant (theta)	1.0076	1.0050	1.2	1	1	1
Dispersion Coefficient (m2/d)			27.46			3.4797
Wet Area Calibrated (m2)			2.3			2.2

It was possible observed the same results in the tank B with an exception (tab 4.13): the most efficient implemented model was the P&F one that was characterized by the higher Nash parameter (tab 4.13) -0.503 and the lowest RMSE (tab 4.13).

Table 4.13: The AIC parameter, the Nash-Sutcliffe coefficient and the RMSE values (UFC/100ml) calculated applying the first order kinetics models to describe the Streptococci removal

	Temperature Model			No Temp. Model	
	CSTR	CSTRS	P&F	CSTR	CSTRS
			Tank A		
AIC	118.36	119.81	123.91	116.65	117.76
Nash Sutcliffe Efficiency	0.49	0.38	0.33	0.48	0.39
RMSE (UFC/100ml)	286.77	314.88	328.36	289.24	313.30
Nash Validated Model	-0.11	-0.06	-0.09	-0.14	-0.06
RMSE validated (UFC/100ml)	143.98	140.68	143.04	145.74	140.97
			Tank B		
AIC	75.552	75.401	79.056	73.552	73.407
Nash Sutcliffe Efficiency	-0.616	-0.596	-0.503	-0.616	-0.597
RMSE (UFC/100ml)	52.888	52.560	50.995	52.885	52.566
Nash Validated Model	-0.427	-0.411	-0.497	-0.428	-0.417
RMSE validated (UFC/100ml)	57.853	57.530	59.256	57.865	57.655

4.3.5 The Sensitivity analysis of pathogens removal models

From sensitivity analysis of all models used to describe the pathogens dynamics in both constructed wetlands tanks (table 4.14), it emerges that the mortality rates k increased and decreased by the 30% influence lower than the Arrhenius constants increased and decreased

by the 10% the models behaviour: the condition number of mortality rates k range between 0.25 to 40 (table 4.14), while the Arrhenius constants condition number ranged between 0.68 and 126 (table 4.14).

Table 4.14: Condition Numbers of pathogens mortality rate (k) and Arrhenius Constants (theta) calculated during the sensitivity analysis

	Tank A			Tank B			Tank A		Tank B	
	Clostridi Temperature Model						No Temp. Model			
	CSTR	CSTRs	P&F	CSTR	CSTRs	P&F	CSTR	CSTRs	CSTR	CSTRs
K +30%	0.48	0.64	0.48	0.51	0.7	0.36	0.49	0.65	0.56	0.7
K -30%	0.59	0.95	0.57	0.69	1.29	0.41	0.63	0.96	0.73	1.58
Theta +10%	1.62	2.13	1.37	1.80	3.04	1.03				
Theta -10%	3.11	2.42	2.24	3.75	2.83	1.8				
	Coliformi Temperature Model						No Temp. Model			
K +30%	0.78	2.66	1.7	0.53	0.71	1.51	0.78	2.96	0.76	2.71
K -30%	1.42	>40	5.08	0.67	1.21	3.67	1.43	>40	1.4	>40
Theta +10%	4.96	39.34	10.81	2.01	3.14	8.24				
Theta -10%	4.79	4.03	8.3	3.89	3.08	7.54				
	Escherichia Temperature Model						No Temp. Model			
K +30%	0.78	2.16	1.13	0.53	0.7	5.91	0.78	2.64	0.76	2.7
K -30%	1.39	>40	1.98	0.71	1.29	589.29	1.41	>40	1.4	>40
Theta +10%	4.76	25.79	5.05	2.0144	3.11	126.78				
Theta -10%	4.76	4.04	5.91	3.91	3.04	27.68				
	Streptococci Temperature Model						No Temp. Model			
K +30%	0.55	0.87	0.25	0.77	2.4	1.52	0.53	1.12	0.77	2.41
K -30%	0.65	0.67	0.29	1.4	>40	3.96	0.78	0.52	1.4	>40
Theta +10%	1.88	2.4	0.68	4.76	18.06	7.8				
Theta -10%	3.43	3.31	1.28	5.1	6.34	9.11				

5. DISCUSSION AND CONCLUSION

5.1 The models for nitrogen compounds and total dissolved nitrogen removal

This study shows that the first order kinetics models describe in a good way and with parsimonious simplicity the dynamics of total dissolved nitrogen in the constructed wetland tanks. However, the model performance decrease from calibration to validation suggesting that the models structure does not include some key processes: in general, the RMSE tends to increase and the Nash-Sutcliffe parameter tends to decrease. Anyway an average RMSE of 1.5-1.6 could be define acceptable for the evaluation of constructed wetland plants designed such as tertiary treatments when the total nitrogen is already below the legislation limits.

Regarding the spatial structure of the model, by taking the Akaike's information criterion (AIC) into account, it emerges that the use of a Continuous Stirred Tank Reactor (CSTR) model, and of a CSTR in series model (CSTRs), could represent the best solution associated with an first order kinetics model because it combines simplicity with a good nitrogen dynamics prediction, although in some cases the Plug and Flow reactor models performed better during the validation.

Despite the constructed wetland hydraulics was influenced by the presence of preferential flows and dead zones, the Plug and Flow model with dead zones has not been able to describe better than other models the dynamics of total dissolved nitrogen in both tanks: the model implementation shows that the dead zone area and the exchange rate tends to be 0.

In general, the results show that the tanks hydraulics proposed have not influenced the models accuracy but its complexity only; however, To further test the importance of the presence of dead zones and preferential flows in these plants (an issue well known in wetlands (Kadlec et al. 2008)), based on this hydraulic behaviour, it would be very interesting to implement more accurate models that take the presence of preferential and dead zones into account, by simulating one, two or three spatial dimensions.

Considering the results of models that were built taking into account the nitrogen cycle in wetland (model n°2 and 3), it emerges that they were able to describe the nitrogen removal in tanks but are resulted less stable, validation performance clearly worsens with respect to calibration. The construction of these models has suffered, principally, the low number of information and observations available for their implementation and the low accuracy of some

data in term of quality (see below); a more accurate sampling campaign would have allowed to improve the calibration phase of these models and to implement a different mathematical formulation able to describe better the Nitrogen conceptual model proposed (fig. 3.31): considering (just an example) the particulate nitrogen in N cycle and investigate some processes such as the clogging (describing the sedimentation in a HSSF wetland) and the hydrolysis, how some authors do (Mayo et al, 2005; Senzia et al, 2002).

Concerning the nitrogen removal models, it would be interesting, so, to implement these having a much larger number of observed data and a more precise information such as: the knowledge of inflow and outflow dissolved oxygen in wastewater, in order to understand if aerobic or anaerobic conditions prevail; the knowledge of inflow and outflow wastewater temperature; a higher frequency of sampling of the inflow and outflow wastewater; informations about the particulate nitrogen concentration in wastewater (in order to understand better the nitrogen cycle).

5.2 The models for pathogens removal

The first order kinetics models, do not describe in a perfect way the pathogens removal observed in the constructed wetland tanks; the modelled data were not capable of fitting well the data observed but in most cases (principally in the tank A) they were characterized by a low RMSE value (compared with the highlighted ones from some authors such Hamaamin et al. (2014)).

The first order kinetics model, in both tanks, has described the Escherichia coli dynamics with low RMSE values: the average RMSE calculated after the calibration (considering both tanks) was 20 UFC/100ml, while was 22 UFC/100ml after the validation. However, the negative Nash parameter calculated (principally after the validation) shows that the models do not fit satisfactorily the observed data.

The Clostridium dynamic was modelled better in the tank A than in the tank B and also in this case the Nash parameter calculated was negative in both cases except after the model calibration in tank B. In tank A, the first order kinetics model describes the Clostridium dynamic with an average RMSE of 30 UFC/100ml and 40 UFC/100ml after the calibration and validation respectively; while in the tank B the average RMSE value was 20 UFC/100ml after the calibration and greater than 220 UFC/100ml after the validation. It was possible to observe a similar model behaviour in the case of Fecal coliform: in tank A, the first order

kinetics model describes the Fecal coliform dynamic with an average RMSE of 13 and 31 after the calibration and validation respectively; while in the tank B the average RMSE was 41 UFC/100ml after the calibration and 195 UFC/100ml after the validation.

In both tanks (and principally in the tank B), excepted when the Clostridium dynamic is simulated, it emerges that the observations do not support a modelization of pathogens removal models dependent by temperature: the CSTR and CSTRs models used to describe the dynamics of Coliform, Escherichia and Streptococci without the temperature dependency were characterized by lower AIC parameters than the same models dependent on temperature and were capable to describe the pathogens dynamics similar or better. Clearly, more observations are required to understand and model the effect of temperature on pathogens in this system.

Globally, from this study it emerges that it could be possible to use a first order kinetics model to predict the pathogen dynamics in an HSSF constructed wetland tank taking into account some prescriptions, that depend on the role of constructed wetland plant in the overall wastewater treatment plant and on the wastewater destiny: for example, these models could be interesting in order to predict the pathogens abatement of a constructed wetland plant installed upstream with respect to other traditional disinfection treatments; on the contrary, for example, a constructed wetland tank implemented for the wastewater re-use requires models that produce more accurate informations; sometime the wastewater reuse limits (for use agronomic, civil and industrial) require pathogens concentration equal to 0, so, this situations needed the use of very precise models.

As described above, also in this case, would be to implement more complex models having a greater number of observations and more accurate measurements. It would be interesting investigate and evaluated models using a pathogens decay dependent by others wastewater and wetland characteristics than I have used in this work or than were collected ones, such as: the dissolved oxygen concentration, the wastewater pH, the adsorption, filtration, sedimentation as showed by Hamaamin et al. (2014) and Mayo et al. (2007).

5.3 The models development and the sampling campaigns

In general, this study shows as the constructed wetland plant for the wastewater treatment, in particular the field-scales ones, are complex systems that can be described by models more or less simple. However, their implementation and validation for the management and the design

of wetlands, requires a meticulous data collection and numerous information (even for the simplest models).

Despite the models comparison have demonstrated that hydraulics sub-models have not influenced much the models accuracy, their prediction capacity could be influenced by a more accurate knowledge of some tanks hydraulics characteristics such as (first of all) the tanks inflow and outflow wastewater; the latter were not sampled accurately during the campaign made by LASA between the years 2011-2012. As I have deduced from some studies conducted by Toscano et al. (2009) and Langergraber (2007), it is fundamental the preliminary tanks hydraulics characterization, that means build and validate the most suitable tanks hydraulics sub-models (0D, 1D, 2D or 3D), before to implement models for predict the removal of nutrients and pathogens. The tanks hydraulics can be modelled having a good number of information about the tanks inflow and outflow wastewater, how showed Toscano et al. (2009) and Langergraber (2007). Then, Rhodamine tracer tests can be implemented to calculated the tanks HRT, to investigate the presences of preferential flow zones (as during this study was made) and to understand something about the solute transport into the HSSF porous medium with which it can calculate the longitudinal and transversal coefficients that could be used successfully in prediction models, as shown by Toscano et al. (2009).

Only after the knowledge of constructed wetland tanks hydraulics, models for prediction of nutrients and pathogens should be implemented. The construction and the validation of these could require: an good number of observations (according to the kind of model to be built); the accurate choice of sampling period (less than one years, one year, two year or more); an efficient campaign useful to understand the wastewater temperature dynamics into the tank; and others useful information such as showed above (wastewater DO, pH, clogging, sedimentation and others).

6. REFERENCES

Alkaeed O., Flores C., Jinno K., Tsutsumi A. (2006): Comparison of several reference evapotranspiration methods for Itoshima Peninsula Area, Fukuoka, Japan. *Memoirs of the Faculty of Engineering, Kyushu University, Vol. 66, No.1, March 2006.*

Anderson D. R. (2008): Model based inference in the life sciences: a primer on evidence. ***Springer-Verlag New York.***

Cirelli G. L., Consoli S., Juanico M. (2009). Modelling Escherichia coli concentration in a wastewater reservoir using an operational parameter MRT%FE and first order kinetics. *Journal of Environmental Management 90 604-614*.

Craggs J. R., Zwart A., Nagels J. W., Davies-Colley R. J. (2004). Modelling sunlight disinfection in a high rate pond. *Ecological Engineering 22 (2004) 113–122*.

Dal Cin L., Berdoricchio G., Coffaro G. (2002). Linee guida per la ricostruzione di aree umide per il trattamento di acque superficiali. Agenzia Nazionale per la protezione dell'Ambiente (ANPA).

Davies-Colley R. J., Donnison A.M., Speed D. J., Ross C. M., Nagel J. W. (1998). Inactivation of faecal indicator microorganisms in waste stabilisation ponds: interactions of environmental factors with sunlight. *Wat. Res. Vol. 33, No. 5, pp. 1220±1230*.

Giraldi D., De Michieli Vitturi M., Iannelli R. (2010). FITOVERT: A dynamic numerical model of subsurface vertical flow constructed wetlands. *Environmental Modelling & Software 25 (2010) 633–640*.

Grady Jr. Leslie C. P., Glen T. D., Nancy G. L., Carlos D. M. Filipe (2011): Biological Wastewater Treatment, Third Edition. *CRC Press, 2011*.

Hamaamin A. Y., Umesh A., Nejadhashemi A. P., Timothy H., Reinhold D. M. (2014). Modeling Escherichia coli removal in constructed wetlands under pulse loading. *Water Research 50 441-454*.

Henze M. (2008). *Biological Wastewater Treatment: Principles, Modelling and Design*. IWA Publishing.

Kadlec R. H, Wallace S. (2008). Treatment Wetlands, Second Edition. *CRC Press, 2008*.

Kadlec R. H. (2008). The inadequacy of first-order treatment wetland models. *Ecological Engineering 15 (2000) 105–119*.

Kivaisi A. K. (2001). The potential for constructed wetlands for wastewater treatment and reuse in developing countries: a review. *Ecological Engineering 16 (2001) 545–560*.

Langergraber G. (2007). Simulation of the treatment performance of outdoor subsurface flow constructed wetlands in temperate climates. *Science of the Total Environment* 380 (2007) 210–219.

Langergraber G., Simunek J. (2005). Modeling Variably Saturated Water Flow and Multicomponent Reactive Transport in Constructed Wetlands. *Vadose Zone Journal 4:924–938 (2005)*.

Langergraber, G., and J. Šimůnek (2006). The Multi-component Reactive Transport Module CW2D for Constructed Wetlands for the HYDRUS Software Package, Manual – Version 1.0, HYDRUS Software Series 2, *Department of Environmental Sciences, University of California Riverside, Riverside, CA, 72 pp., 2006*.

Langergraber, G., Rousseau D., García J., Mena J. (2009). CWM1 - A general model to describe biokinetic processes in subsurface flow constructed wetlands. *Water Sci. Technol., 59(9), 1687-1697, 2009*.

Loro M. (2011): Verifica dell'efficenza depurativa in un impianto di fitodepurazione per il finissaggio di reflui civili con piante ornamentali a confronto con piante tradizionali. *Università degli Studi di Padova. Tesi di Laurea*.

Maynard H. E., Ouky S. K., Williams S.C. (1998). Tertiary lagoons: a review of removal mechanisms and performance. *Wat. Res. Vol. 33, No. 1, pp. 1±13*.

Mayo A.W. (2004). Kinetics of bacterial mortality in granular bed wetlands. *Physics and Chemistry of the Earth 29 1259–1264*.

Mayo A.W., Bigambo T. (2005). Nitrogen transformation in horizontal subsurface flow constructed wetlands I: Model development. *Physics and Chemistry of the Earth 30 (2005) 658–667*.

Mayo A.W., Kalibbala M. (2007). Modelling faecal coliform mortality in water hyacinths ponds. *Physics and Chemistry of the Earth 32 1212–1220*.

Rousseau D.P.L., Vanrolleghem P.A., De Pauw N. (2004). Model-based design of horizontal subsurface flow constructed treatment wetlands: a review. *Water Research 38 (2004) 1484–1493*.

Runkel L.R. (1998). One-dimensional Transport with Inflow and Storage (OTIS): A solute transport model of streams and rivers, *U. S. Geol. Surv. Water Resour. Invest., 98 – 4018*.

Senzia M.A., Mayo A.W., Mbwette T.S.A., Katima J.H.Y., Jørgensen S.E. (2002). Modelling nitrogen transformation and removal in primary facultative ponds. *Ecological Modelling 154 (2002) 207–215.*

Stevik Tor K., Kari A., Geir A., Fredrik Hanssen J. (2004). Retention and removal of pathogenic bacteria in wastewater percolating through porous media: a review. *Water Research 38 1355–1367*.

Tamburini M. (2010): Rimessa in opera di un impianto di fitodepurazione per l'affinamento di reflui civili: verifica della funzionalità e dell'efficenza depurativa e confronto con uno dei metodi di affinamento tradizionale. *Università degli Studi di Padova. Tesi di Laurea*.

Tchobanoglous G., Mohammad A., Franklin L. Burton, Gregory B., Metcalf & Eddy, H. D. Stensel, William Pfrang, McGraw-Hill Education (2014). Wastewater Engineering: Treatment and Resource Recovery. *McGraw-Hill Education, 2014*.

Toscano A., Langergraber G., Consoli S., Cirelli G.L. (2009). *Modelling pollutant removal in a pilot-scale two-stage subsurface flow constructed wetlands*. ecological engineering 3 5 (2009) 281–289.

Trang N.T.D., Konnerup D., Schierup H., Chiem N. H., Tuan L., Brix H. (2010). *Kinetics of pollutant removal from domestic wastewater in a tropical horizontal subsurface flow constructed wetland system: Effects of hydraulic loading rate*. Ecological Engineering 36 (2010) 527–535.

Von Spetling M. (1998). Performance evaluation and mathematical modelling of coliform die-off in tropical and sub-tropical waste stabilization ponds. W*at.Res.Vol.33, No.6, pp. 1435±1448*.

Vymazal J. (2007). Removal of nutrients in various types of constructed wetlands. *Science of the Total Environment 380 (2007) 48–65*.

Vymazal J. (2014). Constructed wetlands for treatment of industrial wastewaters: A review. *Ecological Engineering 73 (2014) 724–751.*

Vymazal J., Brix H., Cooper P. F., Halber R., Perfler R., Laber J. (1998). *Removal mechanisms and type of constructed wetland*. Constructed wetland for wastewater treatment in Europe, pp. 17-56.

Vymazal J., Kröpfelová L. (2008). Wastewater Treatment in Constructed Wetlands with Horizontal Sub-Surface Flow. *Springer Science & Business Media, 2008*.

Wang Yanhua, Jixiang Zhang, Hainan Kong, Yuhei Inamori, Kaiqin Xu, Ryuhei Inamori, Takashi Kondo (2009). A simulation model of nitrogen transformation in reed constructed wetlands. *Desalination 235 (2009) 93–101*.

Wu Haiming, Jian Zhang, Huu Hao Ngo, Wenshan Guo, Zhen Hu, Shuang Liang, Jinlin Fan, Hai Liu (2015). A review on the sustainability of constructed wetlands for wastewater treatment: Design and operation. *Bioresource Technology 175 (2015) 594–60.*

Xu P, F. Brissaud, A. Fazio. (2002). Non-steady-state modelling of faecal coliform removal in deep tertiary lagoons. *Water Research 36 (2002) 3074–3082*.

ATTACHMENT 1

1.1 Results of implementation of first order kinetic models in tank A

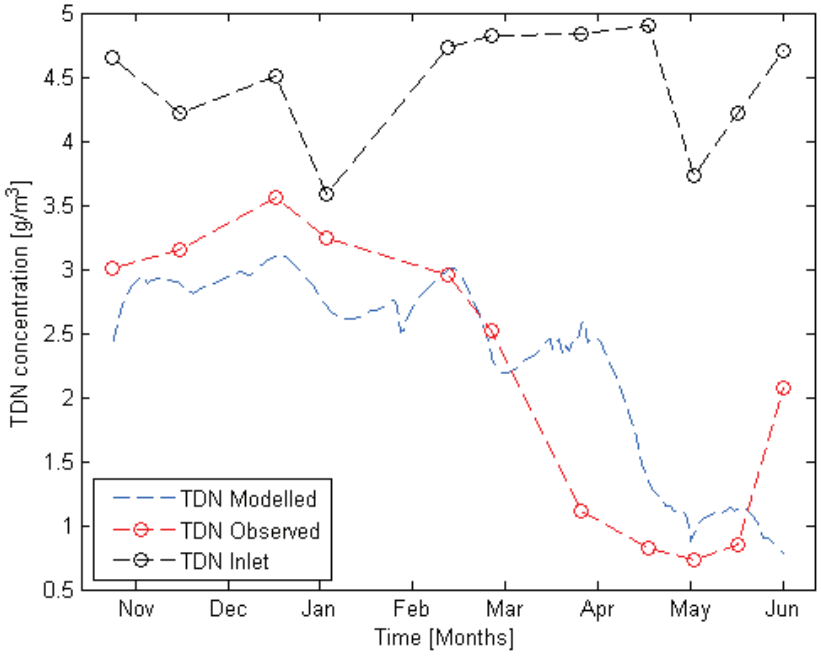

Figure 1.1.1: TDN inlet and observed in tank A and modelled using a CSTR with a first order kinetic model

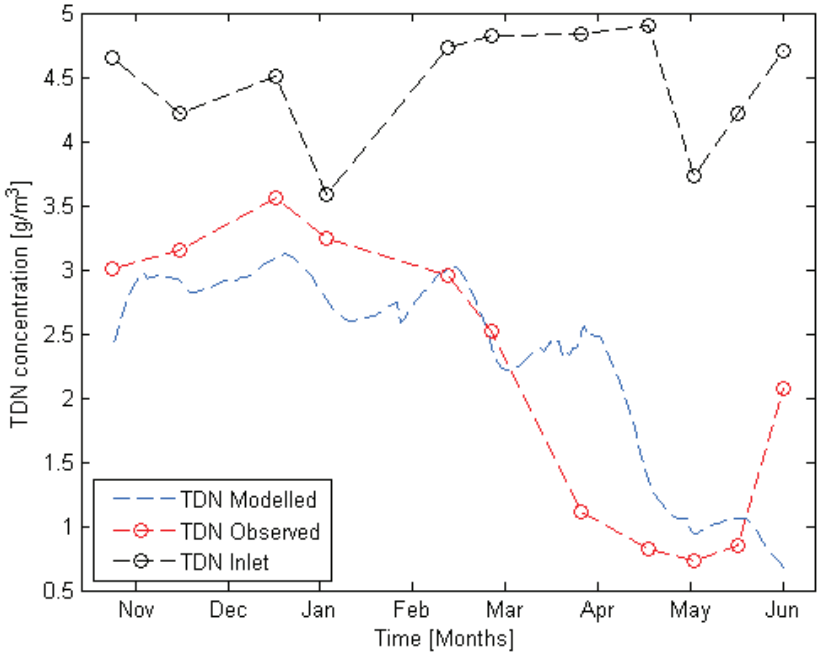

Figure 1.1.2: TDN inlet and observed in tank A and modelled using a CSTR in series with a first order kinetic model

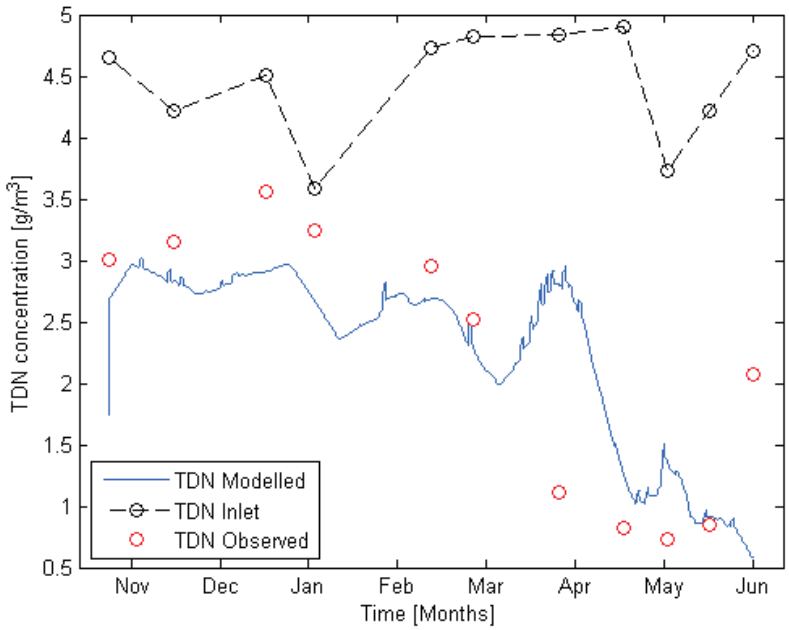

Figure 1.1.3: TDN inlet and observed in tank A and modelled using a Plug and Flow with a first order kinetic model

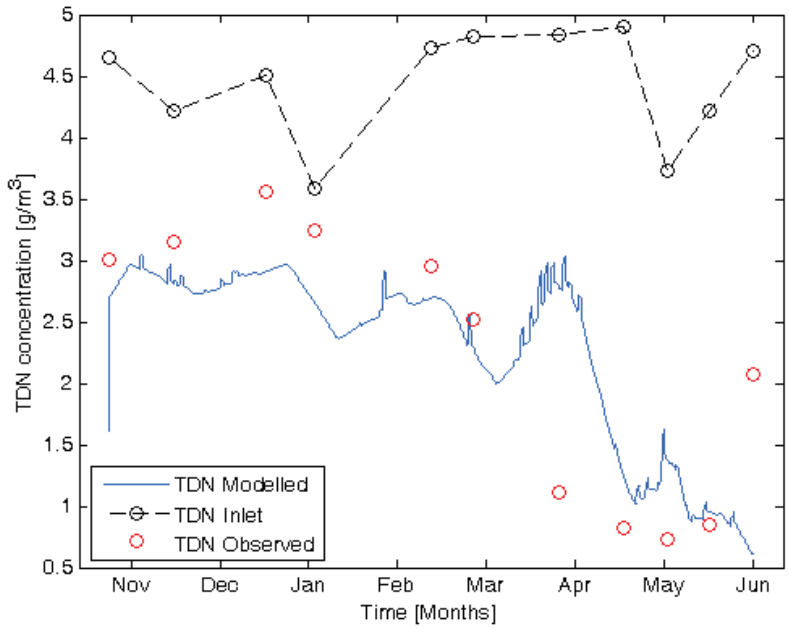

Figure 1.1.4: TDN inlet and observed in tank A and modelled using a Plug and Flow with dead zone and a first order kinetic model

1.2. Results of validation of first order kinetic models in tank A

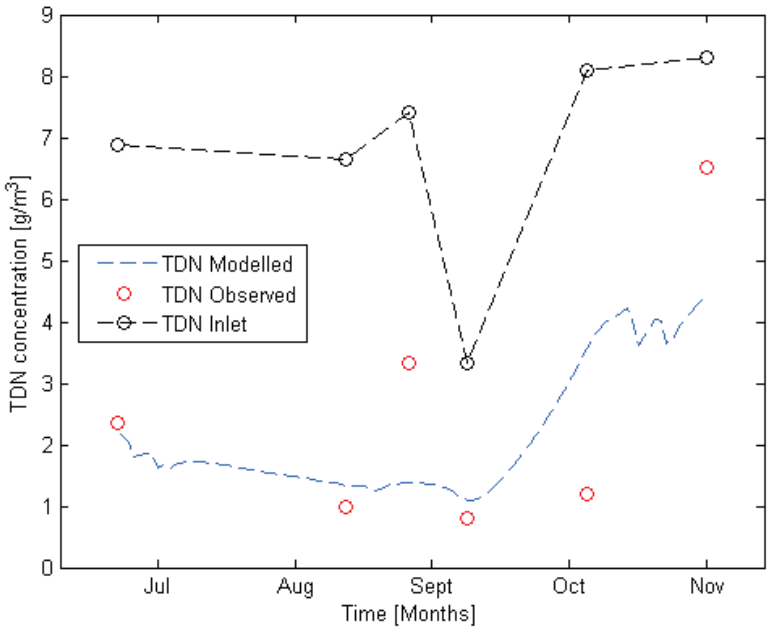

Figure 1.1.5: TDN inlet and observed in tank A and modelled using a CSTR with a first order kinetic model: validated model

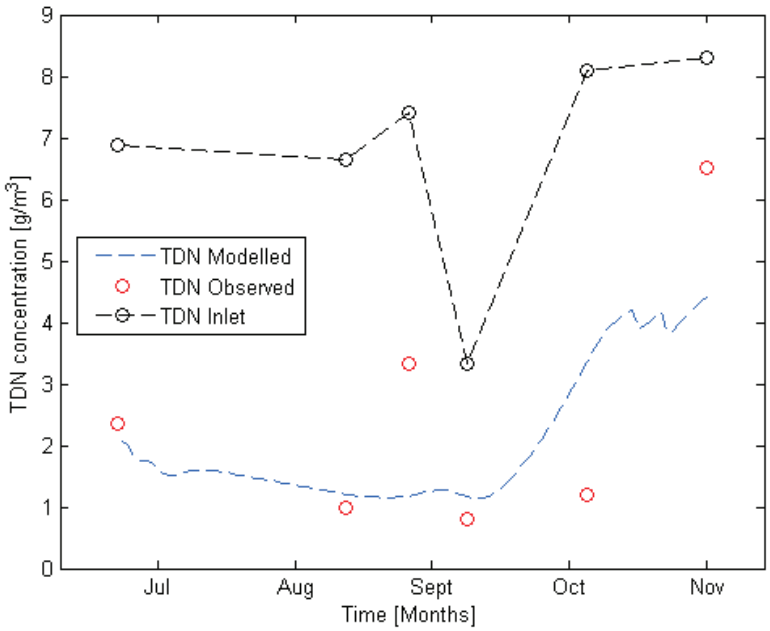

Figure 1.1.6: TDN inlet and observed in tank A and modelled using a CSTR in series with a first order kinetic model: validated model

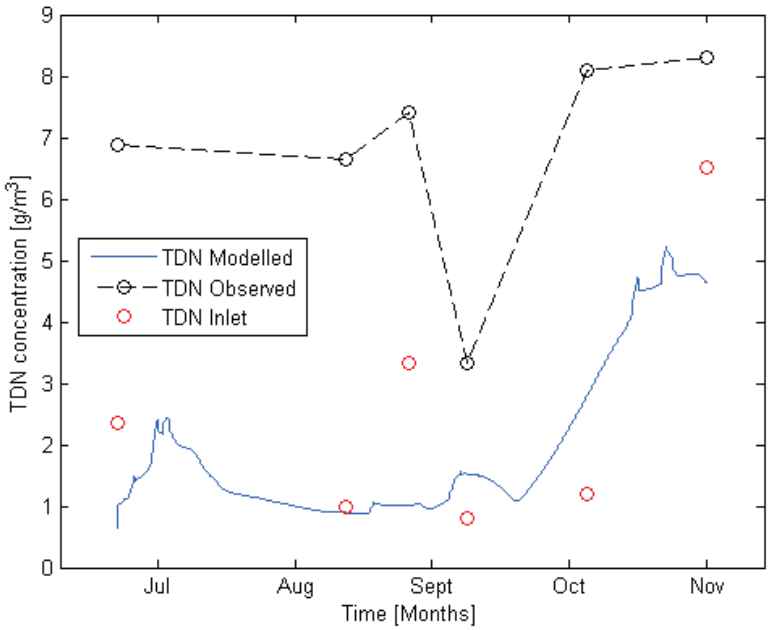

Figure 1.1.7: TDN inlet and observed in tank A and modelled using a Plug and Flow with a first order kinetic model: validated model

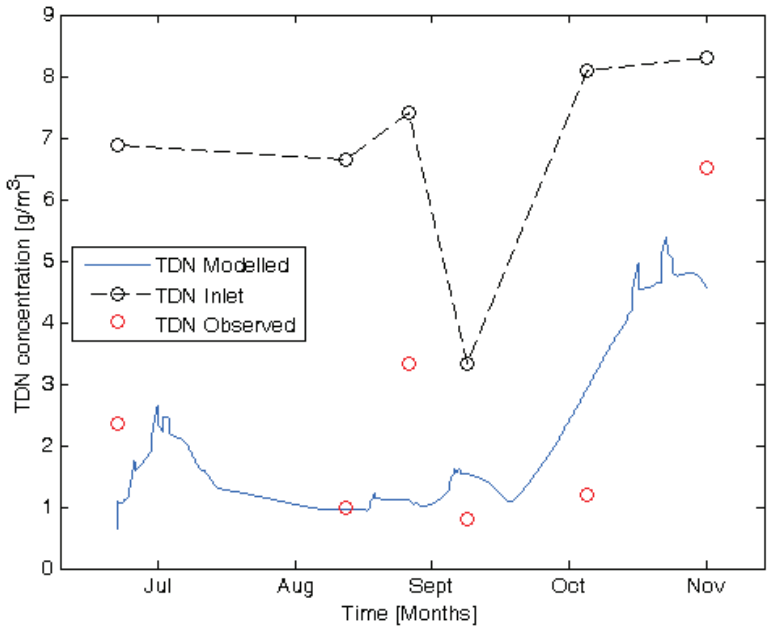

Figure 1.1.8: TDN inlet and observed in tank A and modelled using a Plug and Flow with dead zone and a first order kinetic model: validated model

1.3. Results of implementation of first order kinetic models in tank B

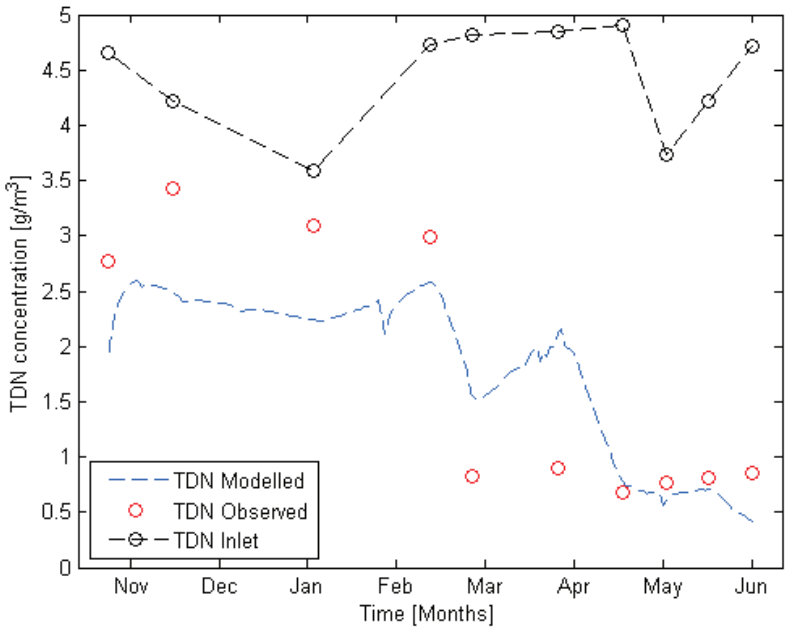

Figure 1.1.9: TDN inlet and observed in tank B and modelled using a CSTR with a first order kinetic model

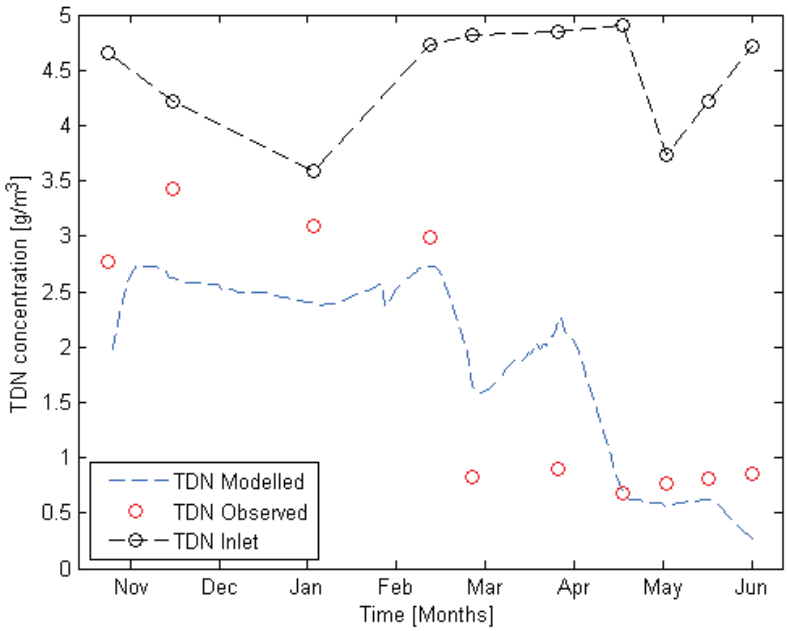

Figure 1.1.10: TDN inlet and observed in tank B and modelled using a CSTR in series with a first order kinetic model

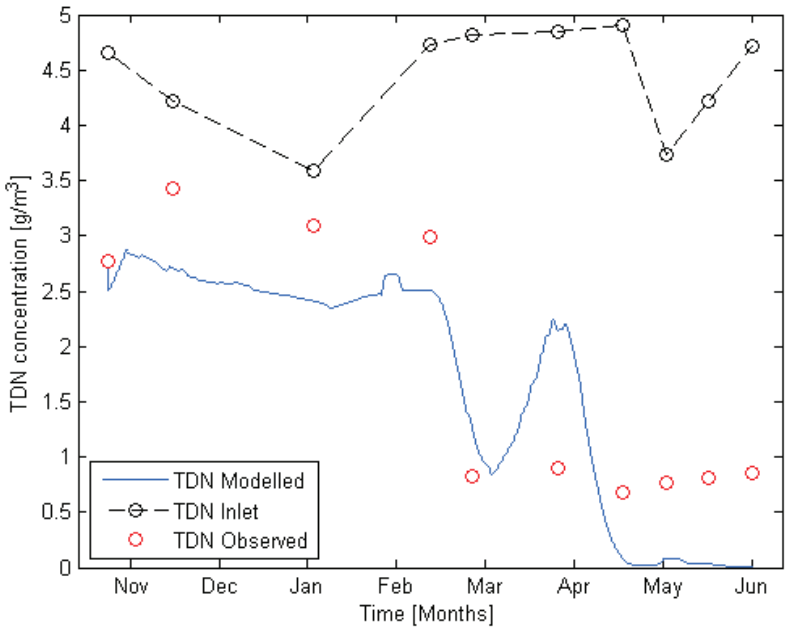

Figure 1.1.11: TDN inlet and observed in tank B and modelled using a Plug and Flow with a first order kinetic model

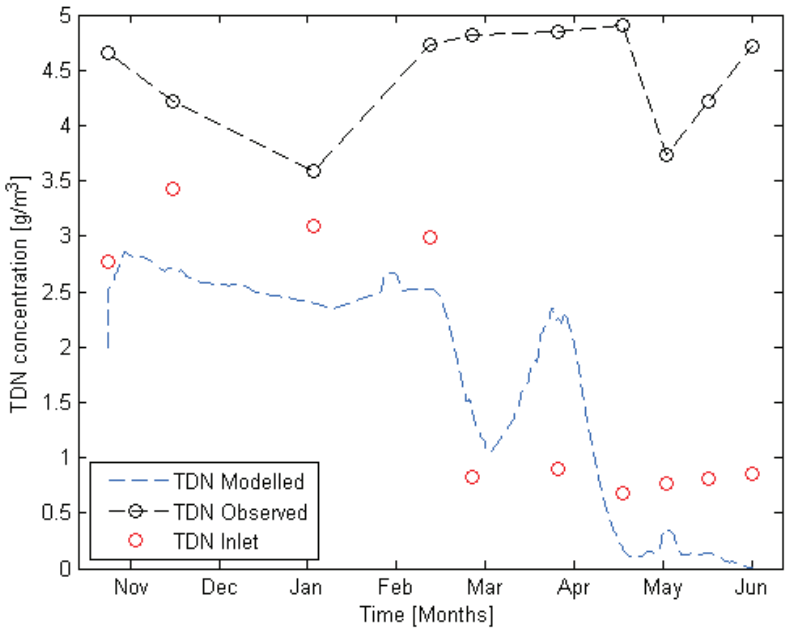

Figure 1.1.12: TDN inlet and observed in tank B and modelled using a Plug and Flow with dead zone and a first order kinetic model

1.4. Results of validation of first order kinetic models in tank B

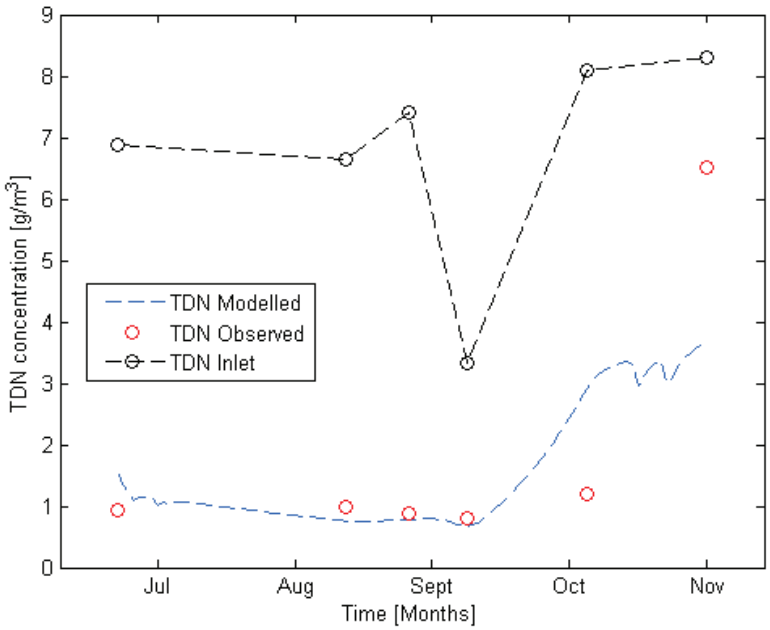

Figure 1.1.13: TDN inlet and observed in tank B and modelled using a CSTR with a first order kinetic model: validated model

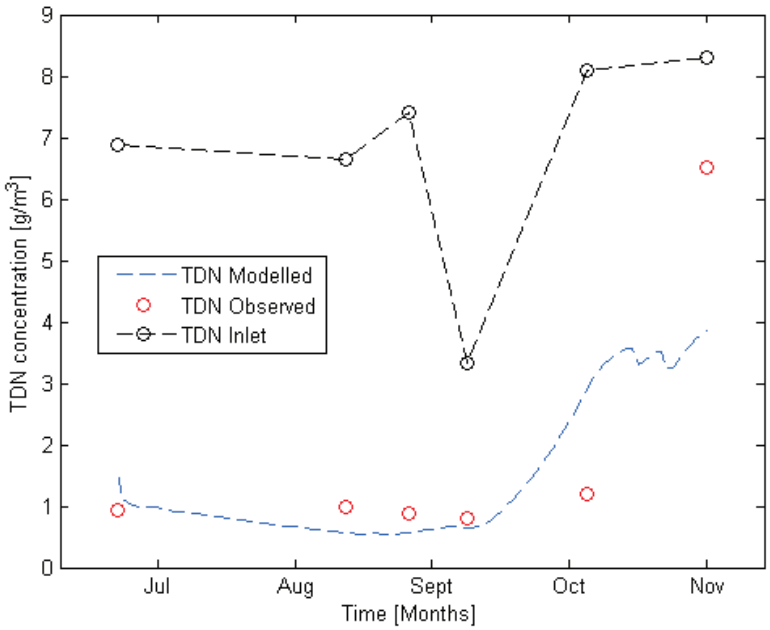

Figure 1.1.14: TDN inlet and observed in tank B and modelled using a CSTR in series with a first order kinetic model: validated model

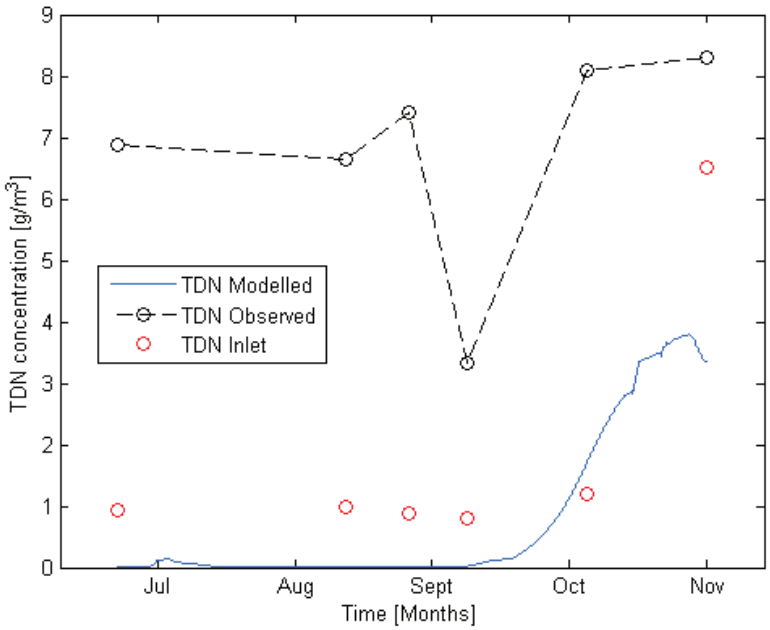

Figure 1.1.15: TDN inlet and observed in tank B and modelled using a Plug and Flow with a first order kinetic model: validated model

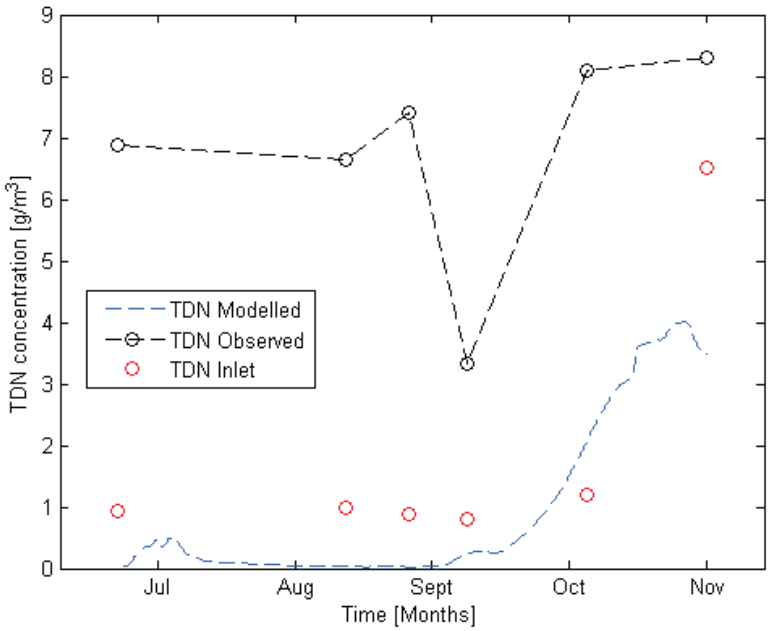

Figure 1.1.16: TDN inlet and observed in tank A and modelled using a Plug and Flow with dead zone and a first order kinetic model: validated model

ATTACHMENT 2

2.1. Results of implementation of model n°2 in tank A

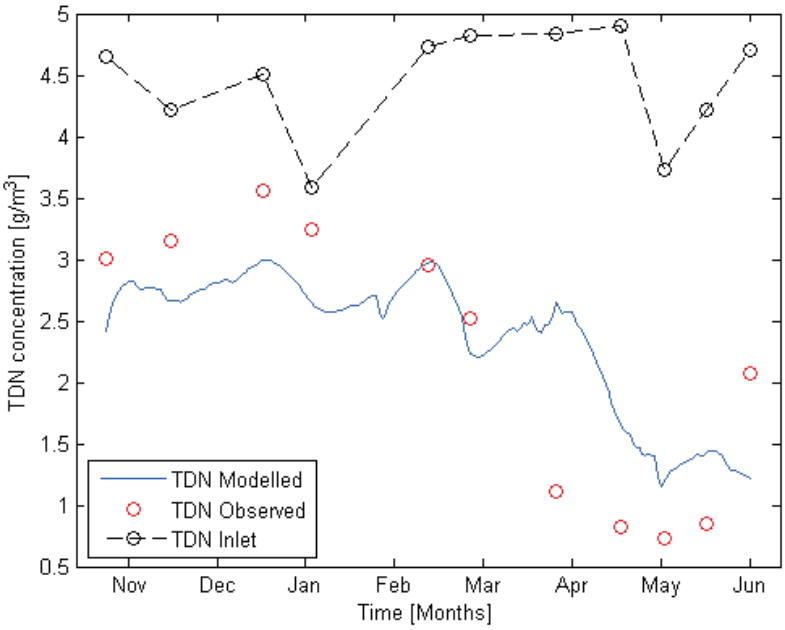

Figure 2.1.1: TDN inlet and observed in tank A and modelled using the model n°2 with a CSTR reactor model

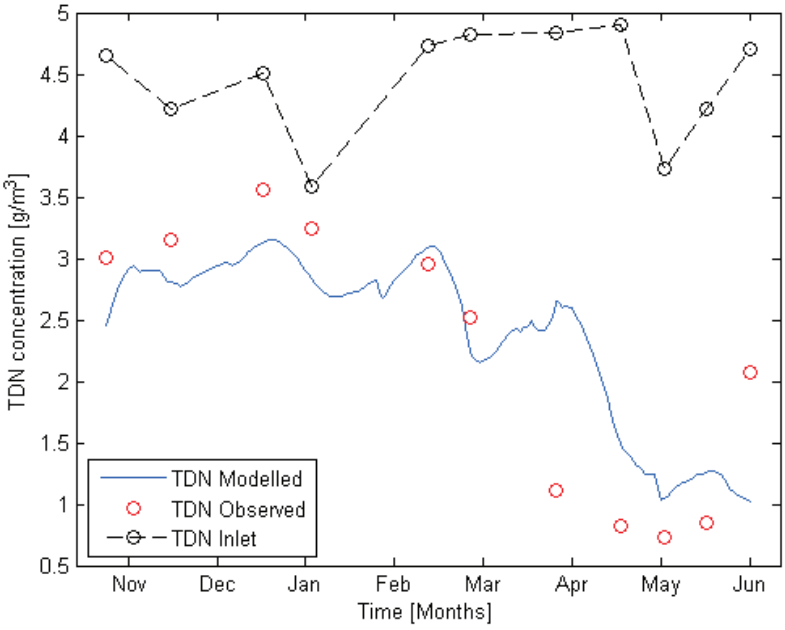

Figure 2.1.2: TDN inlet and observed in tank A and modelled using the model n°2 with a CSTR in series reactor model

2.2 Results of validation of model n°2 in tank A

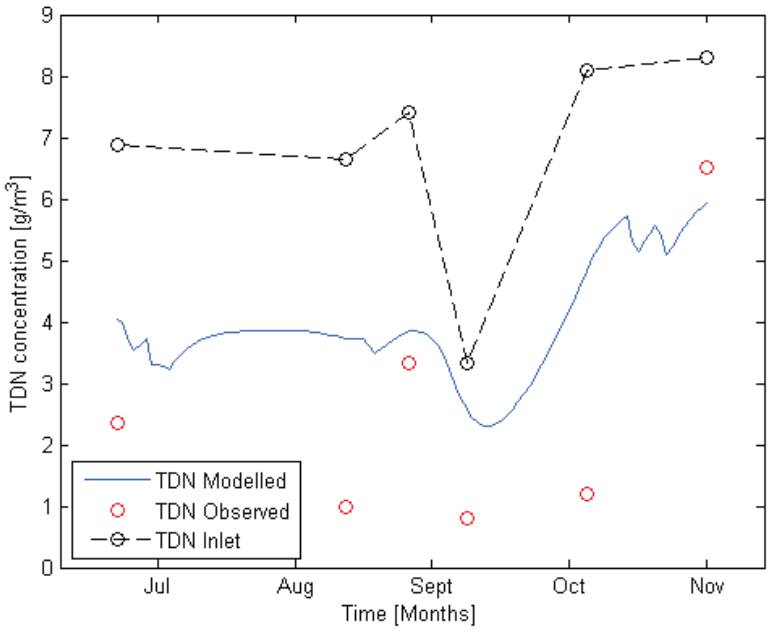

Figure 2.1.3: TDN inlet and observed in tank A and modelled using the model n°2 with a CSTR reactor model: validated model

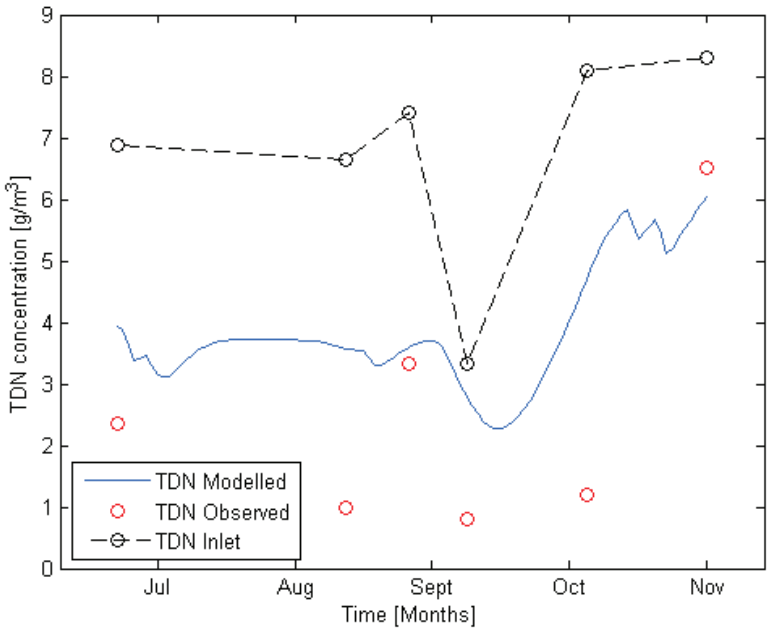

Figure 2.1.4: TDN inlet and observed in tank A and modelled using the model n°2 with a CSTR in series reactor model: validated model

2.3 Results of implementation of model n°2 in tank B

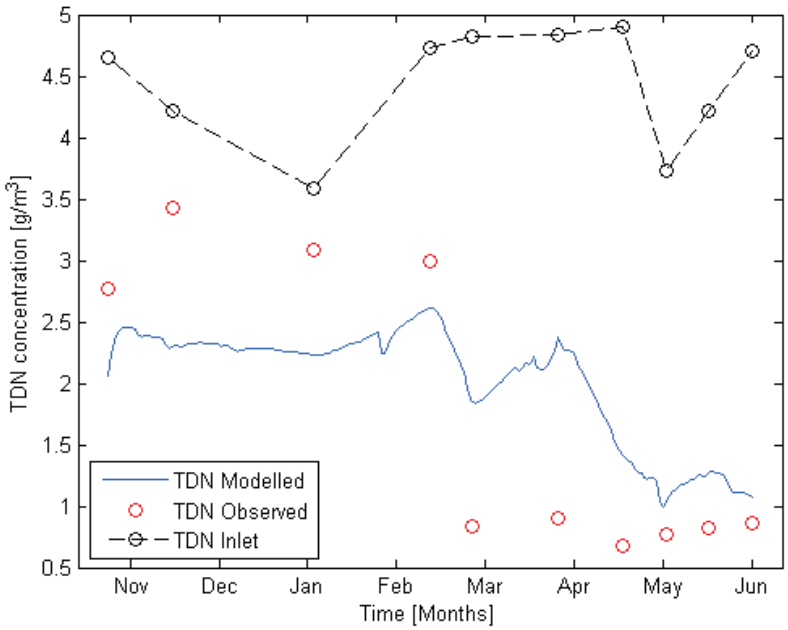

Figure 2.1.5: TDN inlet and observed in tank B and modelled using the model n°2 with a CSTR reactor model

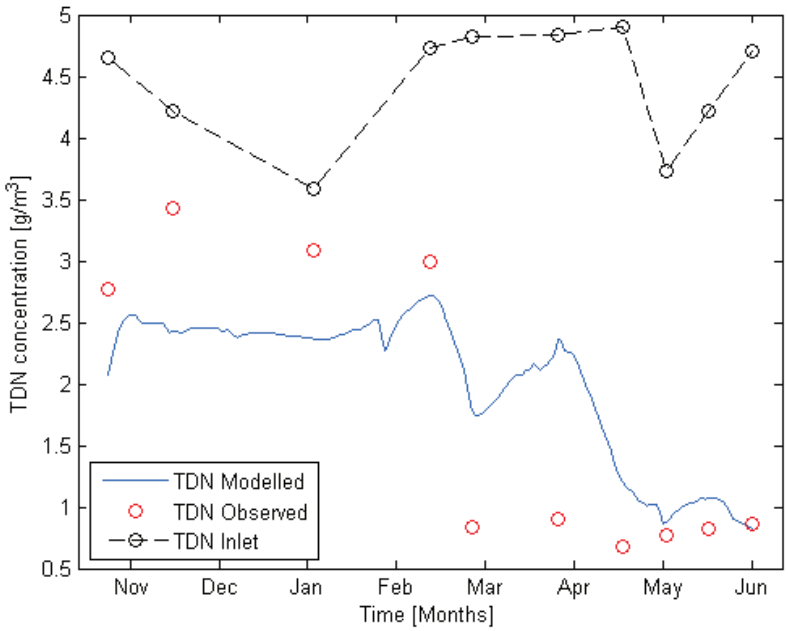

Figure 2.1.6: TDN inlet and observed in tank B and modelled using the model n°2 with a CSTR in series reactor model

2.4 Results of validation of model n°2 in tank B

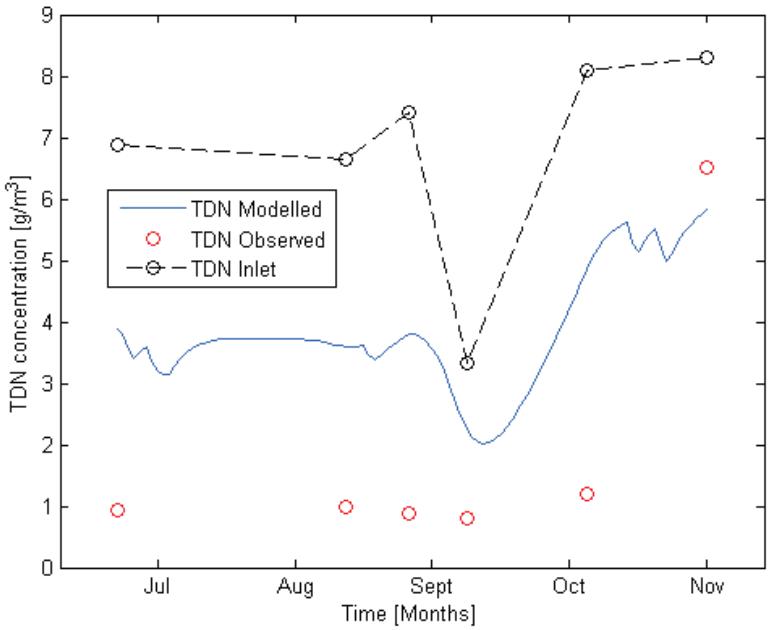

Figure 2.1.7: TDN inlet and observed in tank B and modelled using the model n°2 with a CSTR reactor model: validated model

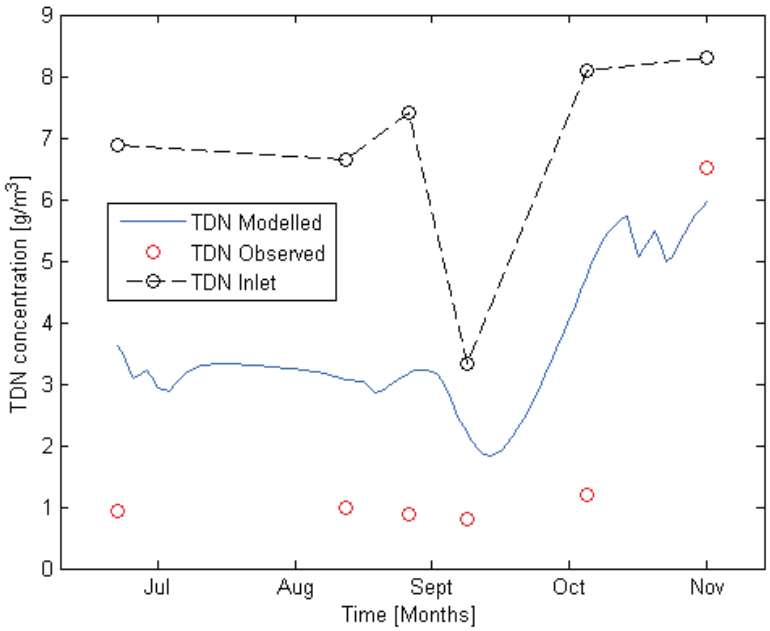

Figure 2.1.8: TDN inlet and observed in tank B and modelled using the model n°2 with a CSTR i series reactor model: validated model

2.5 Results of implementation of model n°3 in tank A

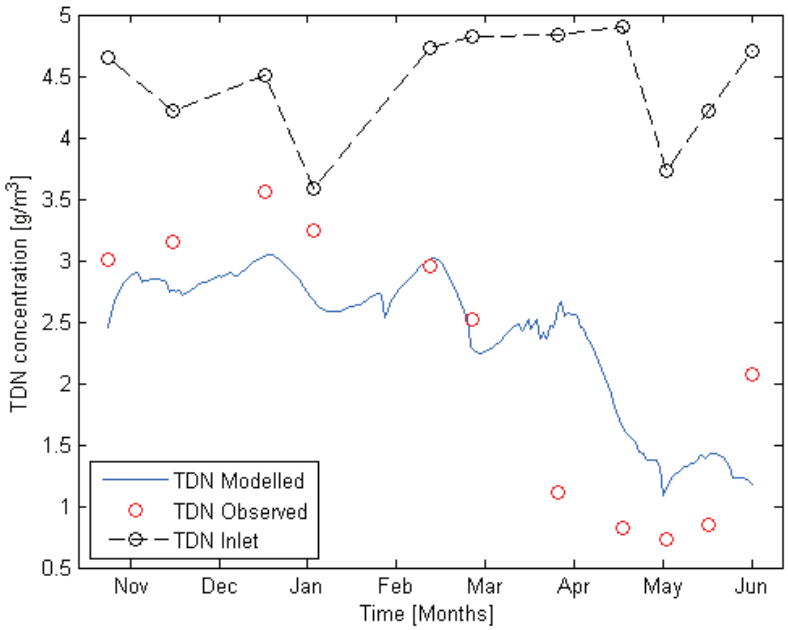

Figure 2.1.9: TDN inlet and observed in tank A and modelled using the model n°3 with a CSTR reactor model

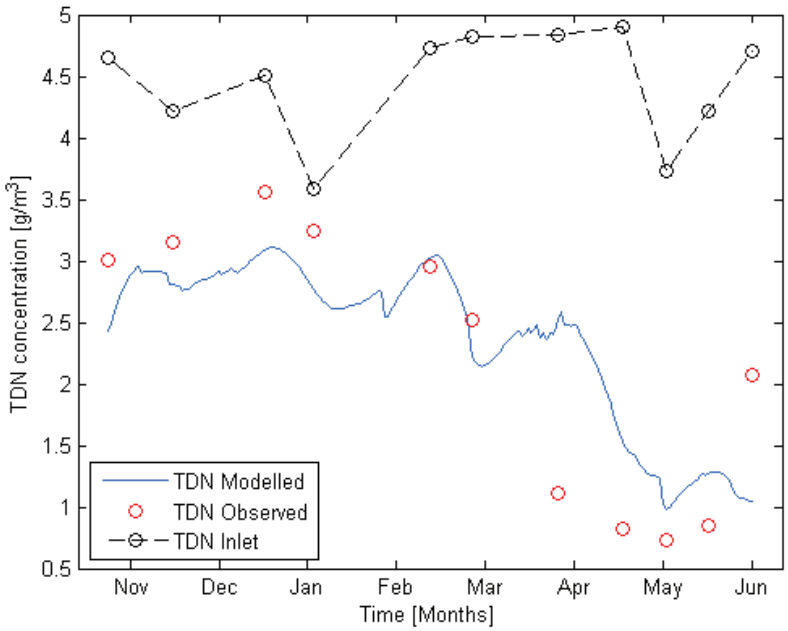

Figure 2.1.10: TDN inlet and observed in tank A and modelled using the model n°3 with a CSTR is series reactor model

2.6 Results of validation of model n°3 in tank A

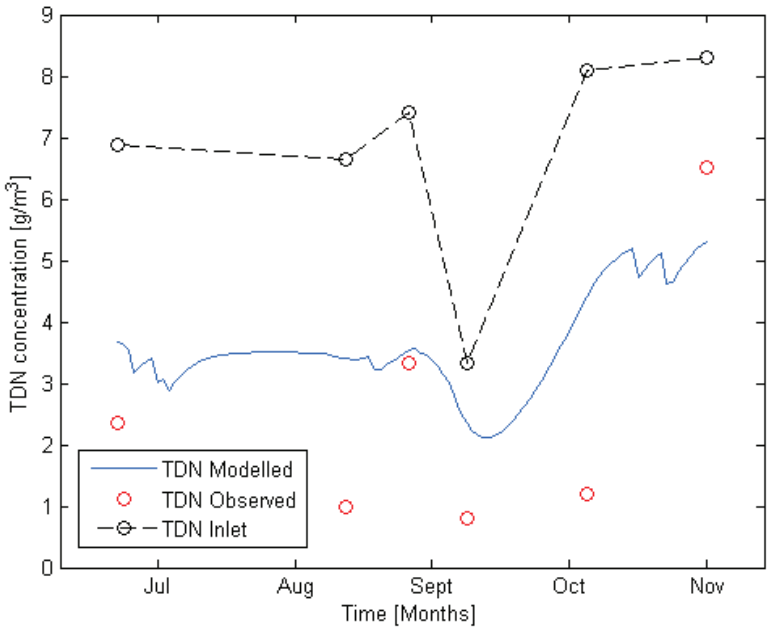

Figure 2.1.11: TDN inlet and observed in tank A and modelled using the model n°3 with a CSTR reactor model: validated model

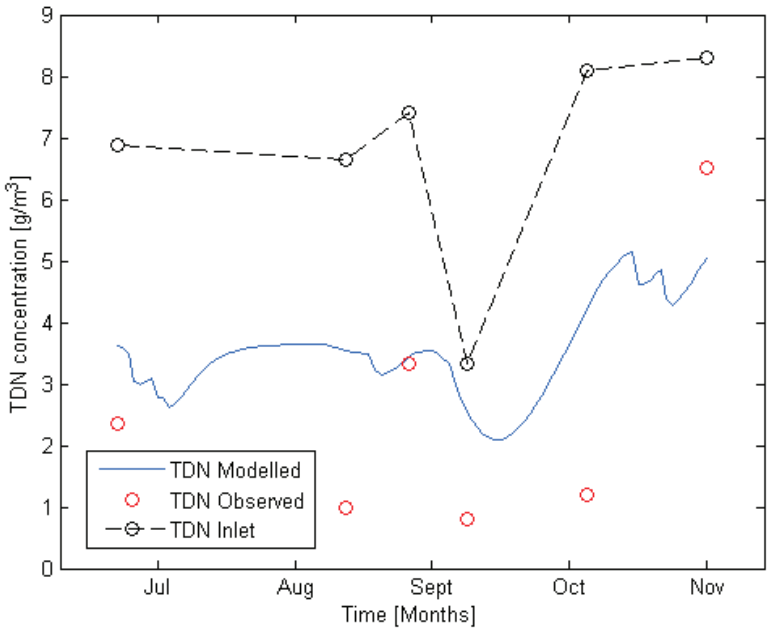

Figure 2.1.12: TDN inlet and observed in tank A and modelled using the model n°3 with a CSTR in series reactor model: validated model

2.6 Results of implementation of model n°3 in tank B

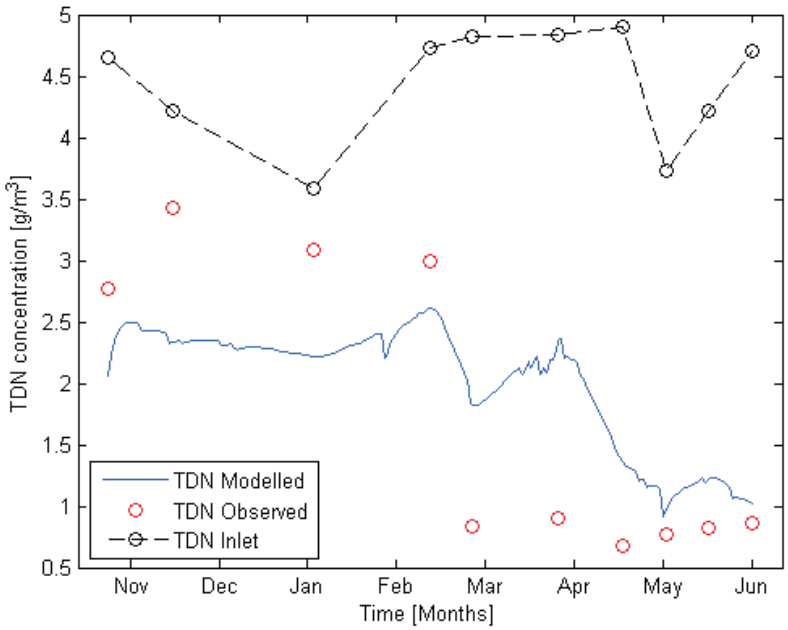

Figure 2.1.13: TDN inlet and observed in tank B and modelled using the model n°3 with a CSTR reactor model

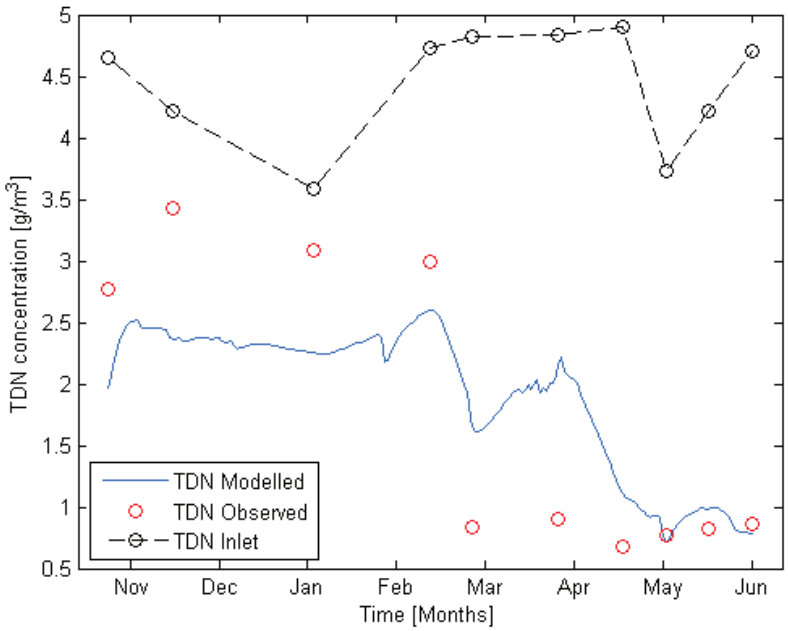

Figure 2.1.14: TDN inlet and observed in tank B and modelled using the model n°3 with a CSTR in series reactor model

2.8 Results of validation of model n°3 in tank B

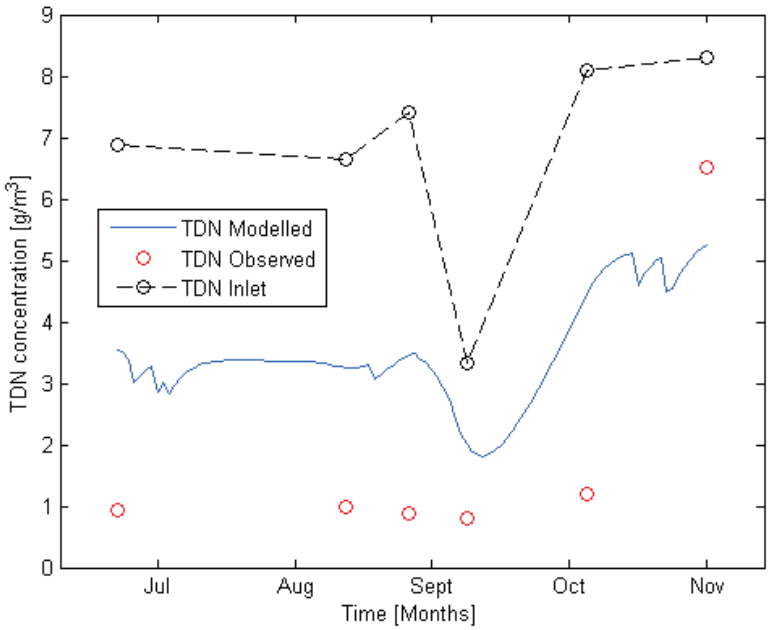

Figure 2.1.15: TDN inlet and observed in tank B and modelled using the model n°3 with a CSTR reactor model: validated model

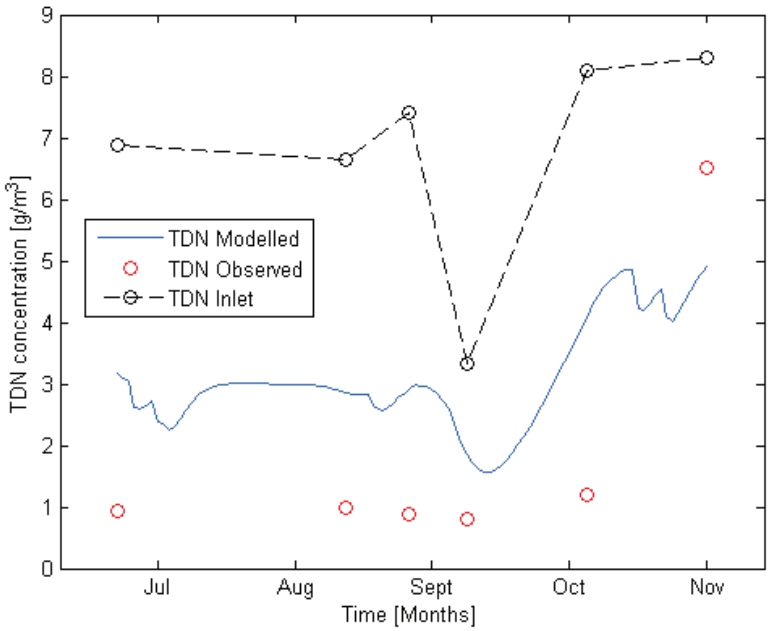

Figure 2.1.16: TDN inlet and observed in tank B and modelled using the model n°3 with a CSTR in series reactor model: validated model

ATTACHMENT 3

3.1. Results of implementation of first order kinetic models in tank A

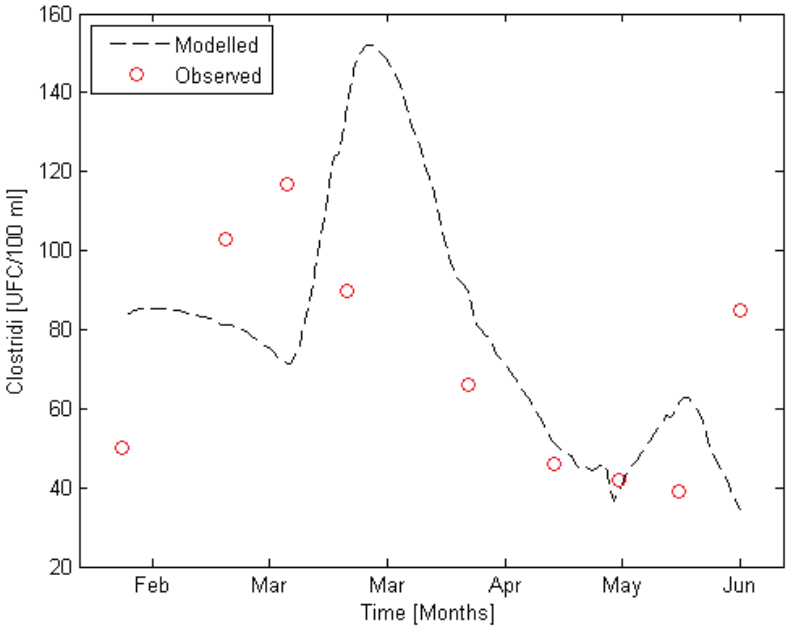

Figure 3.1.1: Clostridium observed in tank A and modelled using the first order kinetic model dependent on temperature with a CSTR reactor model

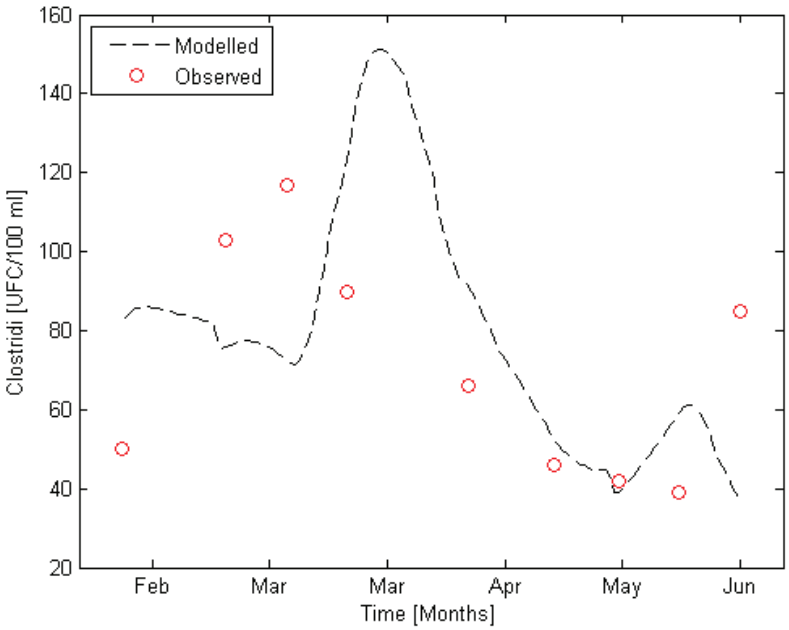

Figure 3.1.2: Clostridium observed in tank A and modelled using the first order kinetic model dependent on temperature with a CSTR in series reactor model

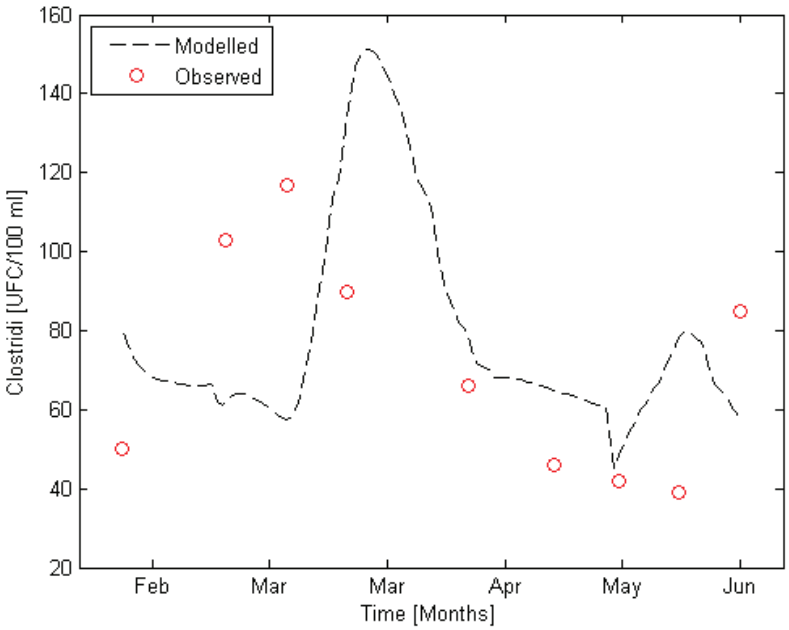

Figure 3.1.3: Clostridium observed in tank A and modelled using the first order kinetic model no dependent on temperature with a CSTR reactor model

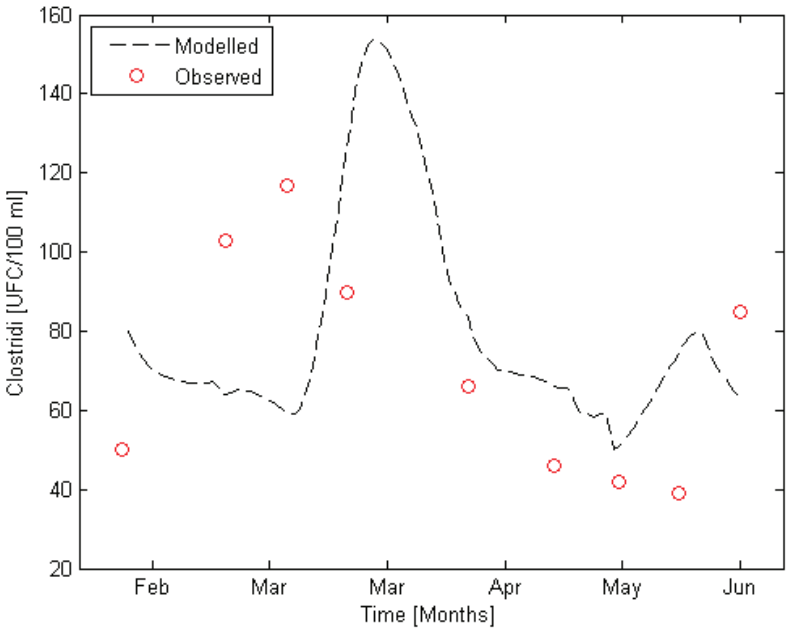

Figure 3.1.4: Clostridium observed in tank A and modelled using the first order kinetic model no dependent on temperature with a CSTR in series reactor model

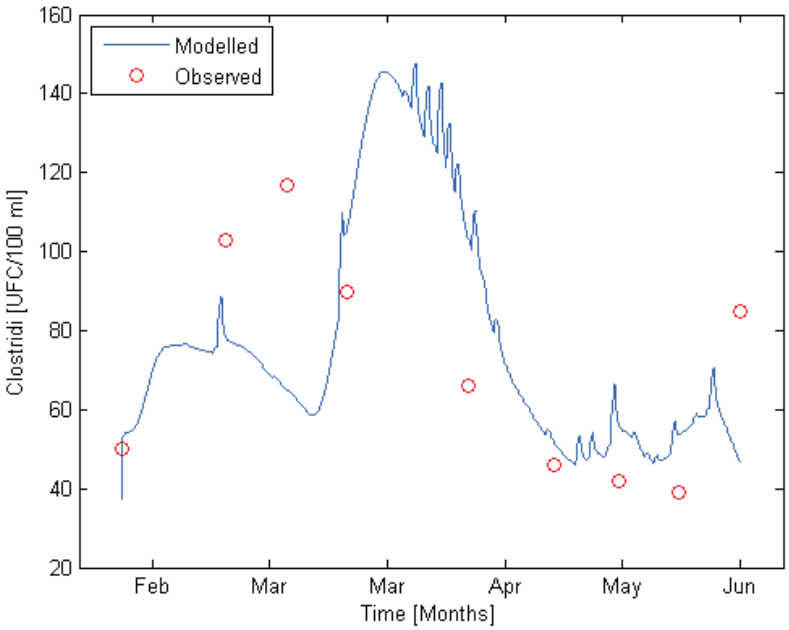

Figure 3.1.5: Clostridium observed in tank A and modelled using the first order kinetic model dependent on temperature with a P&F reactor model

3.2 Results of Validation of first order kinetic models in tank A

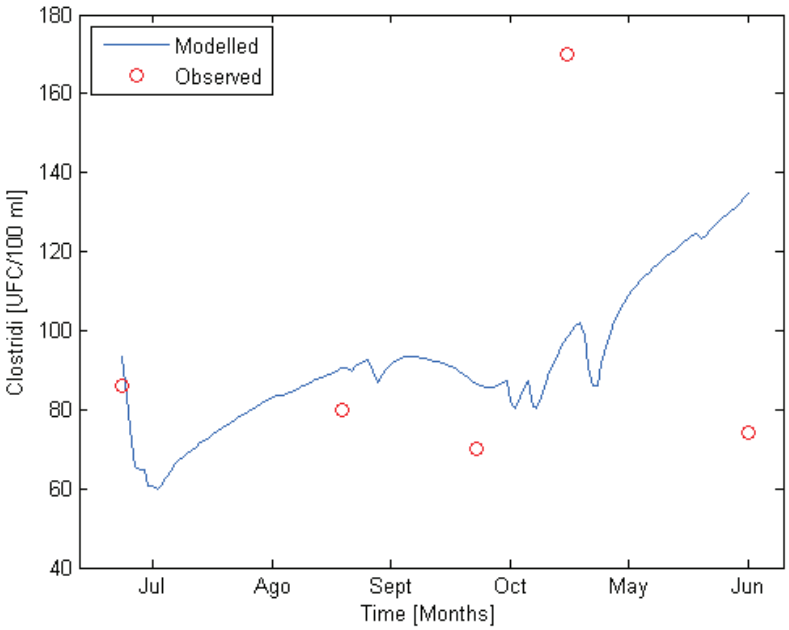

Figure 3.1.6: Clostridium observed in tank A and modelled using the first order kinetic model dependent on temperature with a CSTR reactor model. Model Validated

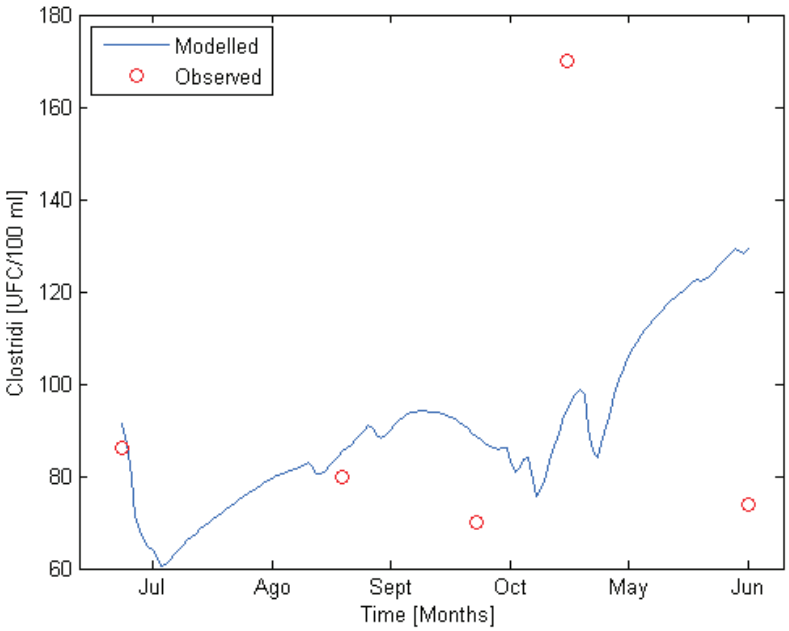

Figure 3.1.7: Clostridium observed in tank A and modelled using the first order kinetic model dependent on temperature with a CSTR in series reactor model: Validated Model

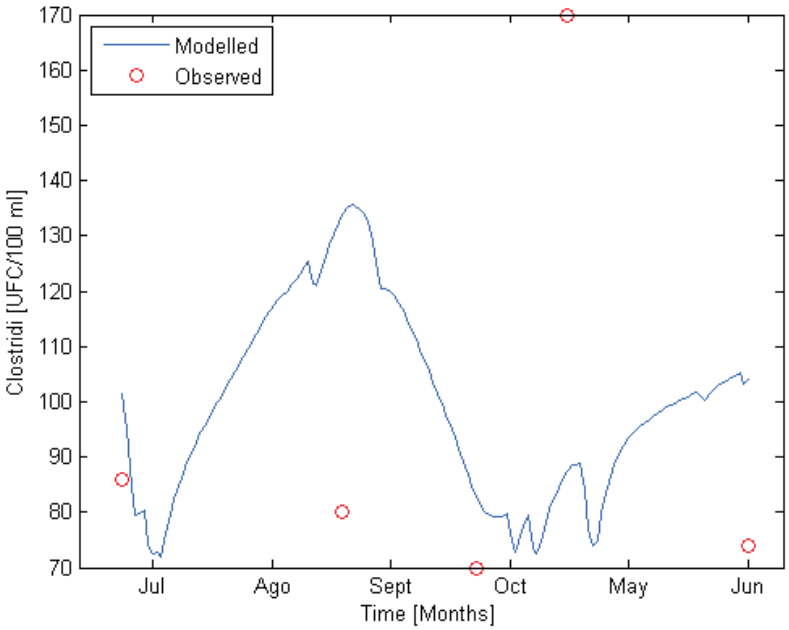

Figure 3.1.8: Clostridium observed in tank A and modelled using the first order kinetic model no dependent on temperature with a CSTR reactor model. Model Validated

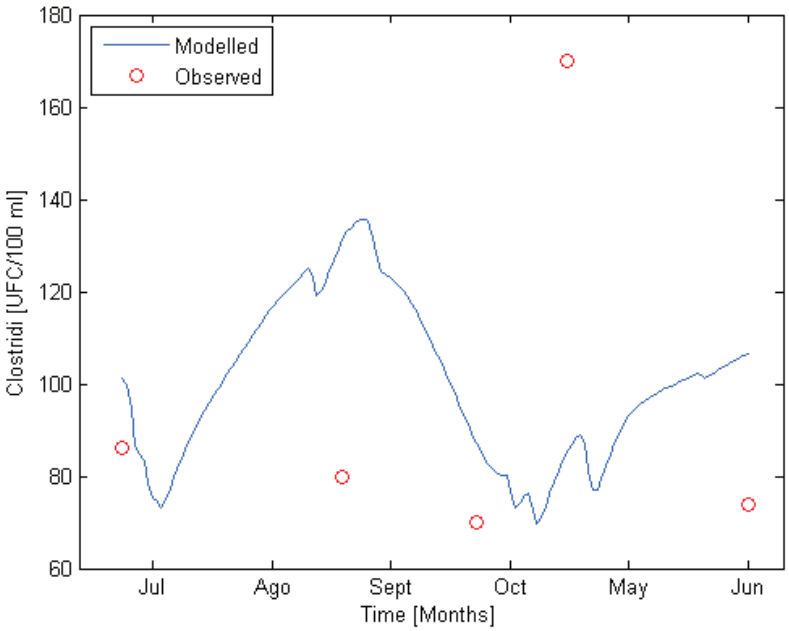

Figure 3.1.9: Clostridium observed in tank A and modelled using the first order kinetic model no dependent on temperature with a CSTR in series reactor model: Validated Model

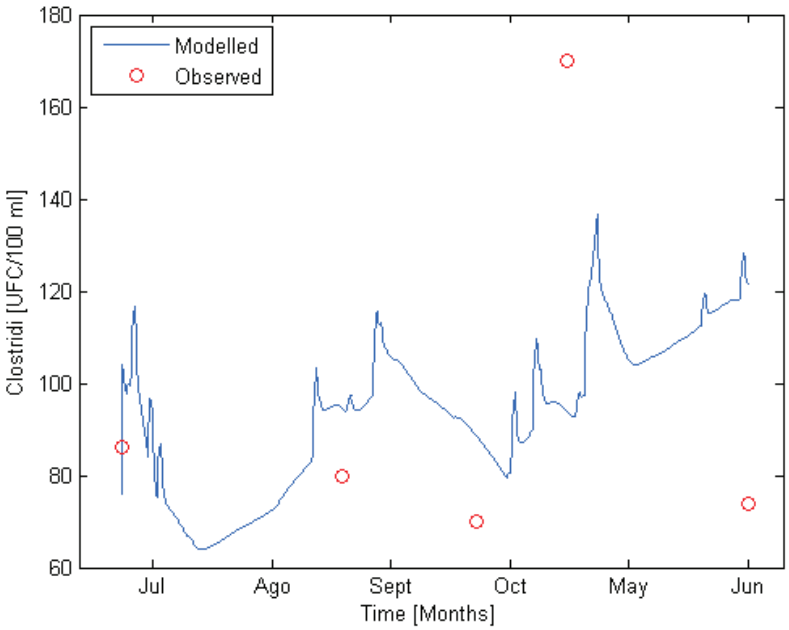

Figure 3.1.10: Clostridium observed in tank A and modelled using the first order kinetic model dependent on temperature with a P&F reactor model: Validated model

3.3 Results of implementation of first order kinetic models in tank B

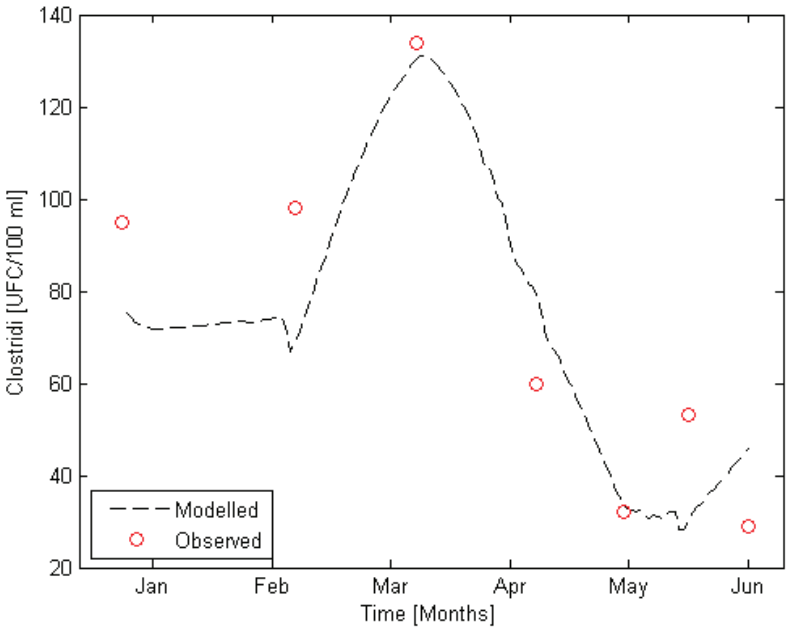

Figure 3.1.11: Clostridium observed in tank B and modelled using the first order kinetic model dependent on temperature with a CSTR reactor model

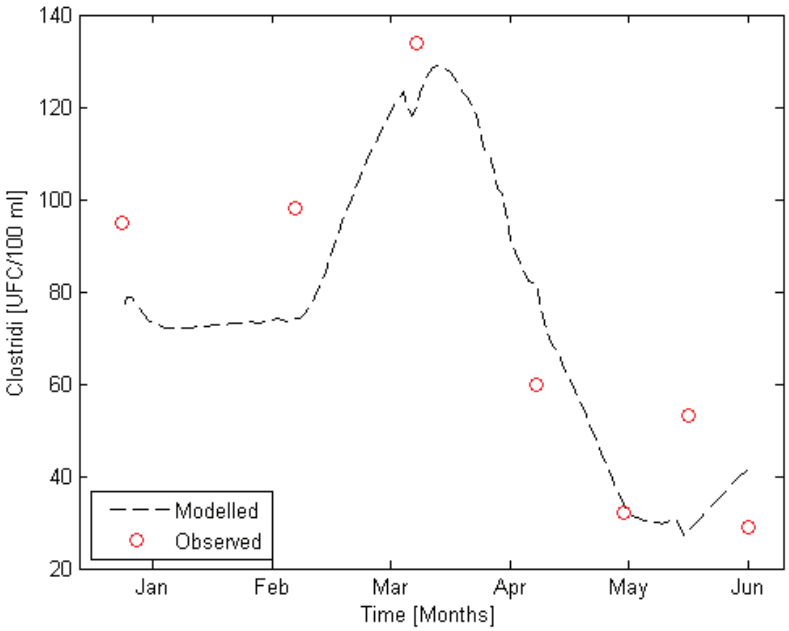

Figure 3.1.12: Clostridium observed in tank B and modelled using the first order kinetic model dependent on temperature with a CSTR in series reactor model

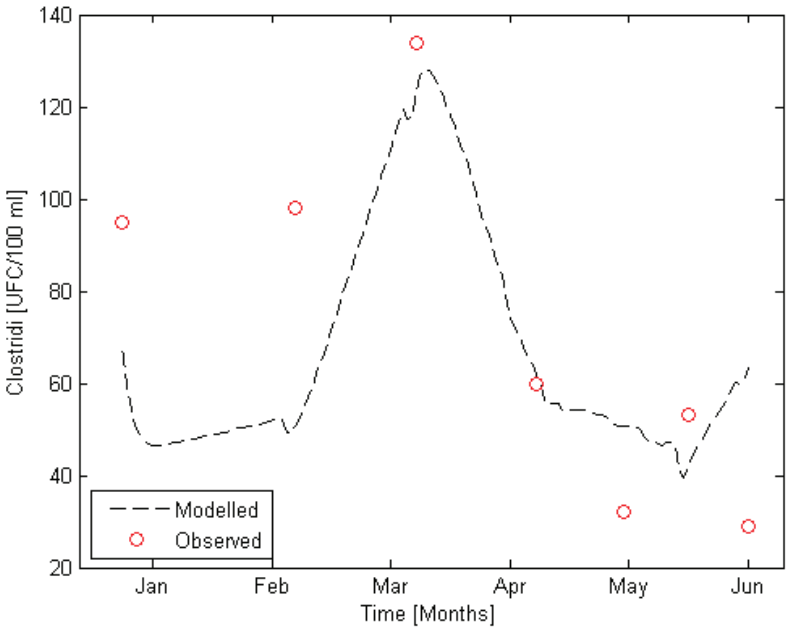

Figure 3.1.13: Clostridium observed in tank B and modelled using the first order kinetic model no dependent on temperature with a CSTR reactor model

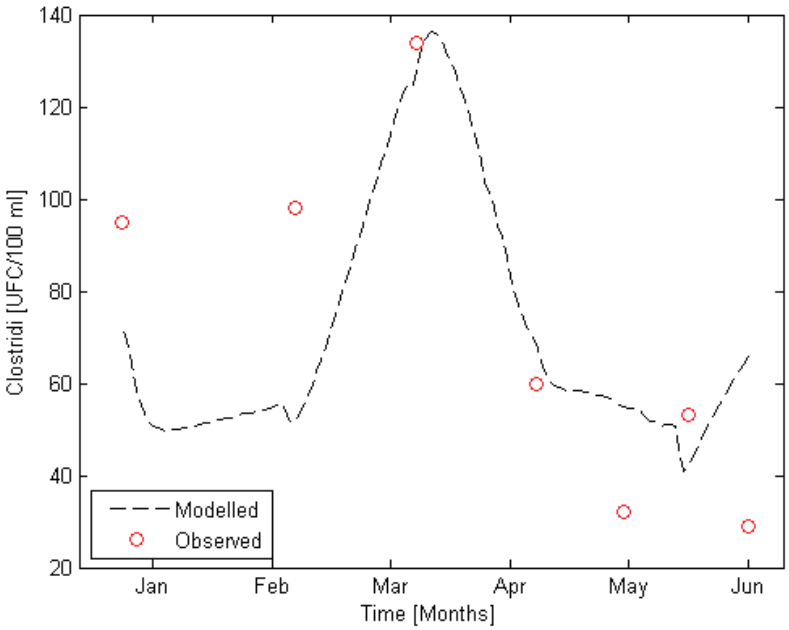

Figure 3.1.14: Clostridium observed in tank B and modelled using the first order kinetic model no dependent on temperature with a CSTR in series reactor model

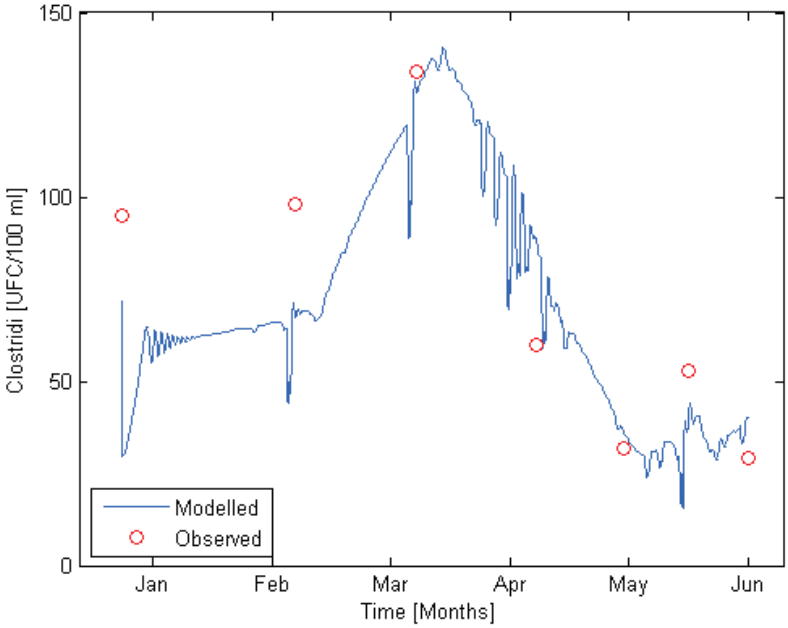

Figure 3.1.15: Clostridium observed in tank B and modelled using the first order kinetic model dependent on temperature with a P&F reactor model

3.4 Results of validation of first order kinetic models in tank B

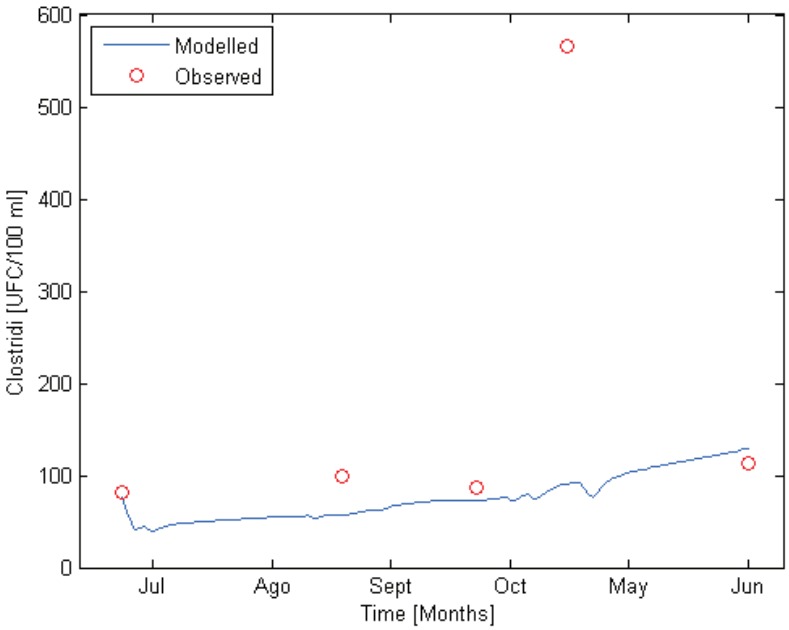

Figure 3.1.16: Clostridium observed in tank B and modelled using the first order kinetic model dependent on temperature with a CSTR reactor model. Model Validated

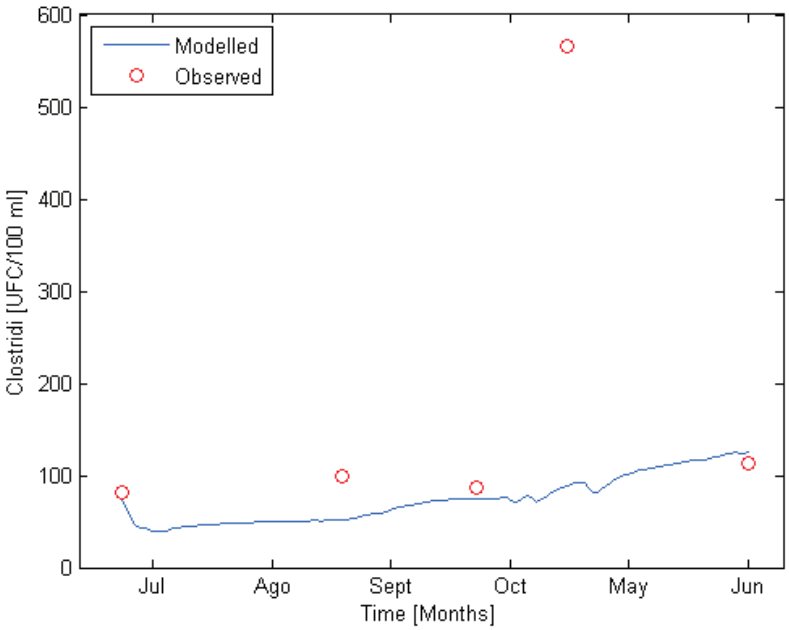

Figure 3.1.17: Clostridium observed in tank B and modelled using the first order kinetic model dependent on temperature with a CSTR in series reactor model. Model Validated

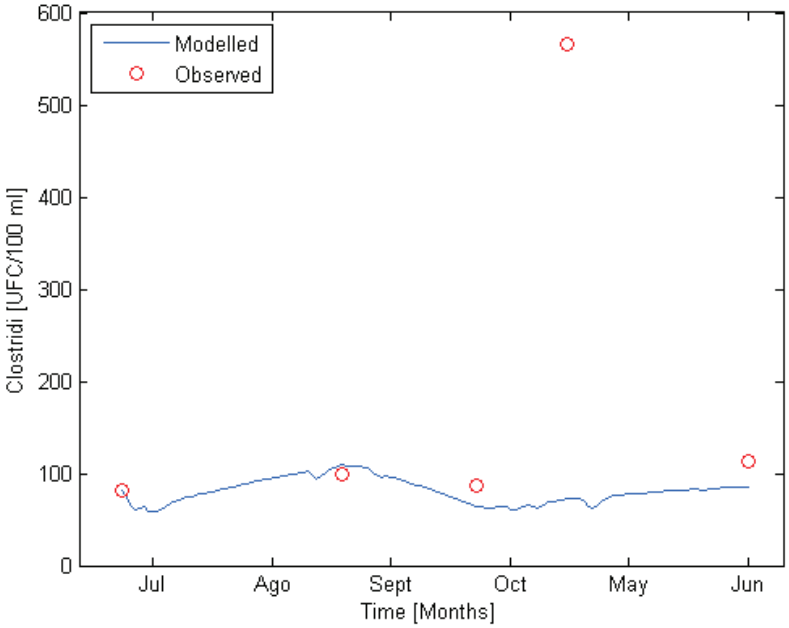

Figure 3.1.18: Clostridium observed in tank B and modelled using the first order kinetic model no dependent on temperature with a CSTR reactor model. Model Validated

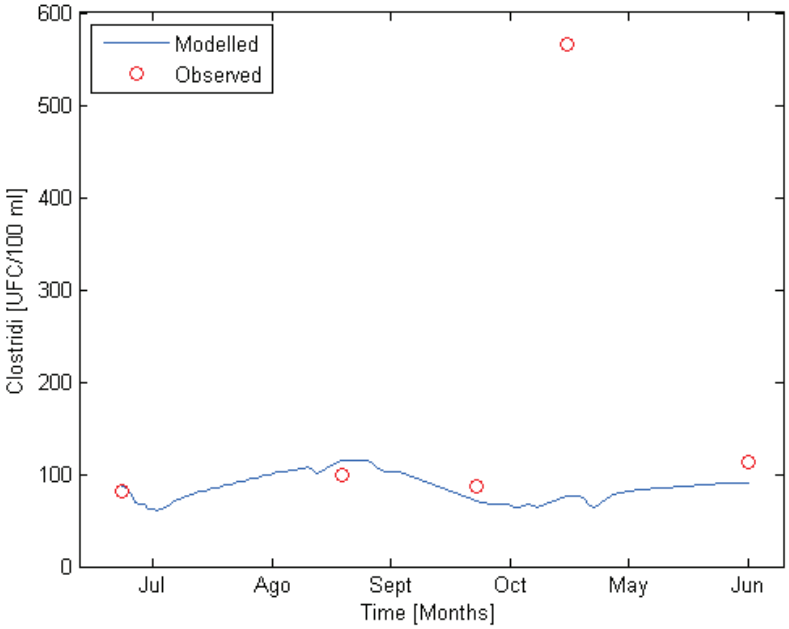

Figure 3.1.19: Clostridium observed in tank B and modelled using the first order kinetic model no dependent on temperature with a CSTR in series reactor model. Model Validated

ATTACHMENT 4

4.1. Results of implementation of first order kinetic models in tank A

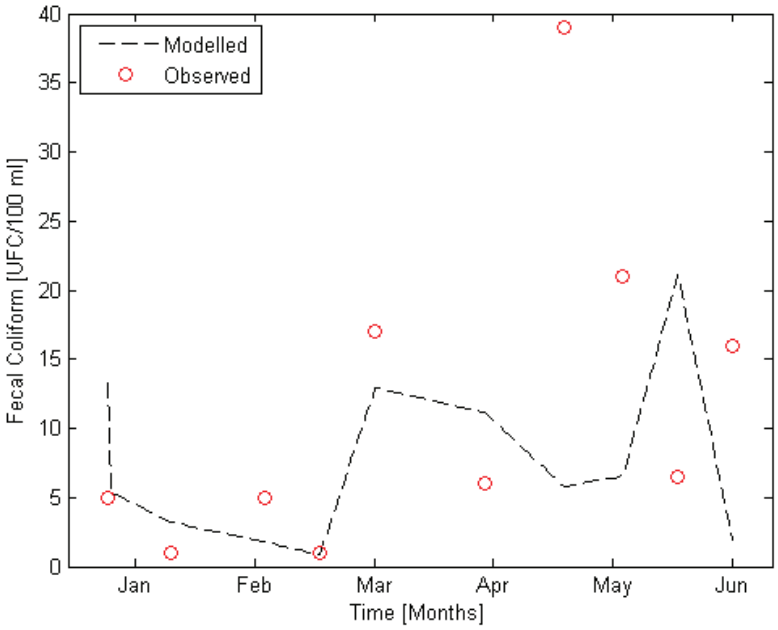

Figure 4.1.1: Fecal Coliform observed in tank A and modelled using the first order kinetic model dependent on temperature with a CSTR reactor model

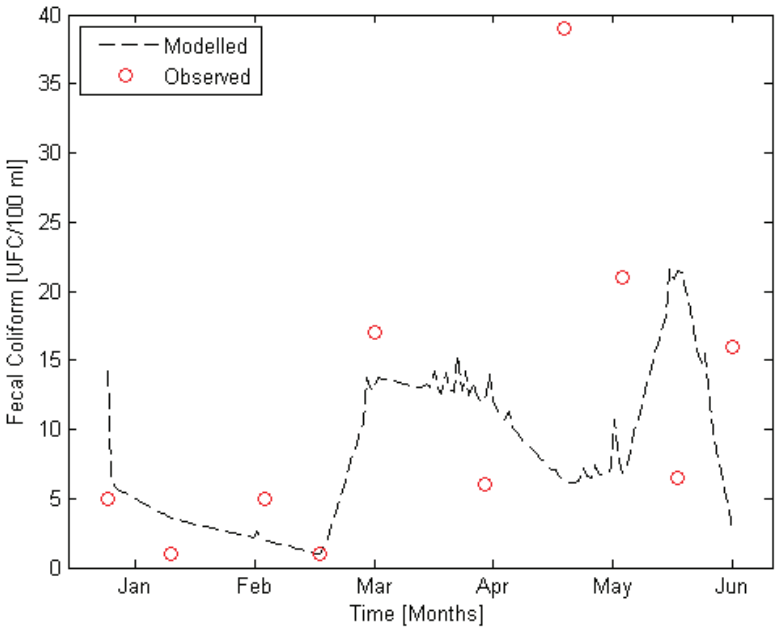

Figure 4.1.2: Fecal Coliform observed in tank A and modelled using the first order kinetic model dependent on temperature with a CSTR in series reactor model

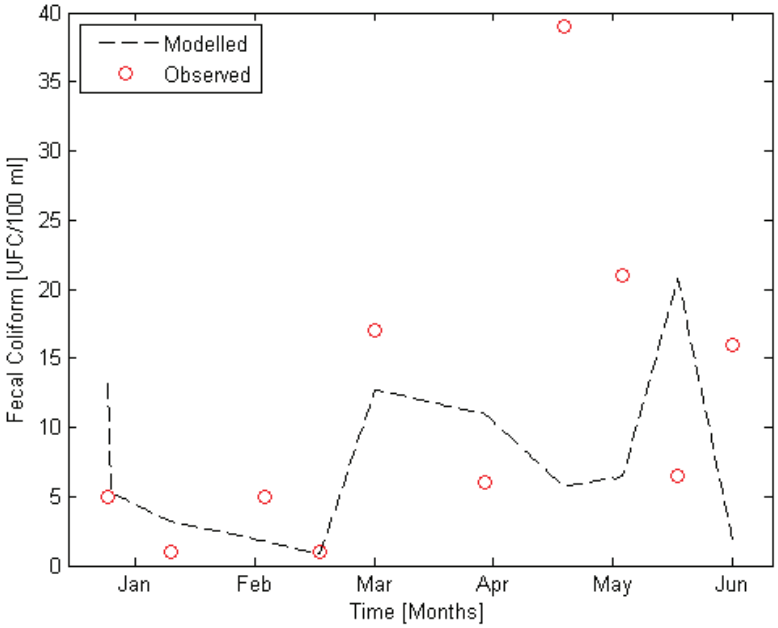

Figure 4.1.3: Fecal Coliform observed in tank A and modelled using the first order kinetic model no dependent on temperature with a CSTR reactor model

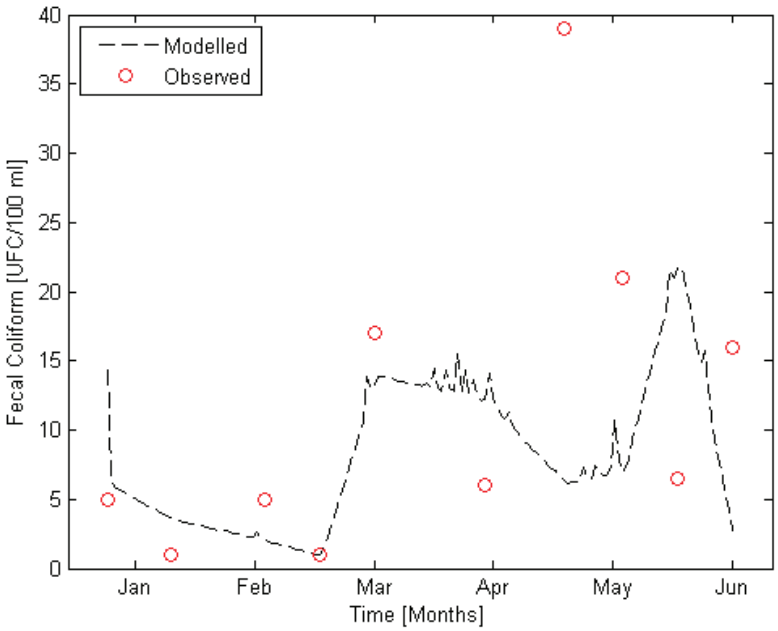

Figure 4.1.4: Fecal Coliform observed in tank A and modelled using the first order kinetic model no dependent on temperature with a CSTR in series reactor model

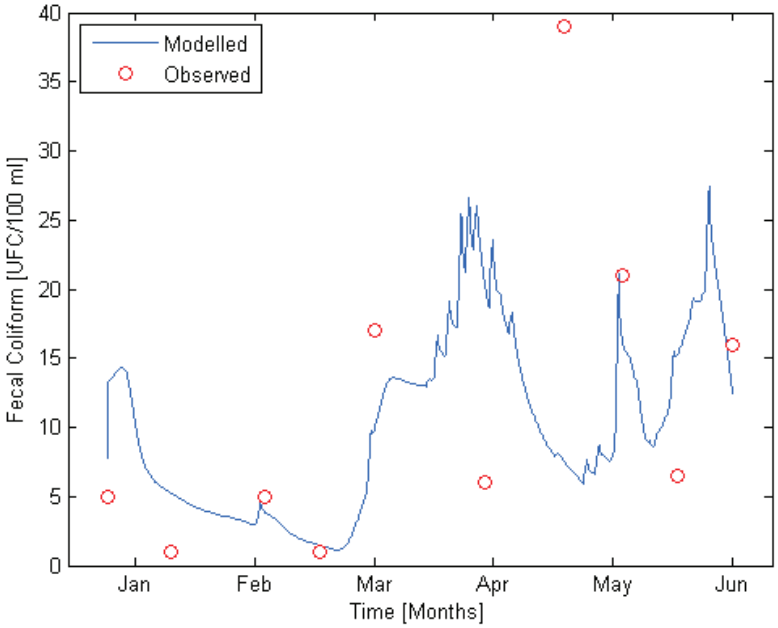

Figure 4.1.5: Fecal Coliform observed in tank A and modelled using the first order kinetic model dependent on temperature with a P&F reactor model

4.2 Results of Validation of first order kinetic models in tank A

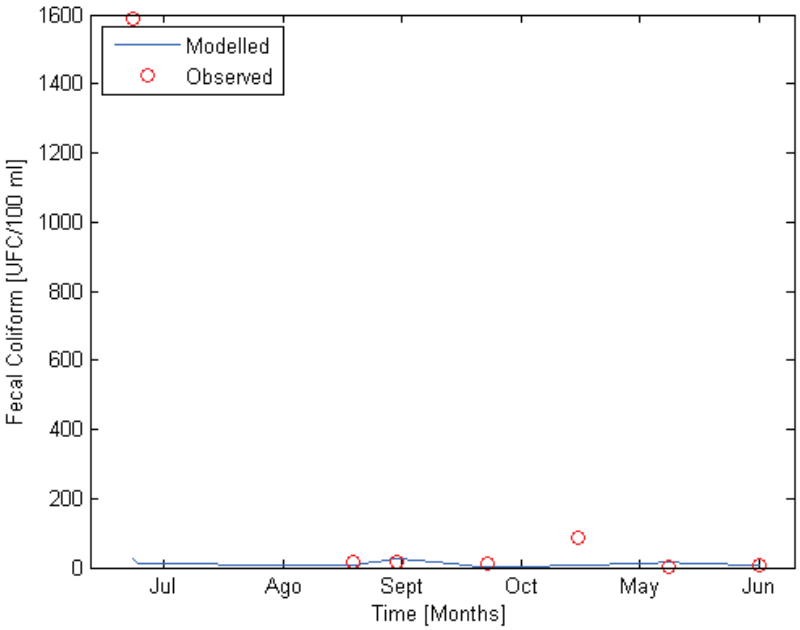

Figure 4.1.6: Fecal Coliform observed in tank A and modelled using the first order kinetic model dependent on temperature with a CSTR reactor model. Model Validated

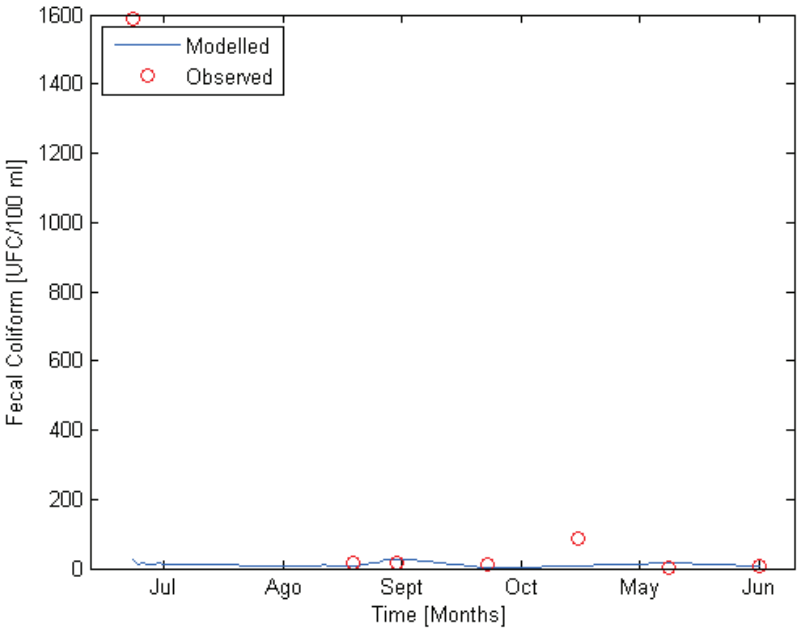

Figure 4.1.7: Fecal Coliform observed in tank A and modelled using the first order kinetic model dependent on temperature with a CSTR in series reactor model: Validated Model

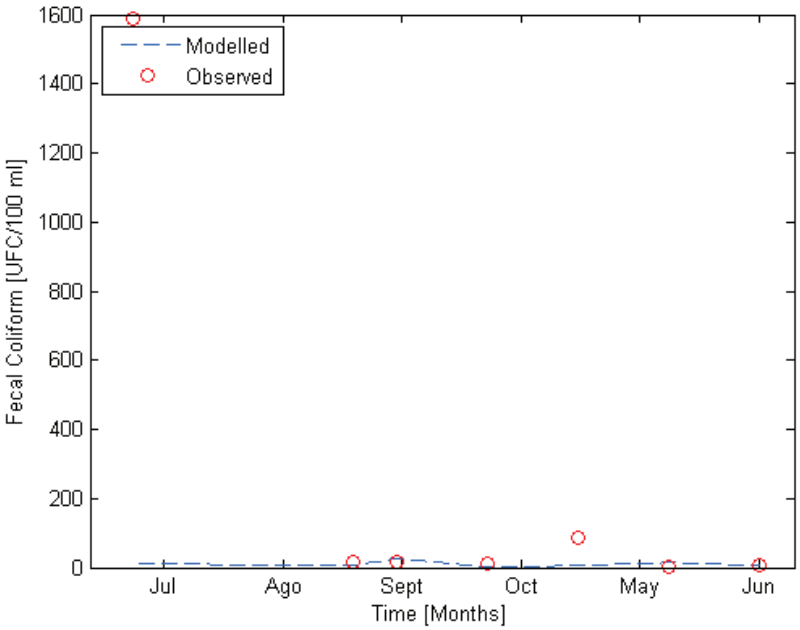

Figure 4.1.8: Fecal Colifom observed in tank A and modelled using the first order kinetic model no dependent on temperature with a CSTR reactor model. Model Validated

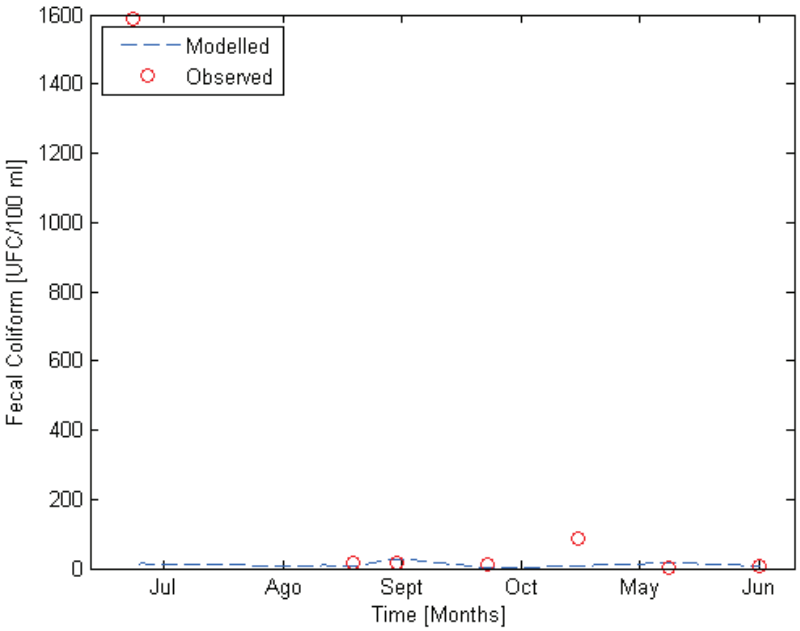

Figure 4.1.9: Fecal Coliform observed in tank A and modelled using the first order kinetic model no dependent on temperature with a CSTR in series reactor model: Validated Model

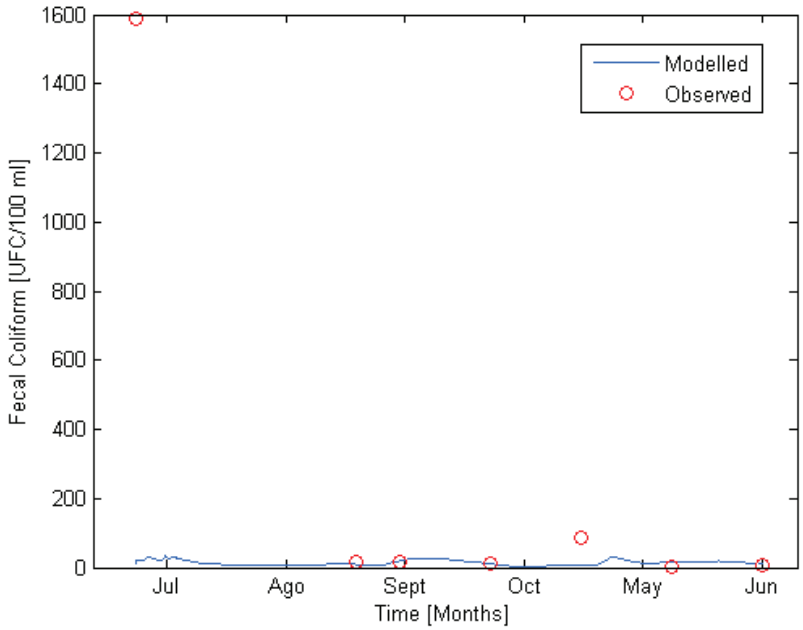

Figure 4.1.10: Fecal Coliform observed in tank A and modelled using the first order kinetic model dependent on temperature with a P&F reactor model: Validated model

4.3 Results of implementation of first order kinetic models in tank B

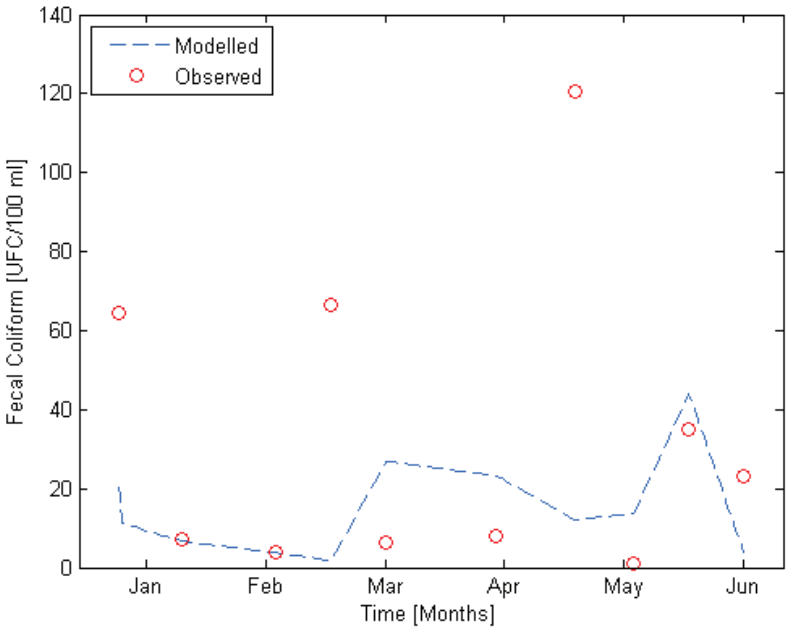

Figure 4.1.11: Fecal Coliform observed in tank B and modelled using the first order kinetic model dependent on temperature with a CSTR reactor model

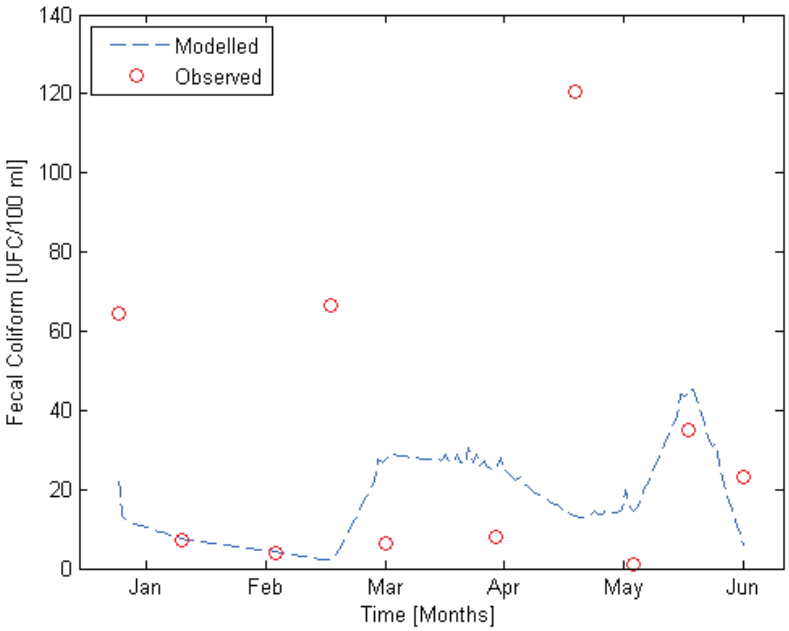

Figure 4.1.12: Fecal Coliform observed in tank B and modelled using the first order kinetic model dependent on temperature with a CSTR in series reactor model

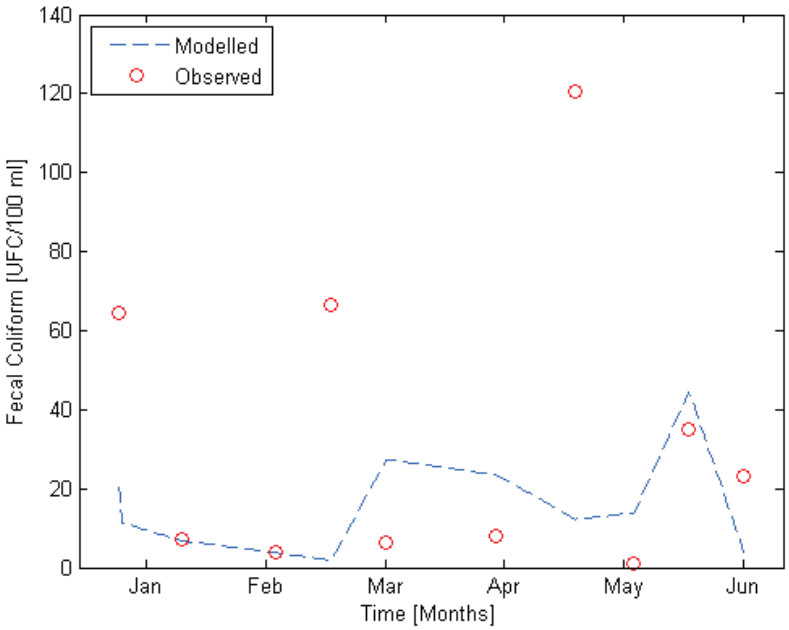

Figure 4.1.13: Fecal Coliform observed in tank B and modelled using the first order kinetic model no dependent on temperature with a CSTR reactor model

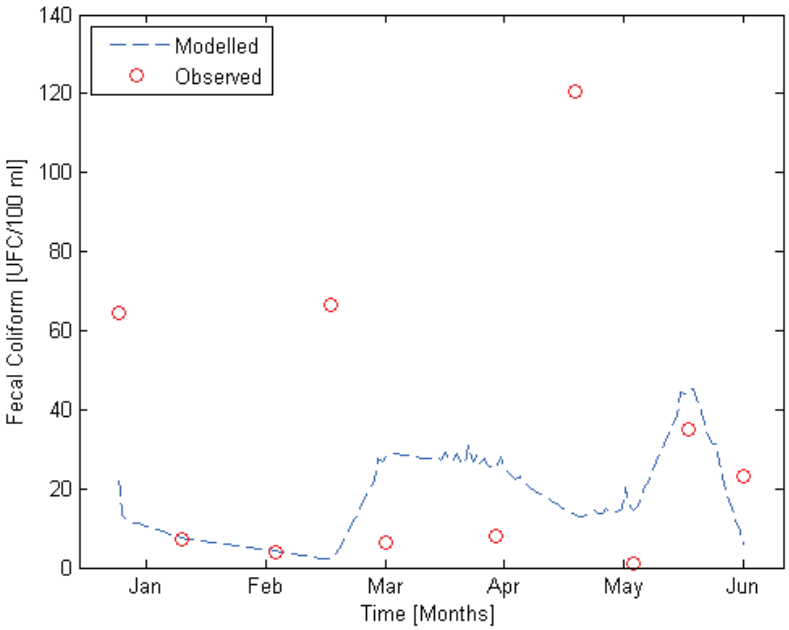

Figure 4.1.14: Fecal Coliform observed in tank B and modelled using the first order kinetic model no dependent on temperature with a CSTR in series reactor model

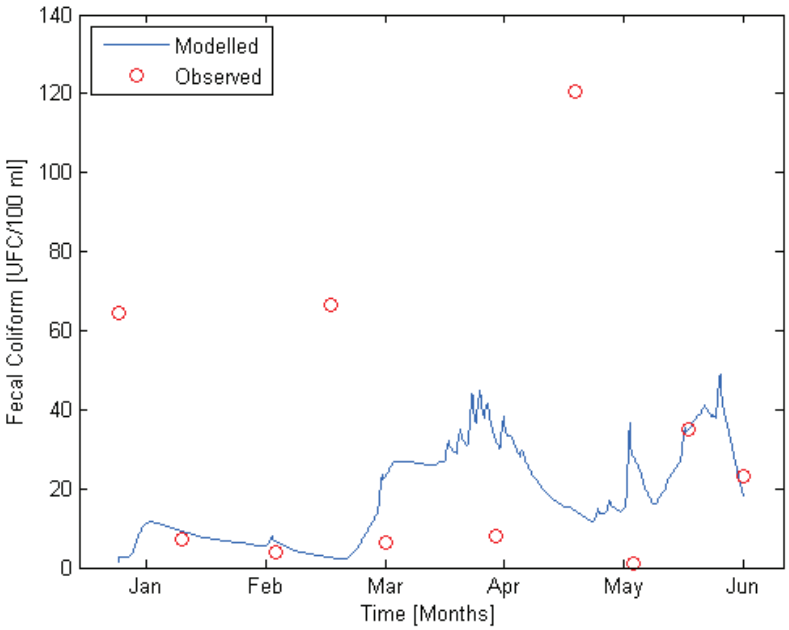

Figure 4.1.15: Fecal Coliform observed in tank B and modelled using the first order kinetic model dependent on temperature with a P&F reactor model

4.4 Results of validation of first order kinetic models in tank B

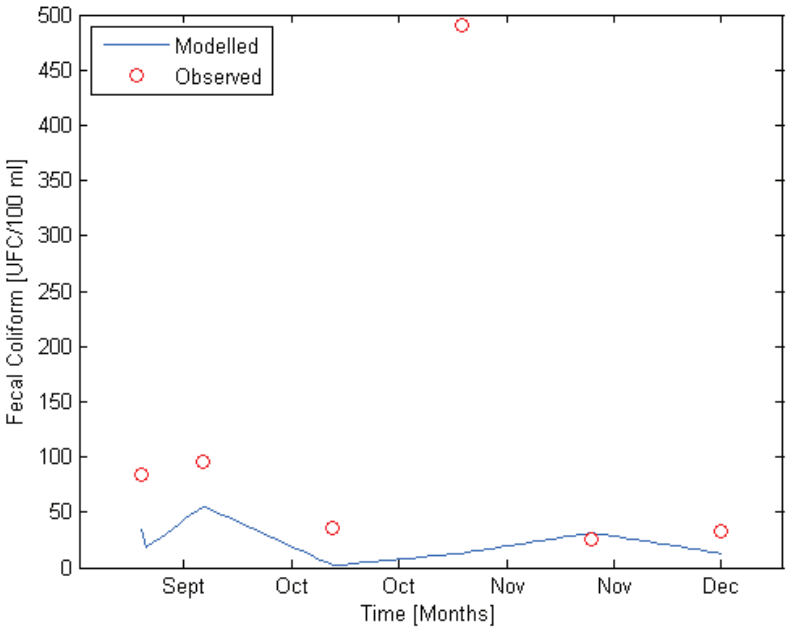

Figure 4.1.16: Fecal Coliform observed in tank B and modelled using the first order kinetic model dependent on temperature with a CSTR reactor model. Model Validated

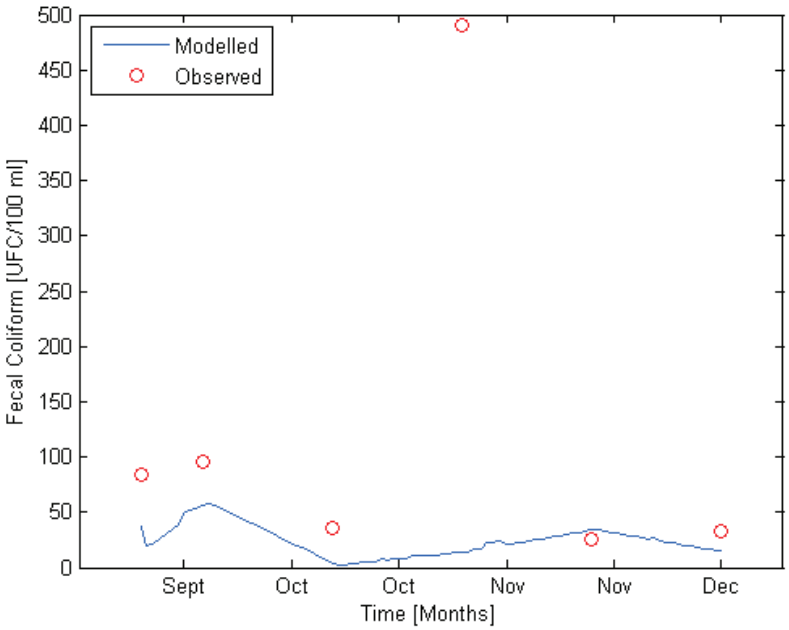

Figure 4.1.17: Fecal Coliform observed in tank B and modelled using the first order kinetic model dependent on temperature with a CSTR in series reactor model. Model Validated

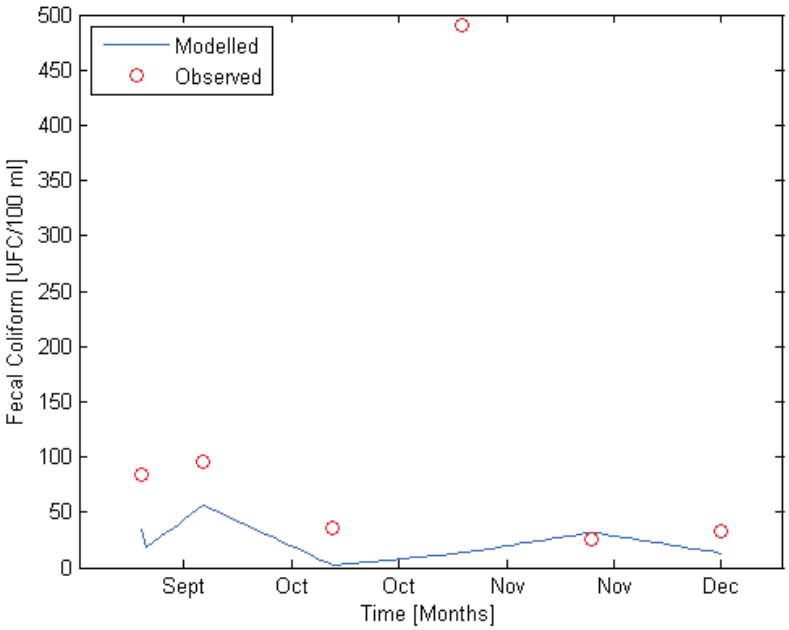

Figure 4.1.18: Fecal Coliform observed in tank B and modelled using the first order kinetic model no dependent on temperature with a CSTR reactor model. Model Validated

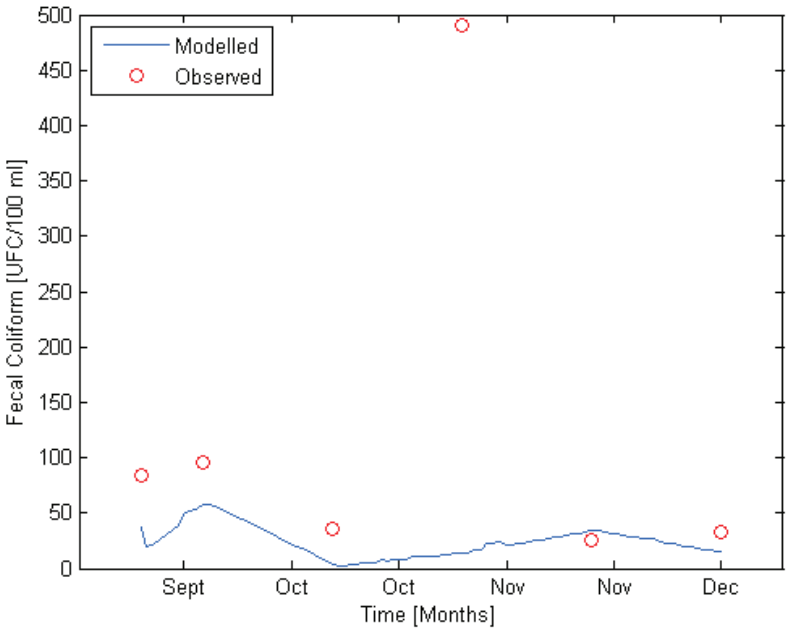

Figure 4.1.19: Fecal Coliform observed in tank B and modelled using the first order kinetic model no dependent on temperature with a CSTR in series reactor model. Model Validated

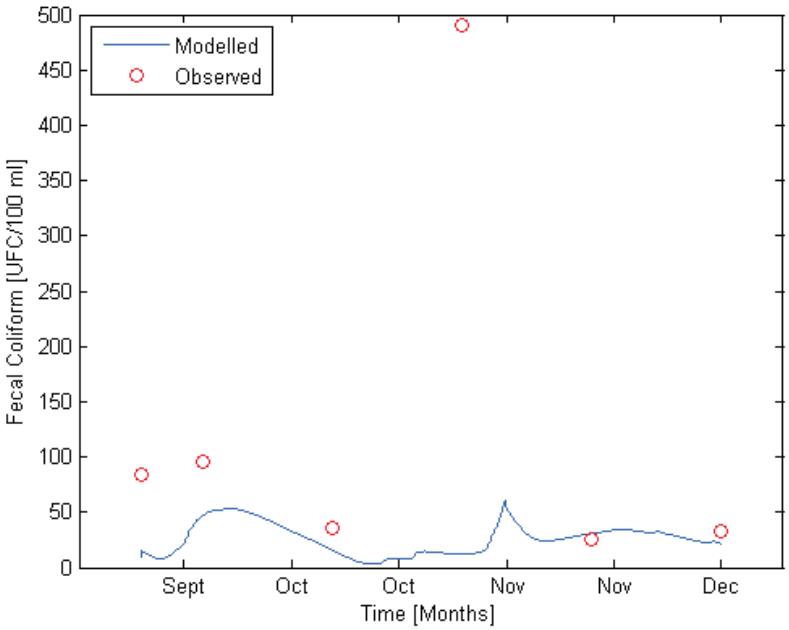

Figure 4.1.20: Fecal Coliform observed in tank B and modelled using the first order kinetic model dependent on temperature with a P&F reactor model: Validated model

ATTACHMENT 5

5.1. Results of implementation of first order kinetic models in tank A

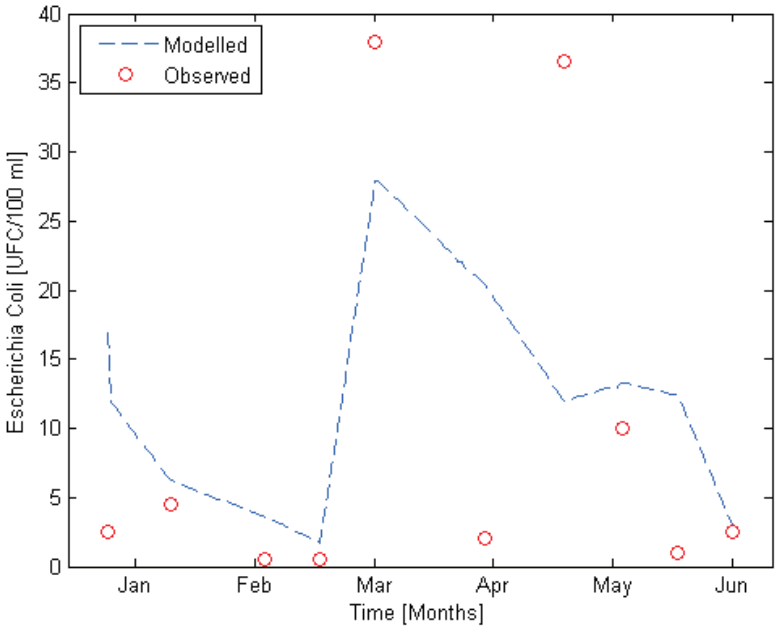

Figure 5.1.1: Escherichia Coli observed in tank A and modelled using the first order kinetic model dependent on temperature with a CSTR reactor model

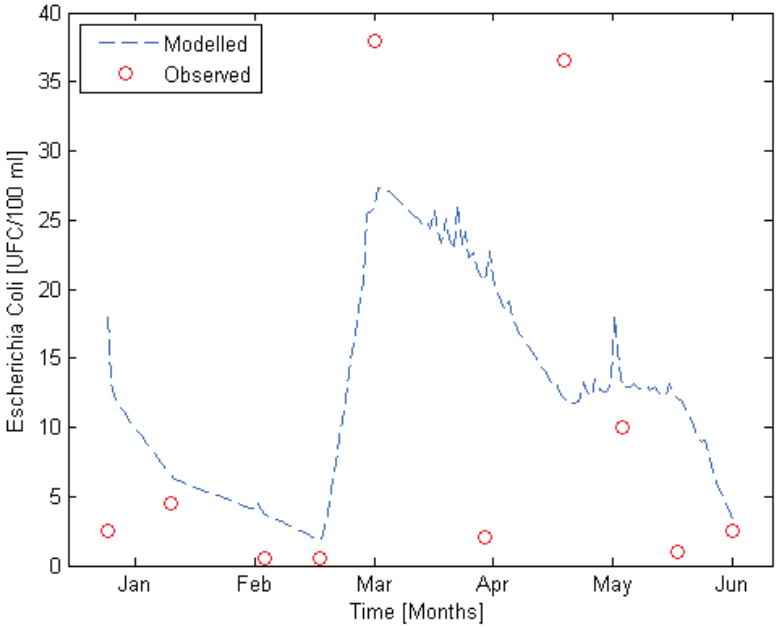

Figure 5.1.2: Escherichia Coli observed in tank A and modelled using the first order kinetic model dependent on temperature with a CSTR in series reactor model

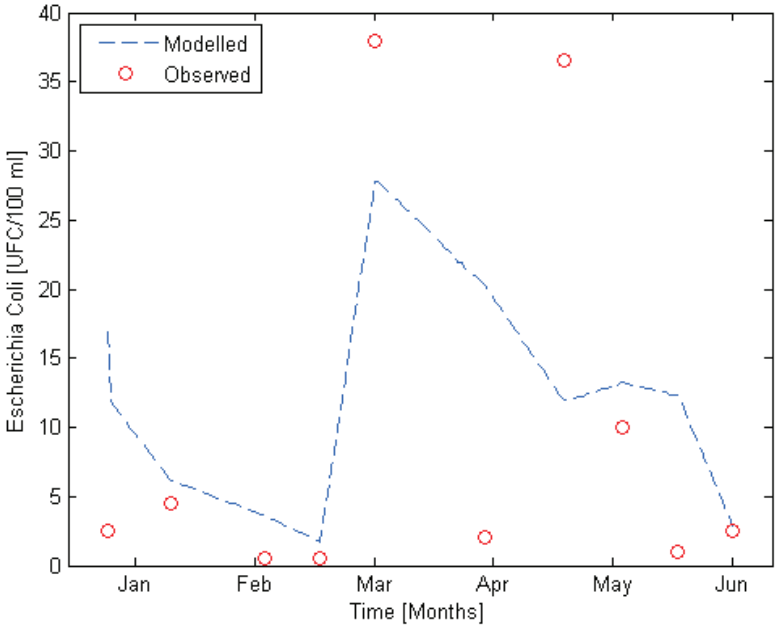

Figure 5.1.3: Escherichi Coli observed in tank A and modelled using the first order kinetic model no dependent on temperature with a CSTR reactor model

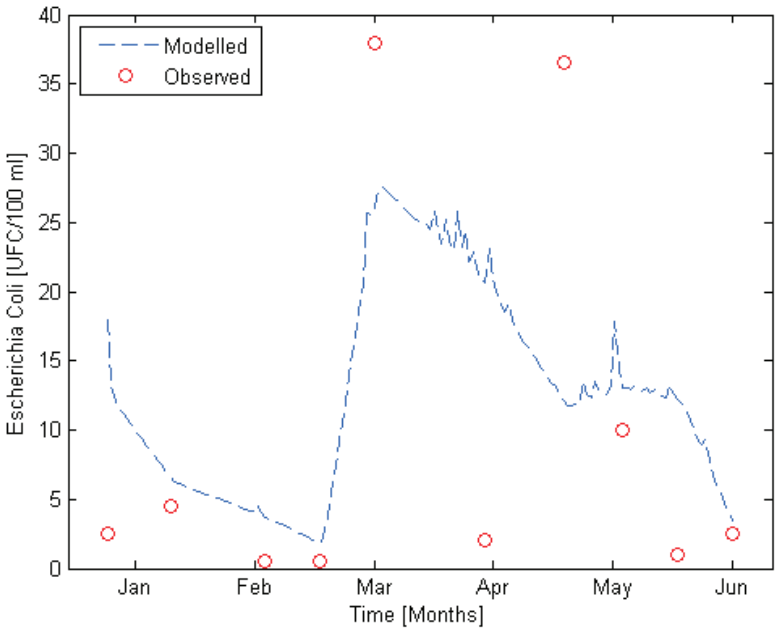

Figure 5.1.4: Escherichia Coli observed in tank A and modelled using the first order kinetic model no dependent on temperature with a CSTR in series reactor model

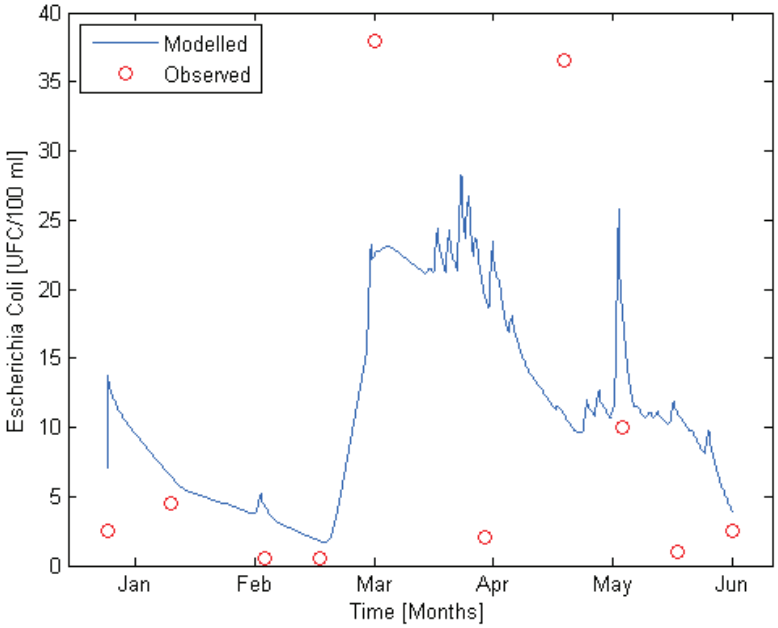

Figure 5.1.5: Escherichia Coli observed in tank A and modelled using the first order kinetic model dependent on temperature with a P&F reactor model

5.2 Results of Validation of first order kinetic models in tank A

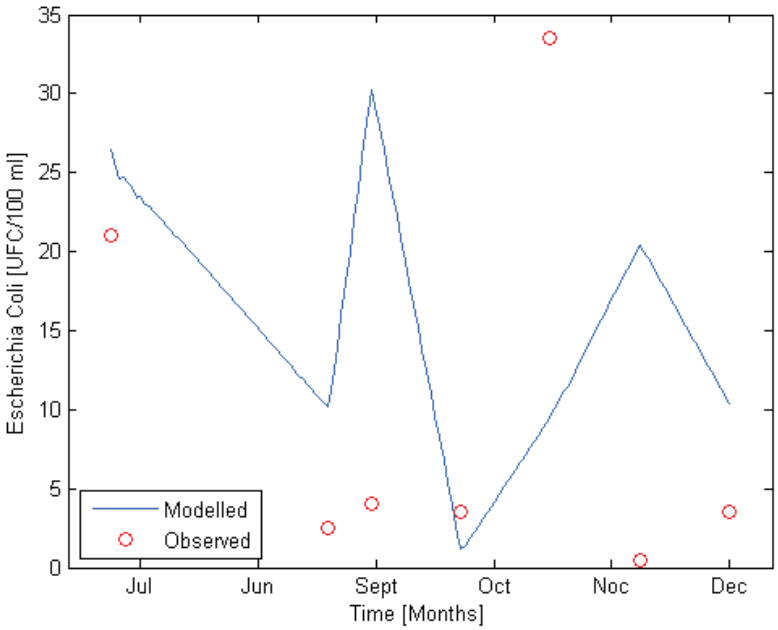

Figure 5.1.6: Escherichia Coli observed in tank A and modelled using the first order kinetic model dependent on temperature with a CSTR reactor model. Model Validated

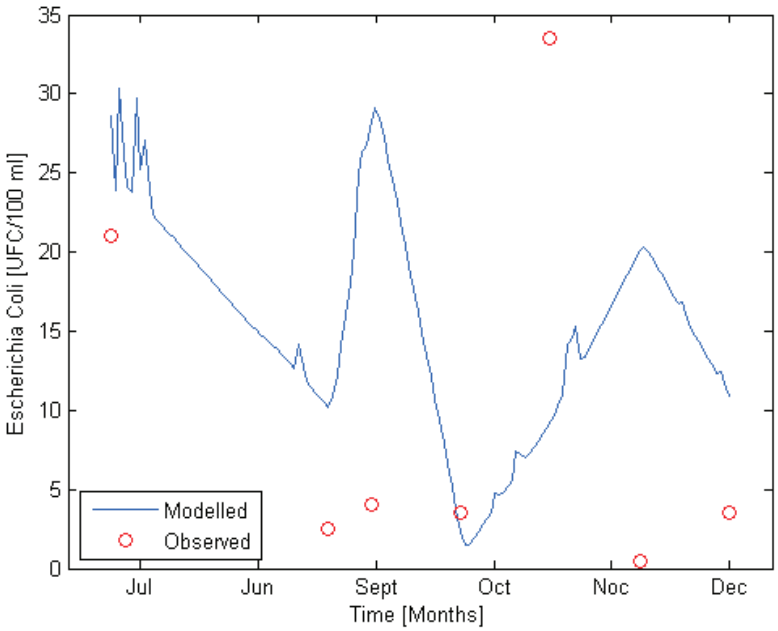

Figure 5.1.7: Escherichia Coli observed in tank A and modelled using the first order kinetic model dependent on temperature with a CSTR in series reactor model: Validated Model

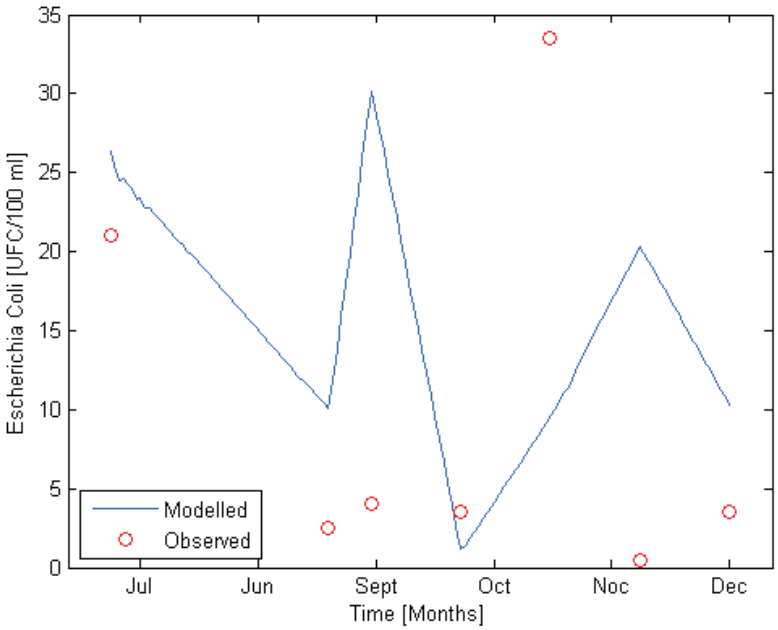

Figure 5.1.8: Escherichia Coli observed in tank A and modelled using the first order kinetic model no dependent on temperature with a CSTR reactor model. Model Validated

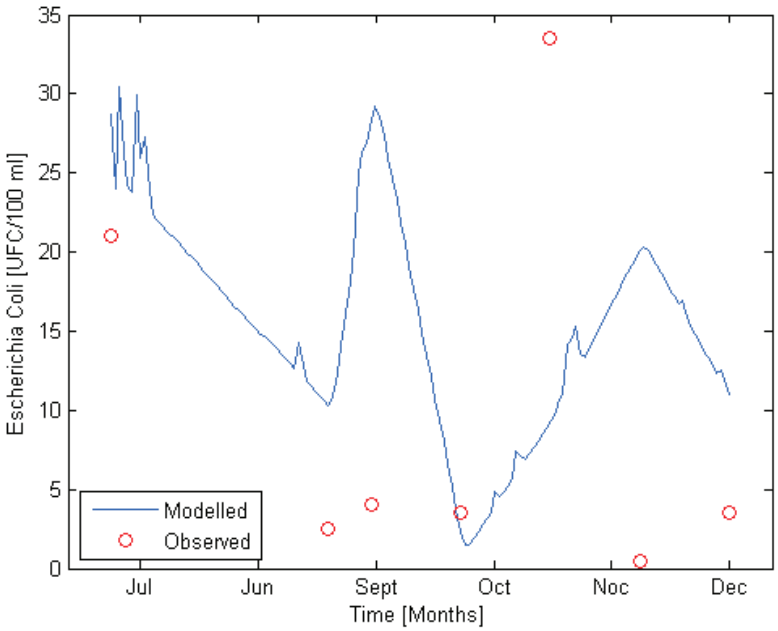

Figure 5.1.9: Escherichia Coli observed in tank A and modelled using the first order kinetic model no dependent on temperature with a CSTR in series reactor model: Validated Model

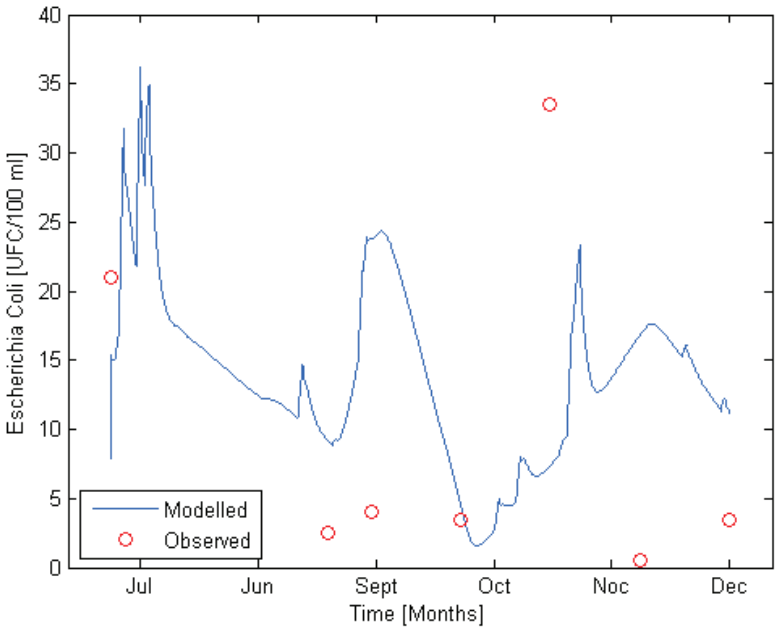

Figure 5.1.10: Escherichia Coli observed in tank A and modelled using the first order kinetic model dependent on temperature with a P&F reactor model: Validated model

5.3 Results of implementation of first order kinetic models in tank B

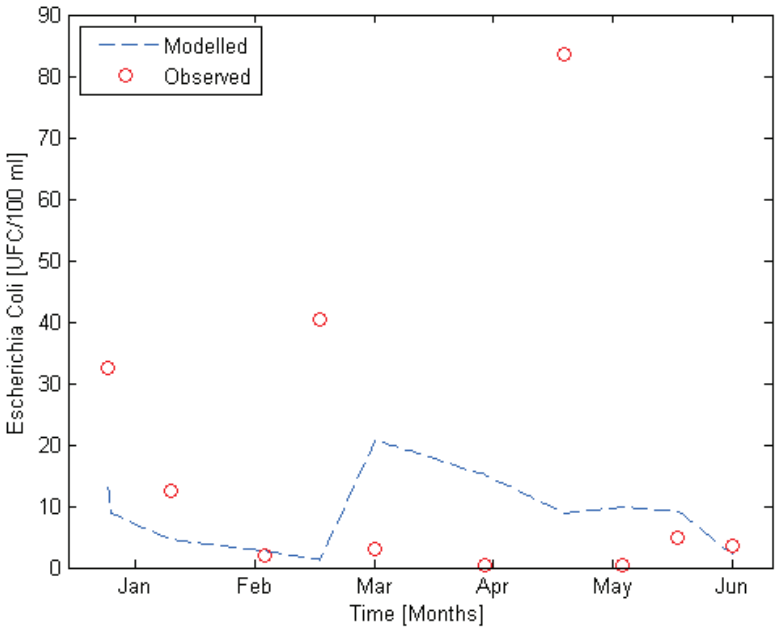

Figure 5.1.11: Escherichia Coli observed in tank B and modelled using the first order kinetic model dependent on temperature with a CSTR reactor model

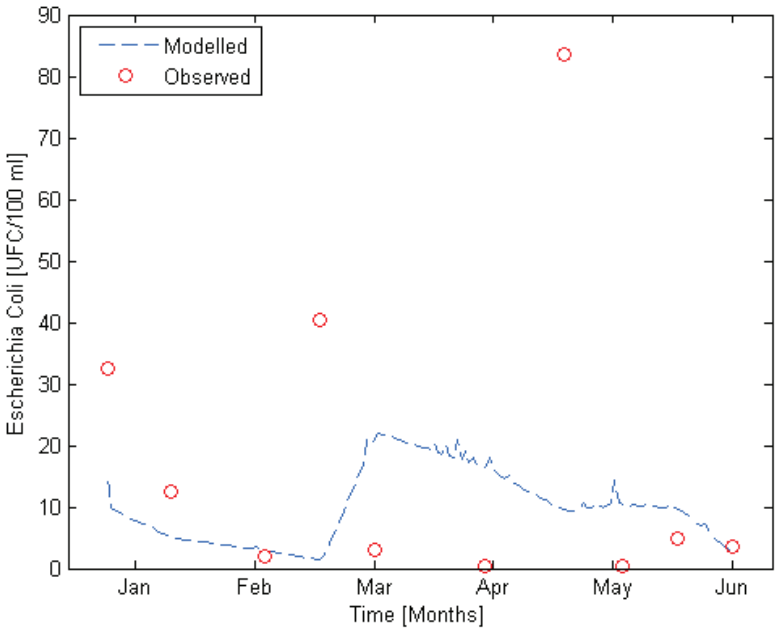

Figure 4.1.12: Escherichia Coli observed in tank B and modelled using the first order kinetic model dependent on temperature with a CSTR in series reactor model

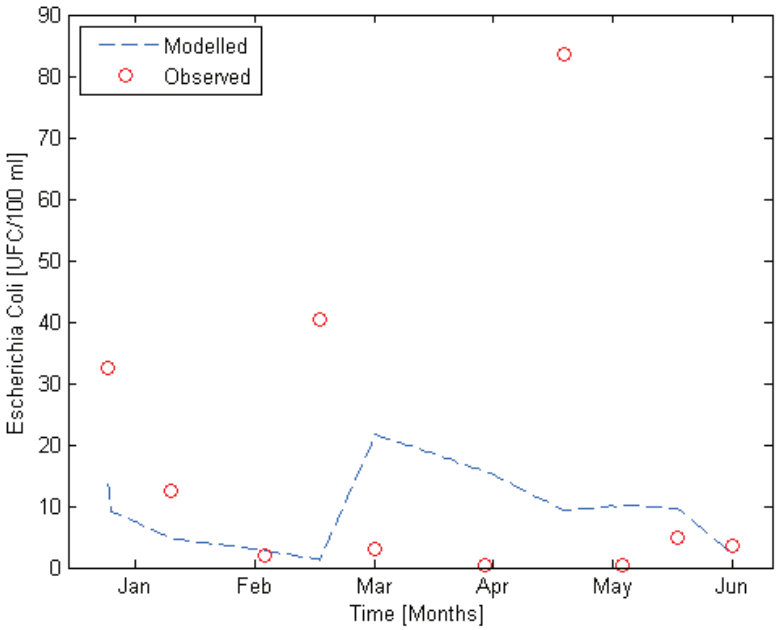

Figure 5.1.13: Escherichia Coli observed in tank B and modelled using the first order kinetic model no dependent on temperature with a CSTR reactor model

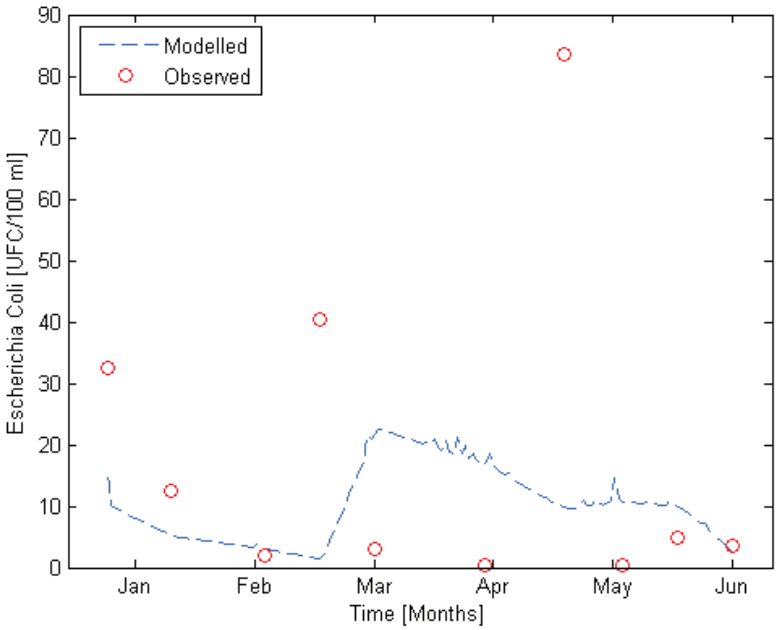

Figure 5.1.14: Escherichia Coli observed in tank B and modelled using the first order kinetic model no dependent on temperature with a CSTR in series reactor model

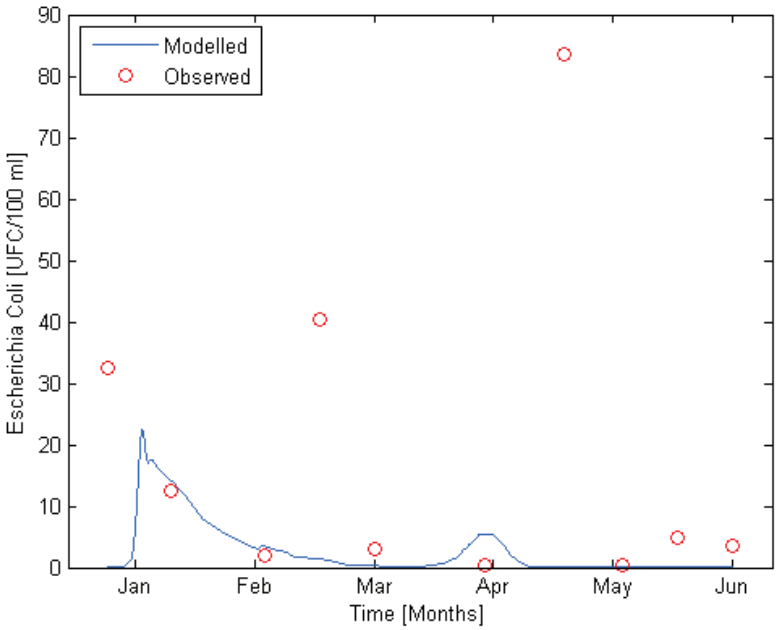

Figure 5.1.15: Escherichia Coli observed in tank B and modelled using the first order kinetic model dependent on temperature with a P&F reactor model

5.4 Results of validation of first order kinetic models in tank B

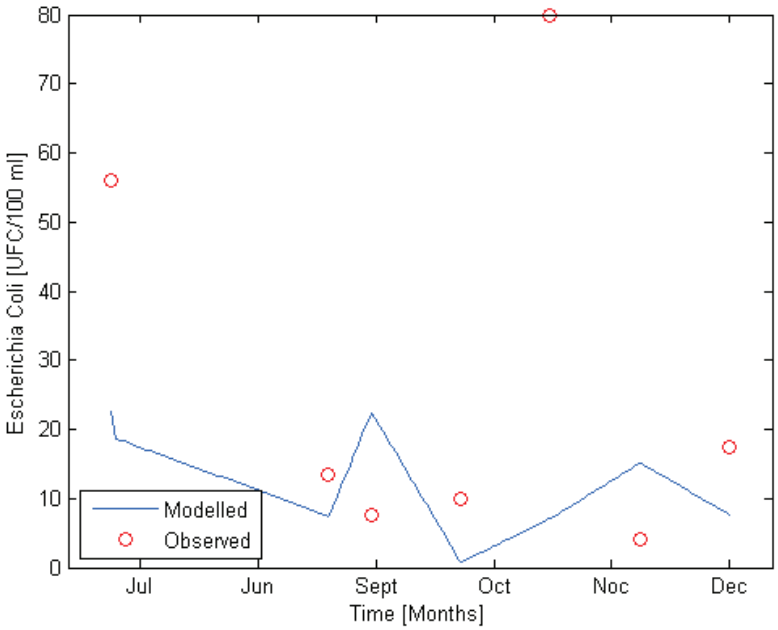

Figure 5.1.16: Escherichia Coli observed in tank B and modelled using the first order kinetic model dependent on temperature with a CSTR reactor model. Model Validated

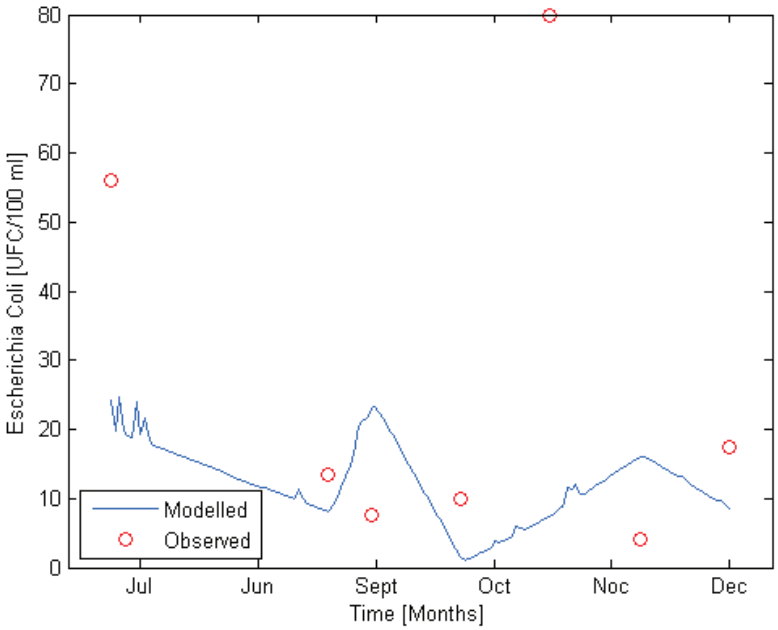

Figure 5.1.17: Escherichia Coli observed in tank B and modelled using the first order kinetic model dependent on temperature with a CSTR in series reactor model. Model Validated

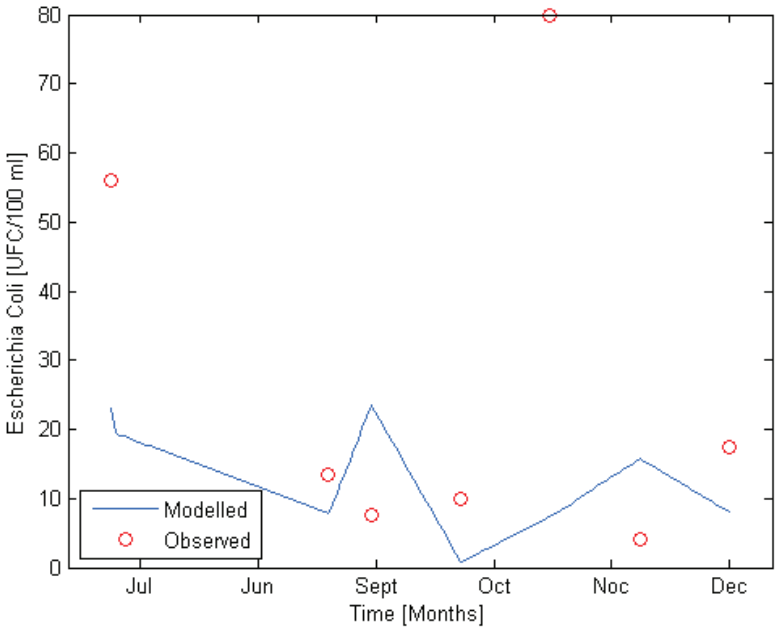

Figure 5.1.18: Escherichia Coli observed in tank B and modelled using the first order kinetic model no dependent on temperature with a CSTR reactor model. Model Validated

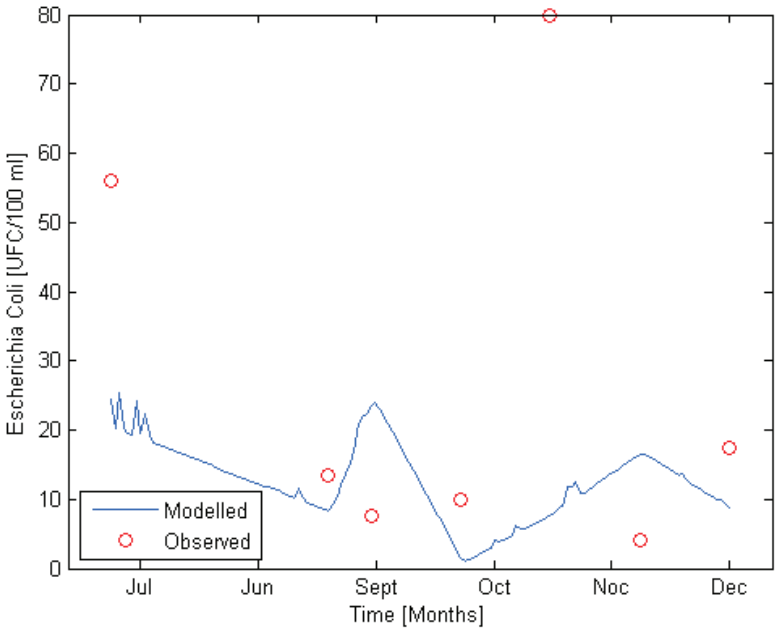

Figure 5.1.19: Escherichia Coli observed in tank B and modelled using the first order kinetic model no dependent on temperature with a CSTR in series reactor model. Model Validated

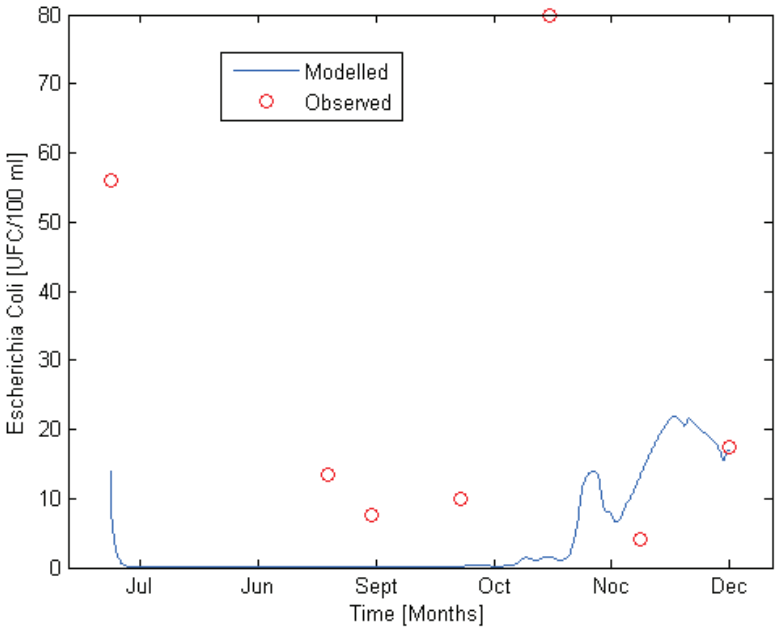

Figure 5.1.20: Escherichia Coli observed in tank B and modelled using the first order kinetic model dependent on temperature with a P&F reactor model: Validated model

ATTACHMENT 6

6.1. Results of implementation of first order kinetic models in tank A

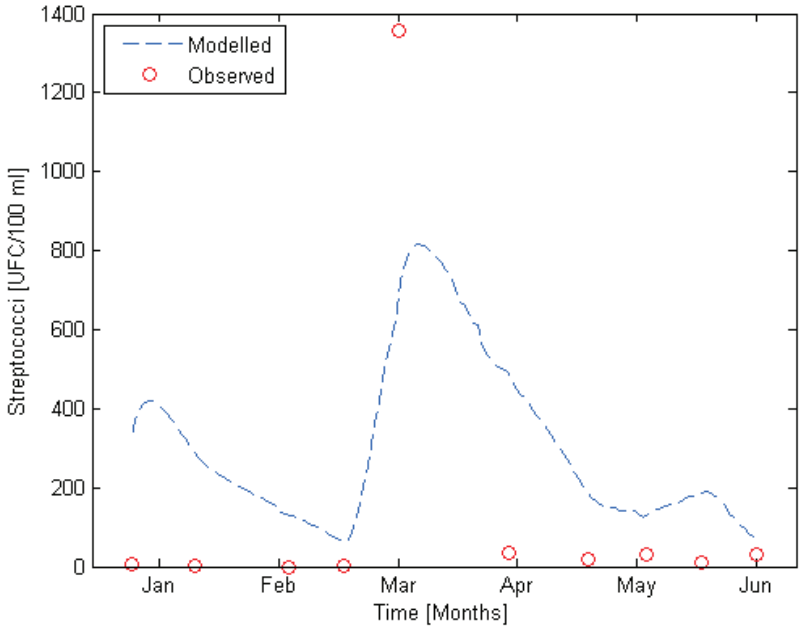

Figure 6.1.1: Streptococci observed in tank A and modelled using the first order kinetic model dependent on temperature with a CSTR reactor model

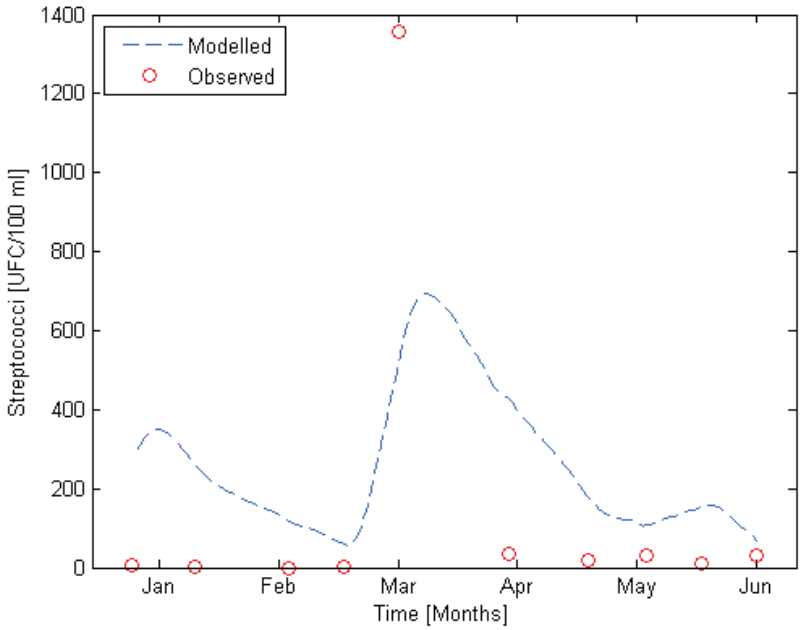

Figure 6.1.2: Streptococci observed in tank A and modelled using the first order kinetic model dependent on temperature with a CSTR in series reactor model

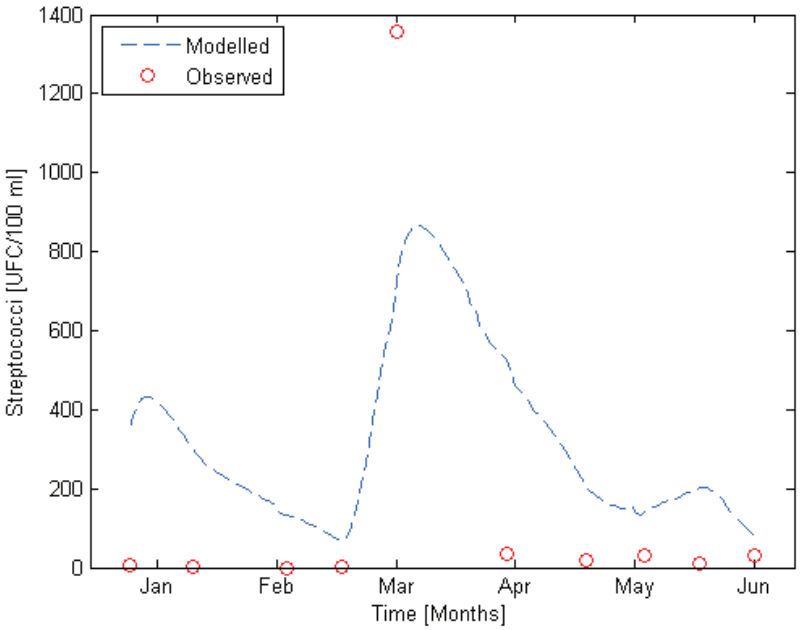

Figure 6.1.3: Streptococci observed in tank A and modelled using the first order kinetic model no dependent on temperature with a CSTR reactor model

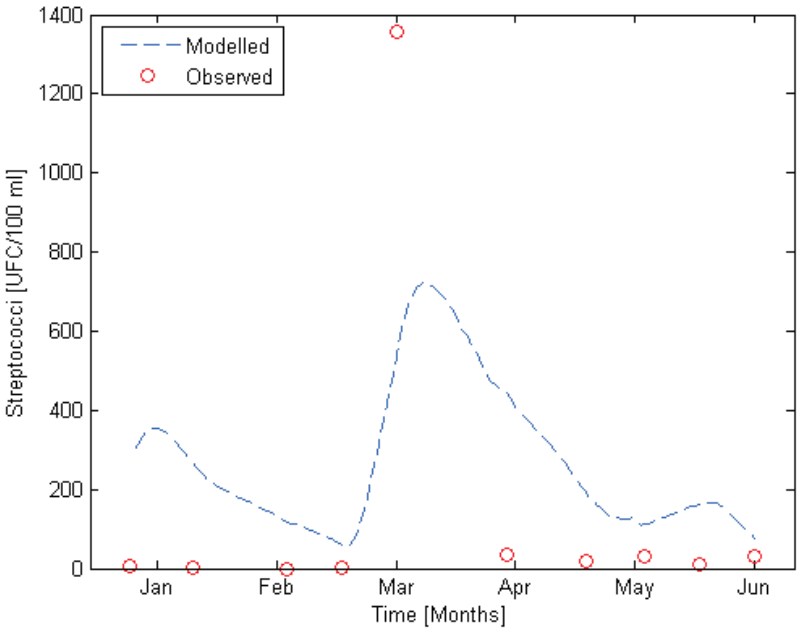

Figure 6.1.4: Streptococci observed in tank A and modelled using the first order kinetic model no dependent on temperature with a CSTR in series reactor model

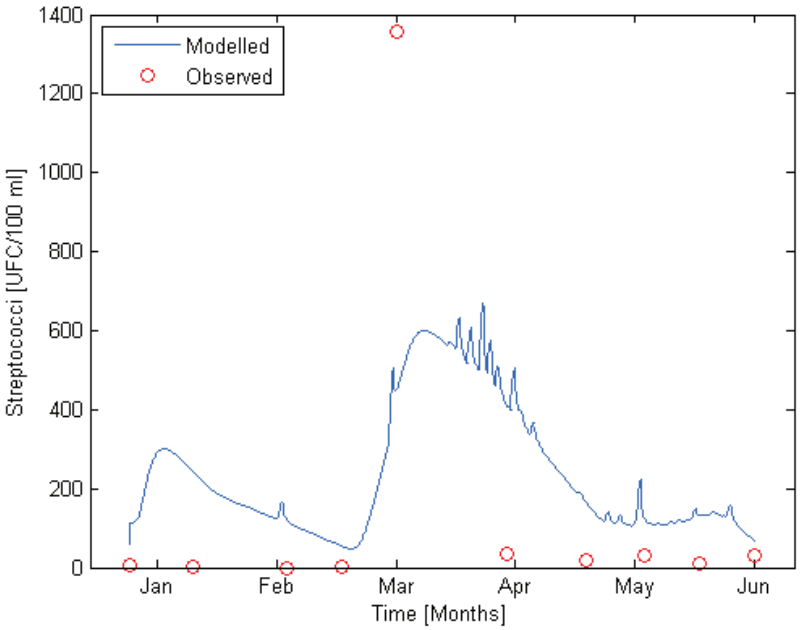

Figure 6.1.5: Streptococci observed in tank A and modelled using the first order kinetic model dependent on temperature with a P&F reactor model

6.2 Results of Validation of first order kinetic models in tank A

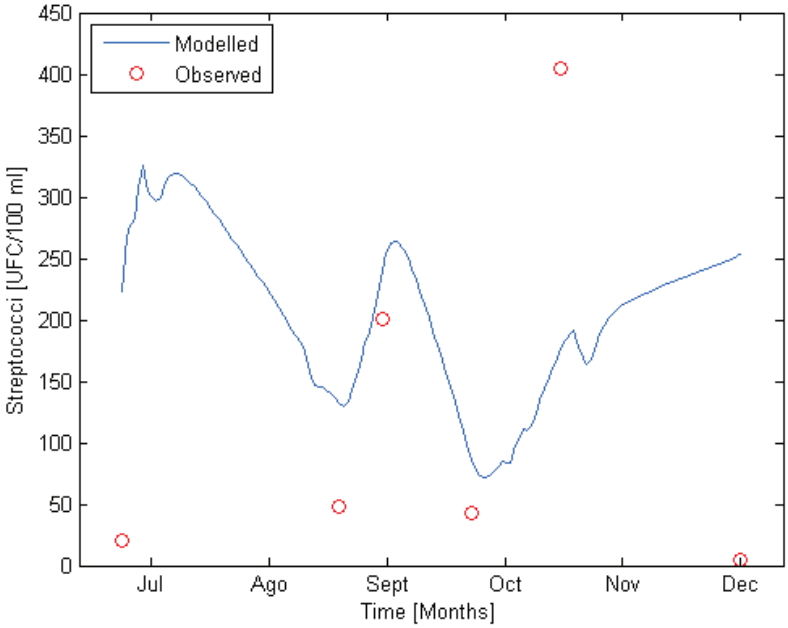

Figure 6.1.6: Streptococci observed in tank A and modelled using the first order kinetic model dependent on temperature with a CSTR reactor model. Model Validated

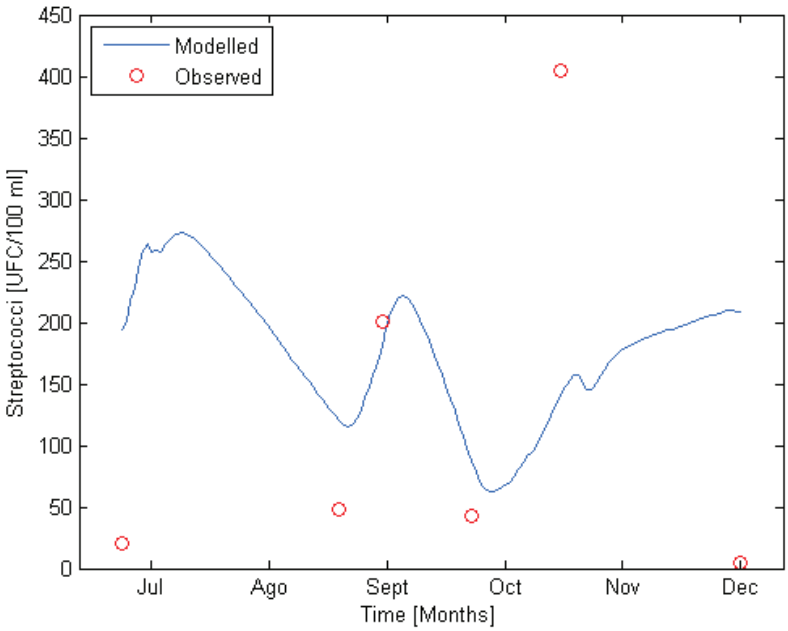

Figure 6.1.7: Streptococci observed in tank A and modelled using the first order kinetic model dependent on temperature with a CSTR in series reactor model: Validated Model

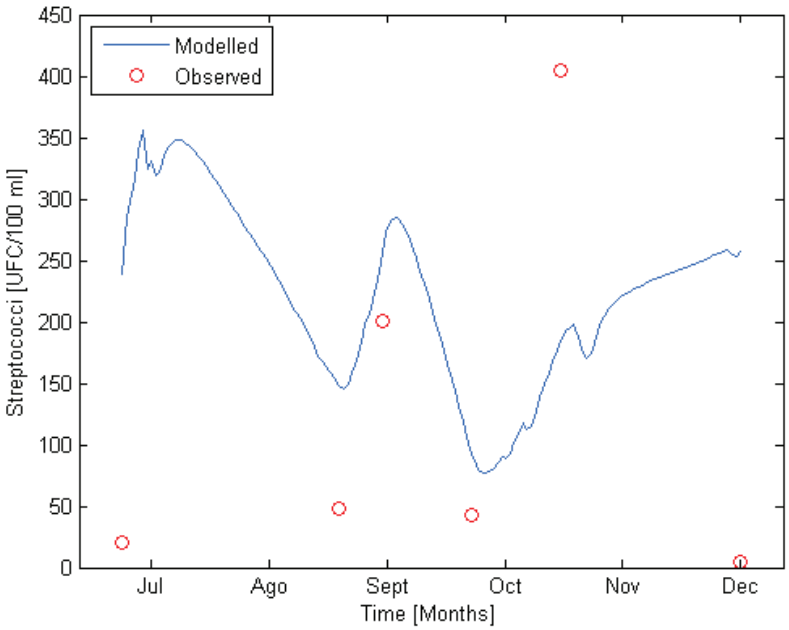

Figure 6.1.8: Streptococci observed in tank A and modelled using the first order kinetic model no dependent on temperature with a CSTR reactor model. Model Validated

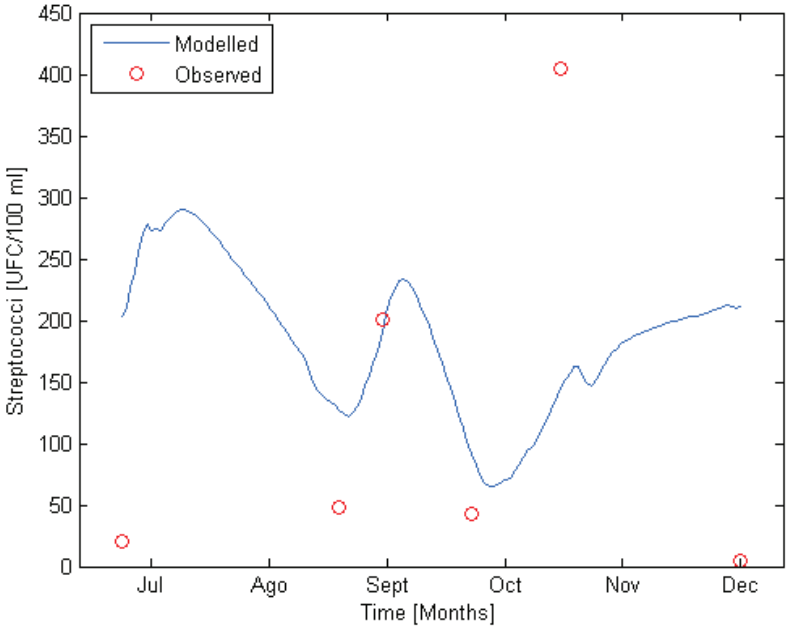

Figure 6.1.9: Streptococci observed in tank A and modelled using the first order kinetic model no dependent on temperature with a CSTR in series reactor model: Validated Model

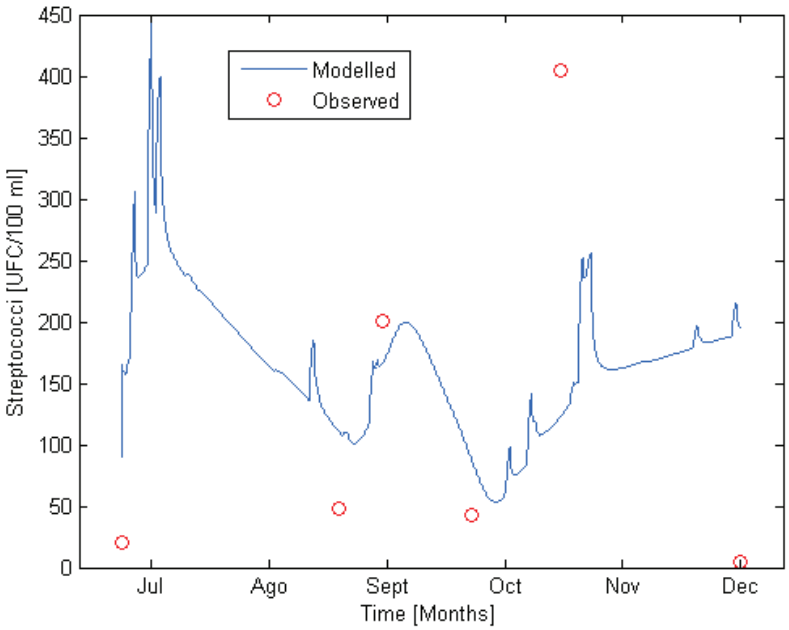

Figure 6.1.10: Streptococci observed in tank A and modelled using the first order kinetic model dependent on temperature with a P&F reactor model: Validated model

6.3 Results of implementation of first order kinetic models in tank B

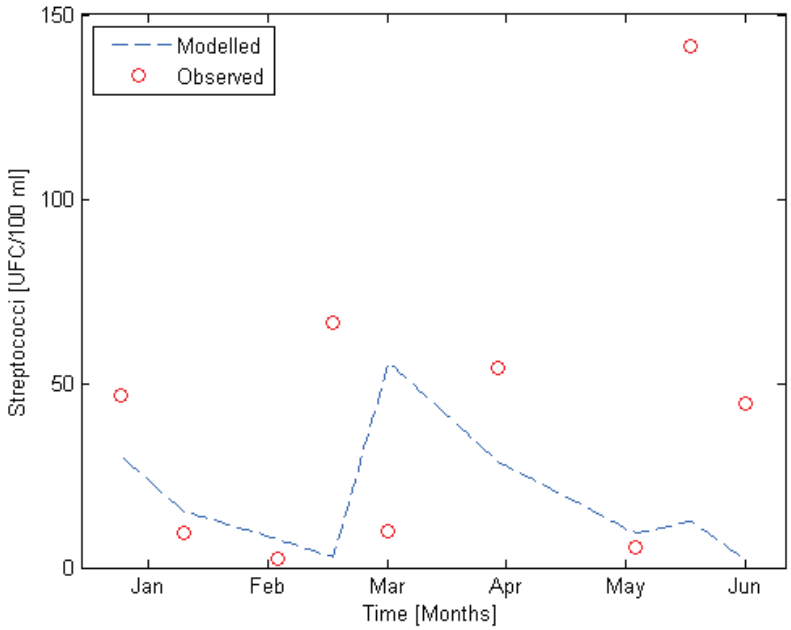

Figure 6.1.11: Streptococci observed in tank B and modelled using the first order kinetic model dependent on temperature with a CSTR reactor model

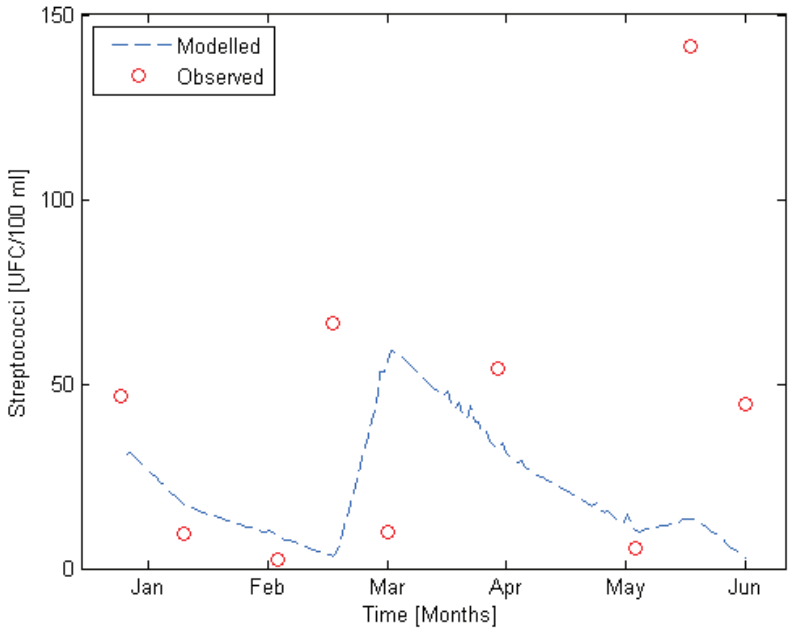

Figure 6.1.12: Streptococci observed in tank B and modelled using the first order kinetic model dependent on temperature with a CSTR in series reactor model

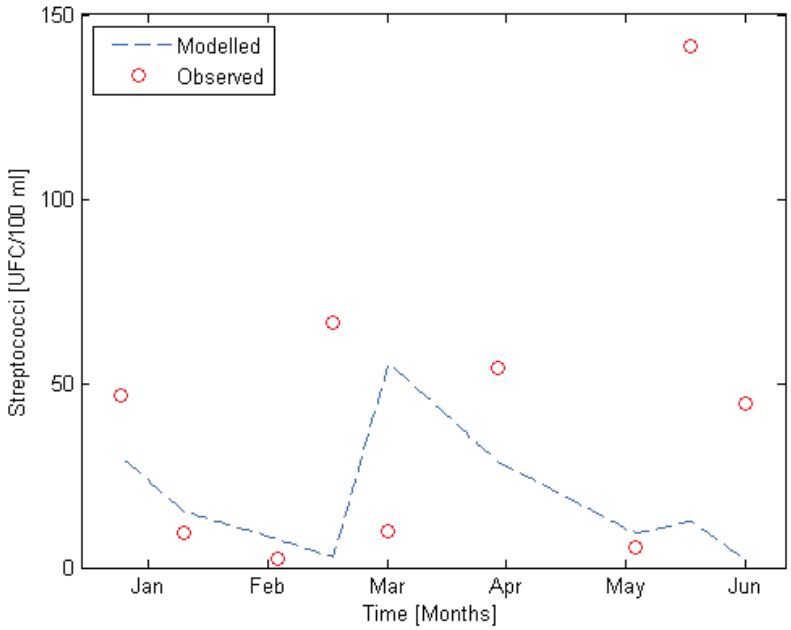

Figure 6.1.13: Streptococci observed in tank B and modelled using the first order kinetic model no dependent on temperature with a CSTR reactor model

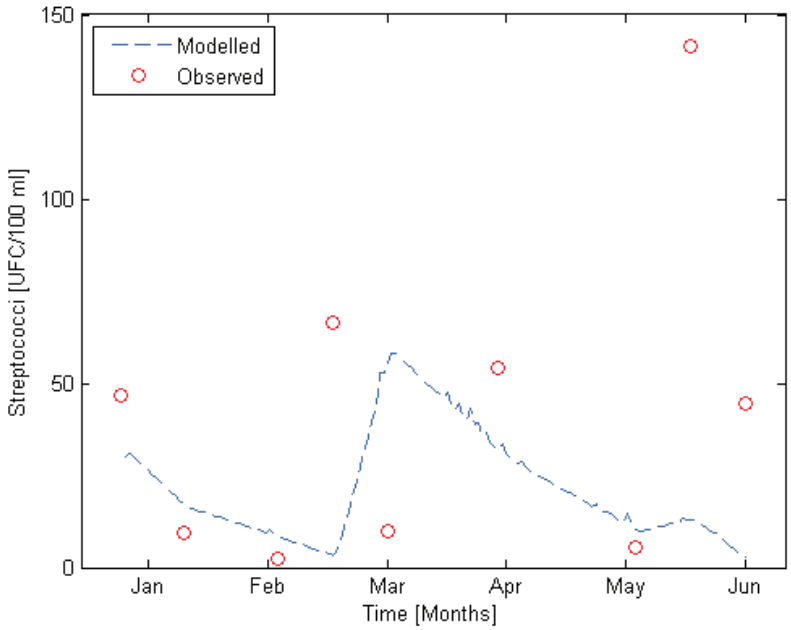

Figure 6.1.14: Streptococci observed in tank B and modelled using the first order kinetic model no dependent on temperature with a CSTR in series reactor model

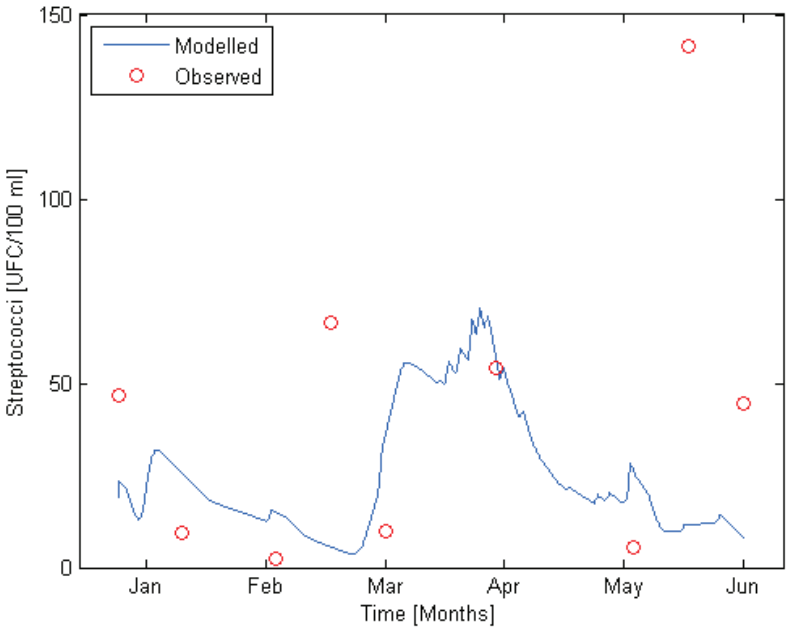

Figure 6.1.15: Streptococci observed in tank B and modelled using the first order kinetic model dependent on temperature with a P&F reactor model

6.4 Results of validation of first order kinetic models in tank B

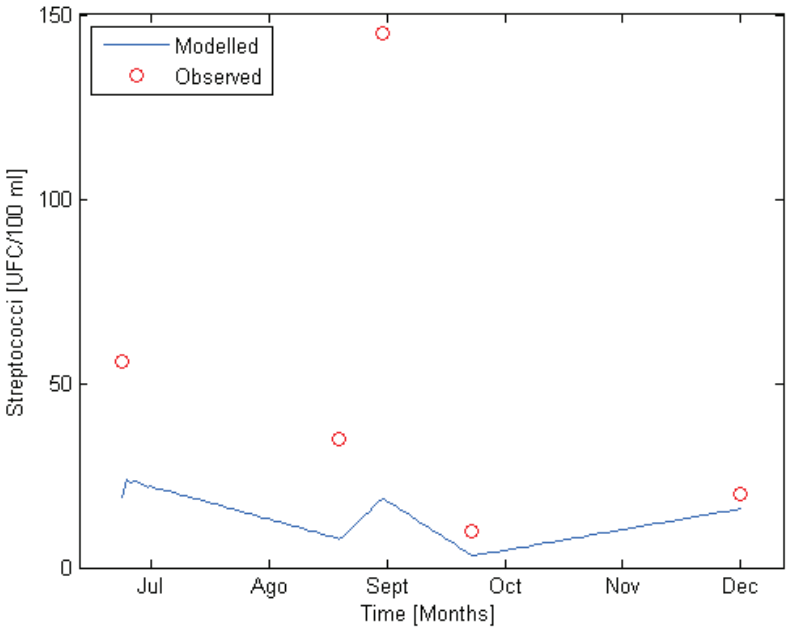

Figure 6.1.16: Streptococci observed in tank B and modelled using the first order kinetic model dependent on temperature with a CSTR reactor model. Model Validated

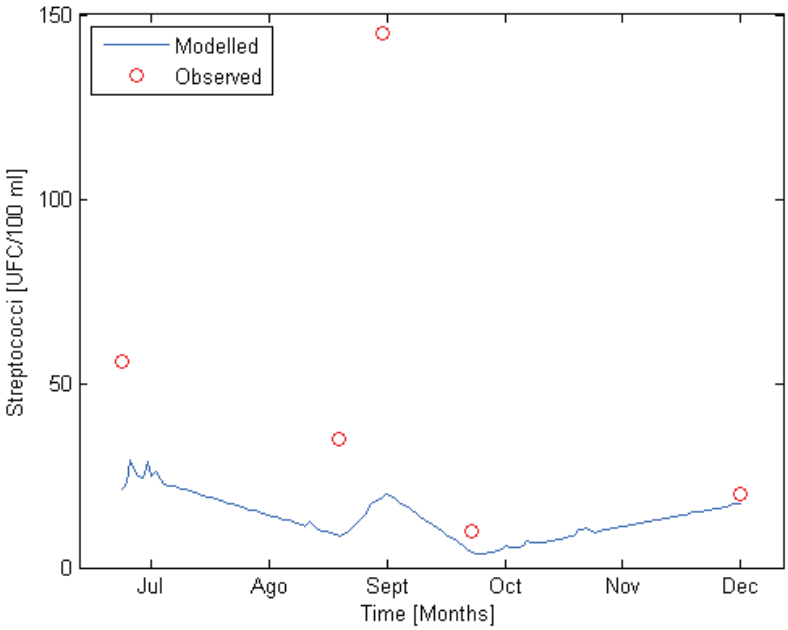

Figure 6.1.17: Streptococci observed in tank B and modelled using the first order kinetic model dependent on temperature with a CSTR in series reactor model. Model Validated

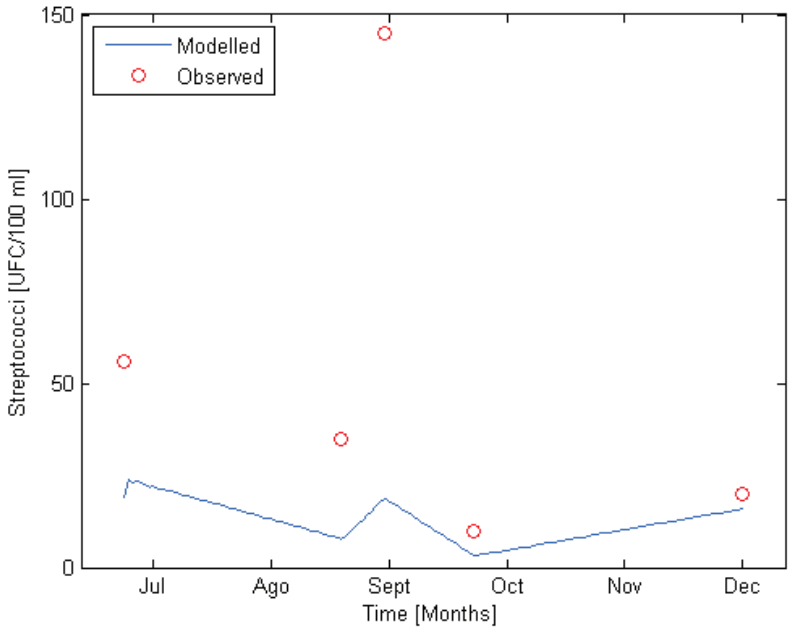

Figure 6.1.18: Streptococci observed in tank B and modelled using the first order kinetic model no dependent on temperature with a CSTR reactor model. Model Validated

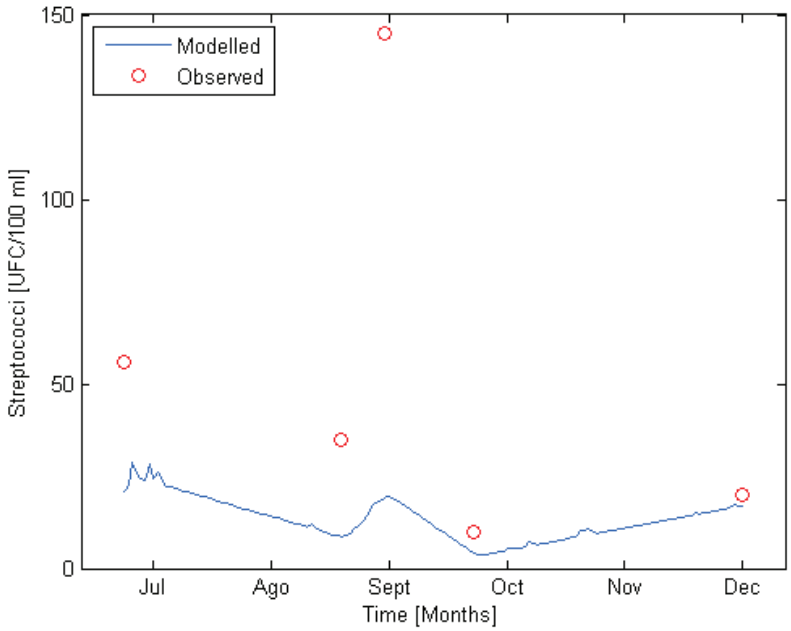

Figure 6.1.19: Streptococci observed in tank B and modelled using the first order kinetic model no dependent on temperature with a CSTR in series reactor model. Model Validated

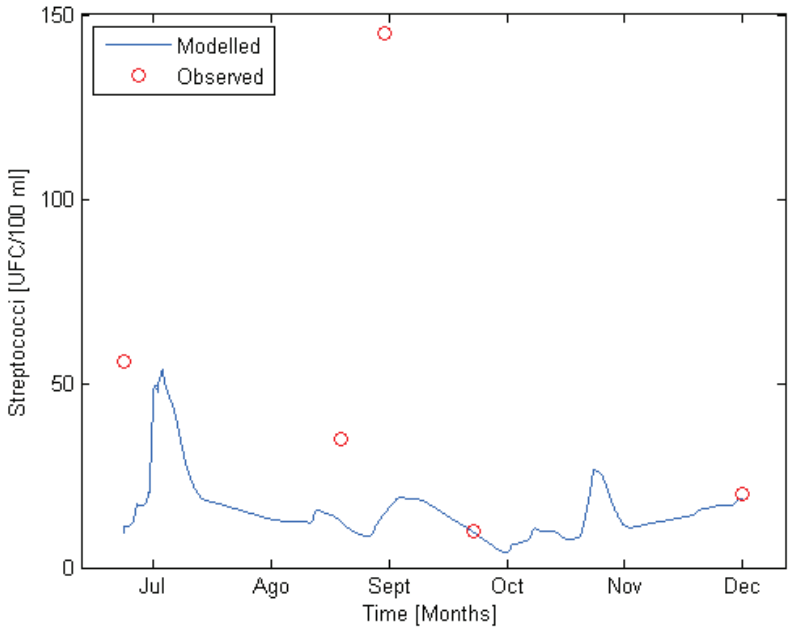

Figure 6.1.20: Streptococci observed in tank B and modelled using the first order kinetic model dependent on temperature with a P&F reactor model: Validated model